Vol.2, No.5, May-2024

# APPLIED SCIENCES
# RESEARCH PERIODICALS

# TABLE OF CONTENTS

# EDITORIAL BOARD

## DISCLAIMER

All the manuscripts are published in good faith and intentions to promote and encourage research around the globe. The contributions are property of their respective authors/owners and Applied Sciences Research Periodicals (ASRP) is not responsible for any content that hurts someone's views or feelings. Authors are responsible for if any plagiarism is found in published material.

Applied Sciences Research Periodicals – ISSN 3033-330X
May 2024, Vol. 2, No. 5, pp. 01-10

# Foundations of Magnetic Field Definition

Stanislav Ordin

1. The Russian Academy of Sciences

**Abstract:**
Any FIELD, by definition, is Force, which is a continuous parameter of space. For the Magnetic Field, this parameter is the Ampere Force, but it was actually neglected. Without fully understanding the ELEMENTARY Lorentz Force, the mystical "Theory" of Magnetism was built - the theory of interaction of Descartes' "gimlets", which was used by Maxwell to build General Electrodynamics. This, strictly speaking, led to the uncertainty of the very concept of the Magnetic Field. So, in practice, when designing magnets, the "Theory" of Magnetism actually did not work and was used by Kirchhoff's rules based on empirical parameters. The analysis of the ELEMENTARY Electric Oscillator made it possible to unambiguously connect the IMAGINARY terms of the Complete Solution of the differential equation of the Complex Elementary Oscillator with the IMAGINARY Parameter initially introduced into its equation, which strictly corresponds to the orthogonal Electric Field - Magnetic. And this made it possible to restore the correct picture of the Magnetic Field.

*Keywords: Orthogonal Frame, Oscillator, Real Solution, Complex Solution, Orthogonal Ampere Force.*

## INVARIANT BASIS AND MAGNETISM

In modern Science, since the description of fragments on the Basis of Local, purely empirical Laws is often used, and not a single Axiomatic Approach on the BASE of a strictly established Orthogonal Frame, many contradictions have accumulated. Likewise, the Magnetic Field, widely used in modern Science and Technology, which is one of the Benchmarks, because of his imaginary "Exceptionalism" [1], there is still not even an unambiguous Definition of it. That is why specialists who use the Magnetic Field in practice invest in its understanding what is more familiar to them - either H or B. This leads to confusion in the development of magnetic materials. And for practical calculations of devices such as electromagnets on the Tokamak, and on the LHC, and in the MRI, and on magnetic levitation trains, they use technical rules of thumb from the "Theoretical Fundamentals of Electrical Engineering," which are borrowed from the design of electromagnets for loading scrap metal. So, it is not at all by chance that in the modern Theory of Magnetism there are many contradictions and inconsistencies, even such large ones as the discrepancy between the Electromagnetic and Optical Descriptions. And in work [2] the most fundamental reasons for the need for a strict Determination of the Magnetic Field were shown. But there are enough contradictions in the Classical Description of Magnetism to try to forget about entire volumes of "mental" constructions in which they tried to eliminate the contradictions in the BASIS of the modern Classical Theory of Magnetism by the method of adjustments. The BASIS must be chosen initially CONSISTENT so as not to hide behind additional Quantum Conditions in the very Definition of the Magnetic Field. Whereas theorists, claiming that without Quantization it is generally impossible to explain Magnetism, act, making a phenomenological mistake, exactly the opposite. And the age-old misconceptions in the BASICS of Quantization and the Theory of Relativity, as shown earlier, arose due to the fact that ideas about the Magnetic Field are inherent in their original form, like the "gimlets of Democritus" passing through the spiral

channels of the Earth from the "North Pole" to "South Pole". And this entailed that "gimlets" were recorded in science, even in Mathematics for hundreds of years.

But, after the bridge was thrown from Quantization to Relativity, it became obvious that one of the reasons for the fundamental difficulties is the finiteness of the speed of light, which they have in common. So, both Quantization and SRT require clarification of the BASIS, which includes the very Definition of the Magnetic Field. After all, it was this that initially demonstrated the finiteness of the speed of light. And if we start in the Definition of the Magnetic Field from Ampere's Law, which actually describes the Magnetic Force, proportional to the relative speed of electrons, then it follows that this is simply the force of interaction between MOVING charges. According to Ampere, it is positive if the charges move parallel and in one direction and negative if they move antiparallel - counter. If we recall Galileo's Principle of Relativity, then Einstein introduced a correction to SRT for charges moving relative to each other only for mass. And if for charges stationary relative to each other there is only the Coulomb force, then between moving charges, in addition to the Coulomb force, an additional force arises, perpendicular to the relative speed, proportional to the relative speed of movement of the charges. And the main question that divided scientists into two believing sects is the question of what to consider the movement of both light and a pair of charges in relation to a stationary observer or relative to the environment. But this "paradox" is also removed if initially, in strict accordance with the Principle of Causality, we take into account the finiteness of the rate of change of the Coulomb field when a charged particle is displaced. At the same time, the imaginary paradox about the absence of interaction between orthogonal coordinates is also eliminated - simply the energy for each of them is calculated through the product of collinear forces and coordinates.

## ELEMENTARY COMPLEX OSCILLATOR

In previous works, the ELEMENTARY Oscillator was analyzed on the basis of the Mechanical Oscillator. For the differential equation of this Oscillator, a Complete REAL Solution was obtained, which is of a General Character for any modifications of the Oscillator [3, 4]. And it was shown that the complex parameters artificially introduced into Newton's Partial Solution for the REAL Oscillator are purely conditional. Imaginaries can be used only under strictly specified conditions. This was simply a technical technique for approximately finding the independent real parameters of a Particular Solution on the complex plane. This purely mathematical confusion in complex Particular Solutions can, as will be shown in this paragraph, be identified and eliminated, taking into account the physical properties of the Magnetic Field.

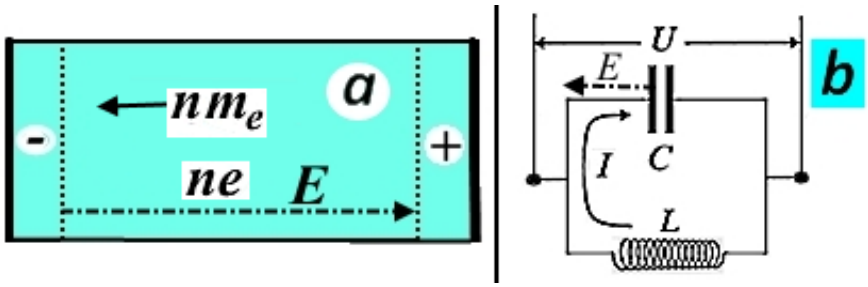


**Fig.1: Model with gravitational inertial force and electrostatic rigidity force (a) and model with magnetic inertial force (b)**

To do this, consider two different modifications of the ELEMENTARY Electric Oscillator. In one, the so-called Plasma - Basic Optical Model, which describes the reaction of free electrons to radiation (electromagnetic), the Electric Oscillator is a modified ELEMENTARY Mechanical

Oscillator, only the rigidity force for charged particles is determined not by a mechanical spring, but by the electric field created by the charges themselves displaced onto the plates (Fig. 1a). In another Basic Electrical Model of the Oscillator, built using purely empirically established technical parameters: capacitance of the capacitor and inductance of the coil, oscillations are described not in the position of charges, but in oscillations of currents in the circuit (Fig. 1b).

For comparison, the basic formulas describing these two models are given in Table 1.

**Table 1: The balance of forces or energies, previously described by one Newton harmonic, the change in the position of charges (in the Plasma model) and the change in currents (in the Skin layer model).**

| | |
|---|---|
| $F_m = m_e \cdot n \cdot a, \;\; F_\xi = -n \cdot e \cdot E = -4\pi e^2 n^2 \cdot x$ | $F_L = L\frac{d^2 J}{dt^2}, \qquad F_C = -\frac{1}{C} J$ |
| $m_e \cdot n \frac{d^2 x}{dt^2} + \xi \cdot x = 0 \Rightarrow \frac{d^2 x}{dt^2} = -\Omega^2 x$ | $L\frac{d^2 J}{dt^2} + \frac{1}{C} J = 0 \Rightarrow \frac{d^2 J}{dt^2} = -\Omega^2 J$ |
| $\xi = 4\pi e^2 n^2, \; \Omega = \sqrt{\frac{4\pi e^2 n_e}{m_e}} = 2e\sqrt{\pi \frac{n_e}{m_e}}$ | $\Omega = \sqrt{\frac{1}{LC}}, \; J = J_{\max} \mathrm{Cos}(\Omega t)$ |
| $\mathcal{E}_T = \frac{m_e \cdot n \cdot (x'[t])^2}{2}$ | $\mathcal{E}_T = \mathcal{E}_C = \frac{CU^2}{2}$ |
| $\mathcal{E}_U = \frac{4\pi e^2 n^2 \cdot (x[t])^2}{2}$ | $\mathcal{E}_U = \mathcal{E}_L = \frac{L \cdot J^2}{2}$ |

In work [5], the limits of applicability of these models were analyzed, when going beyond the limits of applicability of which a borderline "Catastrophe" appears in the description, similar to that eliminated by Planck [6]. Without realizing the very existence of this "Catastrophe" in optics, they always tried to eliminate the "errors" associated with it using the Landau smallness parameter (which, in principle, is not true for giant effects [7]). And in electrodynamics, the same approach of adjustments was veiled by the distance of electromagnetic waves from the emitter, which even tried to justify the coincidence of the phases of the electric and magnetic fields in them. The distance from the emitter of the electromagnetic wave actually hides the fact that both in the emitter itself and in the waves emitted by it there is no instantaneous disappearance of energy, which is obtained without any adjustments for the current and voltage shifted in phase by a quarter of the period, the sum of their energies is - squared amplitudes constant. The product of instantaneous (strength) current and instantaneous ("strength") voltage is not instantaneous total electrical power - it is only a technical method for determining electrical power by the product of effective (equivalent to constant) amplitudes of current and voltage.

Formally, the force balance equation of the Plasma Model (in the table on the left) can be transformed (by taking the derivative) into the equation of the Skin Layer Model (in the table on the right). But this is not the basis for the identity of these equations. This is only a manifestation of the applicability of the Principle of Logarithmic Relativity to the very model of the ELEMENTARY Oscillator for different degrees of derivatives. This "logarithmic" approach was actually used earlier when describing processes using quasiparticles. But under certain boundary conditions (frequencies), mixed vibrations can also play a significant role, for which strict separation of derivatives does not work. Planck described them with the Quantum of Energy of

resonant electromagnetic waves, but purely statistically. And in order to strictly mathematically describe mixed oscillations, it is necessary to take into account all the terms of the equation used in both models, but separately. From a comparison of the equations, it is clear that in the Plasma Model (on the left) the inertial force proportional to the current is neglected, and the force proportional to the mass of charges, which is neglected in the Skin Layer Model, can act as a kind of rigidity.

These neglects are acceptable in different oscillation frequency ranges. Since static gravitational forces are 42 orders of magnitude weaker than electrostatic forces, their comparison by order of magnitude in the equation on the left is possible only at very high frequencies, when the inertial force due to large accelerations is large. Of course, if we assume that the electric force does not depend on frequency - on the acceleration of the charge. The latter, in fact, is indicated by the fact that the Plasma Model well describes the high-frequency edge of plasma reflection by free carriers in metals and semiconductors. But to what extent the inertia of the charge itself is negligible is still an open question [8]. And an additional circumstance that helps equalize the electrical force and the force of gravitational inertia is the high concentration (total mass) of electrons in metals with a small charge that inhibits this entire mass of electrons in a volume proportional to the displacement of electrons in a thin surface layer. It should also be borne in mind that when photons are specularly reflected from a plane for free carriers, there is no real (model, perpendicular to the electric field) boundary on the plane. The role of the boundary is played by locally compressed electrons themselves - plasma waves. And the artificial creation of boundaries perpendicular to the electric field leads to the formation of a spatial Oscillator below the cutoff frequency and to diffraction effects above the cutoff frequency.

Traditionally, the introduction of a term proportional to velocity into the Oscillator equation means friction, the contribution of which, as is known, determines the damping of oscillations. Valid Solutions for the ELEMENTARY Oscillator. Modifications of the ELEMENTARY Oscillator equation to take into account additional forces were carried out earlier, but due to a parametric change in the rigidity force [9]. Those. an influence orthogonal to the forces traditionally used in balance was implicitly implied. But the Orthogonal Force, initially believed, does not produce work (although in reality the force and displacement for each coordinate separately should be collinear). The zero-energy coupling of forces clearly violated Logic, but qualitatively the model of a parametric Oscillator made it possible to describe a number of effects. Although, formally, using Mathieu functions, it did not provide an answer to the Physical Question, and the observed absorption at the vibration frequency along the wave vector of light (Fig. 2) indicated the exchange of energy between normal vibrations in anisotropic crystals [10].

In a rhombohedral boron nitride single crystal, when light propagates along the symmetry axis C, in the transmission spectrum, in addition to the normal absorption band in the frequency range of optical phonons polarized perpendicular to the C axis $\omega_L^{\perp C} \div \omega_T^{\perp C}$ , a non-transmission band anomalous in frequency $\omega_L^{IIC} \div \omega_T^{IIC}$ and shape was discovered.

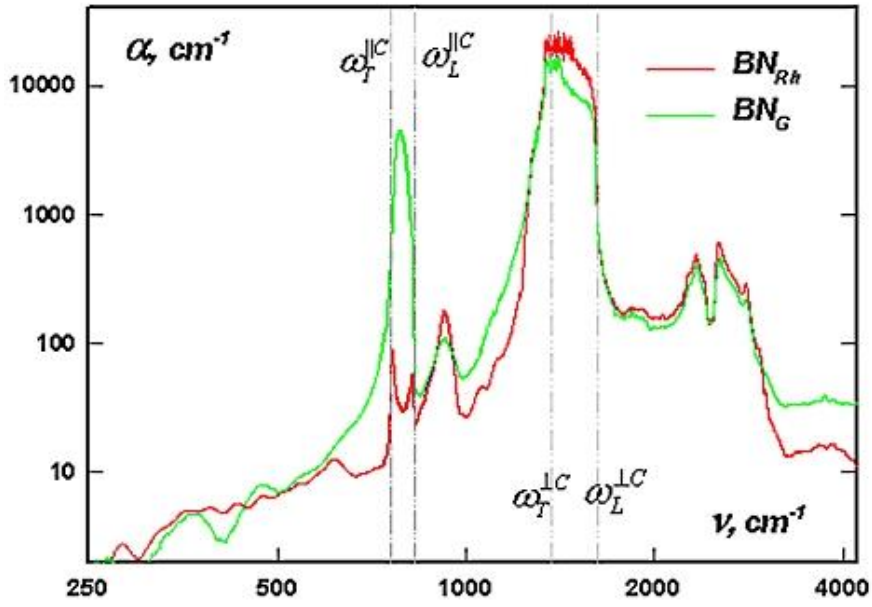


**Fig.2: IR absorption spectra of rhombohedral and hexagonal (with disordered crystallites) boron nitride measured at normal incidence of unpolarized radiation on plates perpendicular to the C axis.**

In the absorption spectrum of a weakly ordered textured sample of hexagonal boron nitride shown in Fig. 2, in which the C axis of its crystallites is deviated from the wave vector of light, the classical crystal-optical contribution to the absorption of vibrations along the C axis appears in the form of a normal absorption band between the transverse and longitudinal vibrations corresponding to interlayer vibrations. phonons. Whereas for a highly ordered single crystal of rhombohedral boron nitride, instead of this usual absorption band, only scattering peaks are observed at phonon frequencies, the polarization of which is orthogonal to the polarization of IR radiation.

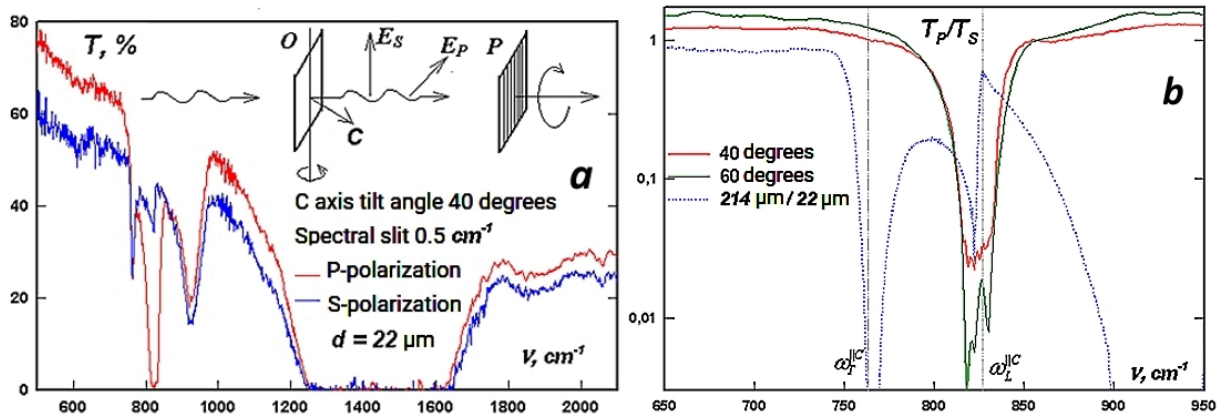


**Fig.3: Dependence of the ratio of the P- and S-components of unpolarized radiation transmitted through an oriented sample of rhombohedral boron nitride on the thickness of the sample and on the angle of rotation of the C axis relative to the wave vector of light.**

The inset to Fig. 3 shows the setup of a polarization experiment to analyze the P- and S-components when the C axis of rhombohedral boron nitride deviates from the direction of light propagation.

Precision polarization measurements of highly ordered crystals of rhombohedral boron nitride presented in Fig. 3 made it possible to associate the anomalous stopband in it with scattering by orthogonal vibrations. And although this did not give a direct answer to the question of the reverse transfer of energy between them, it nevertheless indicated the incompleteness of the description of the Causality Principle by the Kramers-Kronig relation without taking into account the contribution of orthogonal oscillations, at least scattering by them.

But in an electromagnetic wave, not just scattering occurs, but energy transfer between orthogonal oscillations. And from a comparison of the Models of two Electric Oscillators and their equations (Table 1) it is clear that in both of them, separately, this is not taken into account. The Plasma Model does not take into account the Inertia of Current, and the Electrical Model does not take into account the Inertia of Mass, which, as noted above, is permissible only within the limits determined by the limits of applicability of the models.

And, at the same time, since it is ignored that the unaccounted orthogonal terms are directly related to the exchange of energy between orthogonal oscillations, we will not complicate the existing Oscillator models with additional terms. For now, we will limit ourselves to considering a fundamentally new Electric Oscillator with an additional, previously unaccounted for member. And the introduced new Reactive Force orthogonal to the Electric Field, proportional to the speed (current), will be taken into account using IMAGINITY. So let's consider another modification of the ELEMENTARY Oscillator - the Complex Electric Ideal Oscillator based on the balance of only two orthogonal forces.

In this simplest model case, we obtain the balance equation of the Real Electrical Force and the Imaginary Magnetic Force orthogonal to it. In this case, we have the Oscillator equation for the Real and Imaginary (orthogonal to the Electric Force) charge displacement, standardly excited by a single initial condition:

$$\mathrm{i}\gamma x'[t]+x[t]=0,\quad x[0]=1 \tag{1}$$

$$x=\cos\left[\frac{1}{\gamma}t\right]+\mathrm{i}\sin\left[\frac{1}{\gamma}t\right],\qquad \Omega=\frac{1}{\gamma} \tag{2}$$

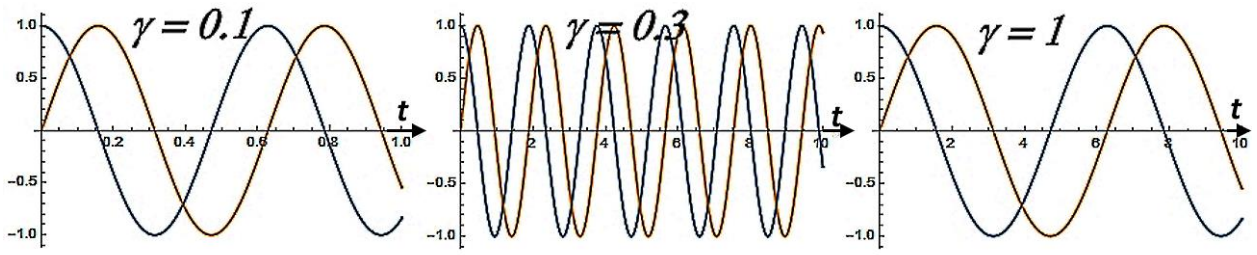


**Fig.4: Associated resonant oscillations of two Orthogonal Forces, the single frequency of oscillations of which is determined by the reactive connection of these Forces.**

The considered simplest equation with reactive "friction" actually gives oscillations of two orthogonal forces even at zero gravitational mass. And it corresponds to oscillations of two orthogonal forces exchanging energy, which is what happens in an electromagnetic wave, without any instantaneous loss of energy.

For simplicity, the solution of the equation with the reactive coupling coefficient at a unit stiffness coefficient was obtained. If we return to the designations of the coefficients of the equation from Table 1, it will become clear that the natural oscillation frequency of the Complex Oscillator is equal to the ratio of the reactive damping coefficient to the stiffness coefficient (without the square root, as for the Real Oscillator):

$$\mathrm{i}\beta x'[t]+\xi x[t]=0\Rightarrow \mathrm{i}x'[t]+\frac{\xi}{\beta}x[t]=0\Rightarrow \Omega=\frac{\xi}{\beta}\Leftrightarrow\frac{1}{\gamma} \qquad (3)$$

Now let's consider the action on the Ideal Complex Oscillator of a single driving Force. But first, let us recall that its action on the ACTUAL Oscillator:

$$x''[t]+\Omega^2*x[t]=\sin[t\omega],\quad x[0]=0,\quad x'[0]=0 \qquad (4)$$

manifests itself in the fact that a driving force of any frequency excites in the Real Oscillator both oscillations at the frequency of the driving force (Newton's harmonic) and oscillations at its own resonant frequency:

$$x[t]=\frac{\Omega\sin[t\omega]-\omega\sin[t\Omega]}{-\omega^2\Omega+\Omega^3}=\frac{1}{-\omega^2+\Omega^2}\sin[t\omega]-\frac{\omega}{-\omega^2\Omega+\Omega^3}\sin[t\Omega] \qquad (5)$$

And these two harmonics have different dependences, shown in Fig. 5, on the frequency of the driving force, where the resonant frequency is taken as a unit of frequency measurement.

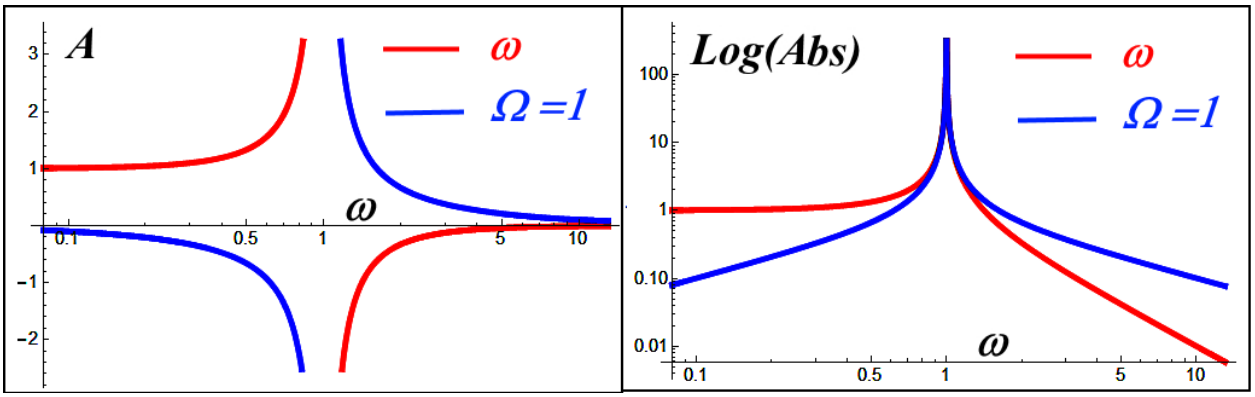


**Fig.5: Frequency dependences of the amplitudes (left) and amplitude modulus (right) of Newton's harmonics (red curves) and oscillations at the resonant frequency (blue curves).**

For an Ideal Complex Oscillator (with purely reactive friction, in accordance with formula (3), the action of a single driving force is described by the expression:

$$\mathrm{i}\cdot x'[t]+\Omega\cdot x[t]=\sin[\omega\cdot t],\quad x'[0]=0 \qquad (6)$$

In this case, for the Ideal Complex Oscillator we obtain the same as for the Ideal Real Oscillator. solution from two harmonics, but for both the real and imaginary parts of the oscillations. In this

case, both Imaginary harmonics are shifted relative to the corresponding Real harmonic by a quarter of the period:

$$x = \mathrm{i}\left(-\frac{\omega\cos[t\omega]}{-\omega^2+\Omega^2}+\frac{\omega\cos[t\Omega]}{-\omega^2+\Omega^2}\right)+\frac{\Omega\sin[t\omega]}{-\omega^2+\Omega^2}-\frac{\omega\sin[t\Omega]}{-\omega^2+\Omega^2}= \\ =\left(\frac{\Omega\sin[t\omega]}{-\omega^2+\Omega^2}-\mathrm{i}\frac{\omega\cos[t\omega]}{-\omega^2+\Omega^2}\right)-\left(\frac{\omega\sin[t\Omega]}{-\omega^2+\Omega^2}-\mathrm{i}\frac{\omega\cos[t\Omega]}{-\omega^2+\Omega^2}\right) \tag{7}$$

Taking, for clarity, the resonant frequency and amplitude of the driving force as unity, we obtain the dependences on the frequency of the driving force of the amplitudes of real and imaginary oscillations of the Ideal Complex Oscillator, both at the frequency of the driving force (Fig. 6, left) and at the resonant frequency (Fig. 6, on right):

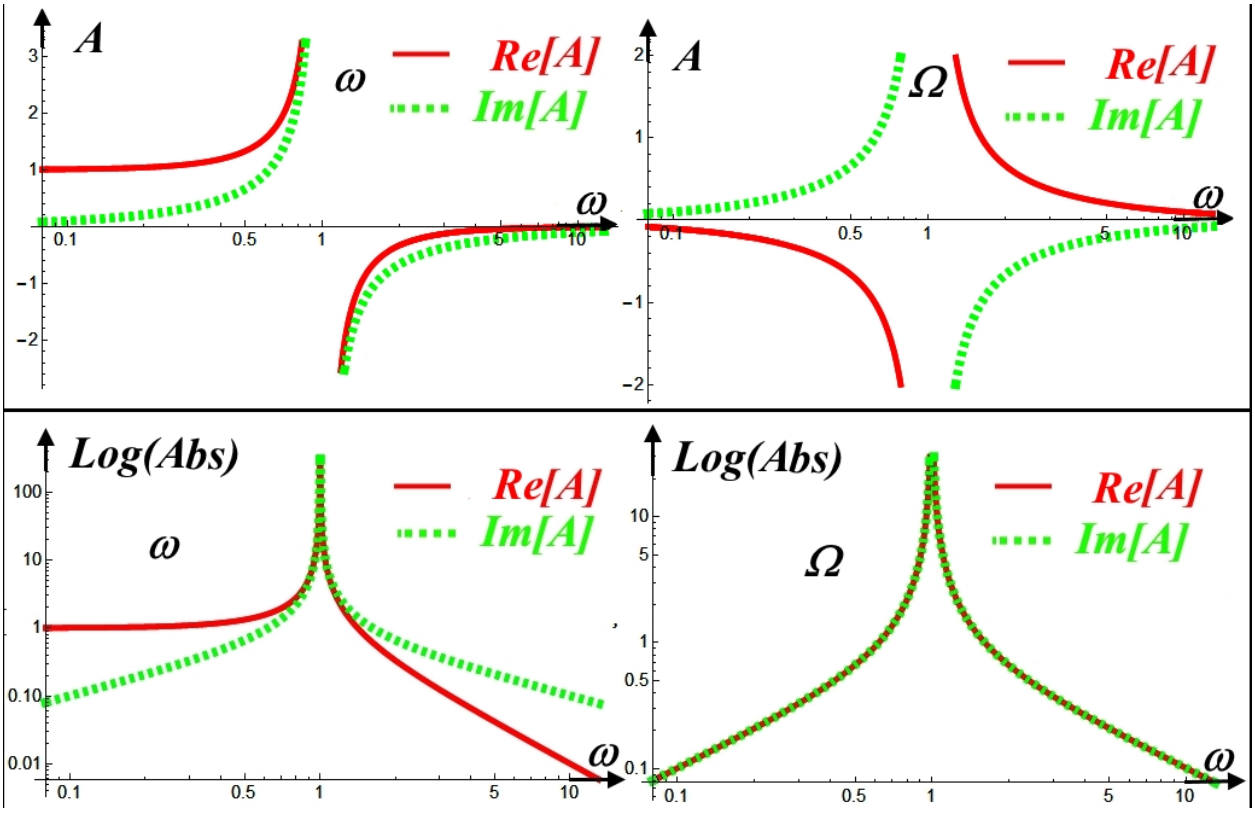


**Fig.6: Frequency dependences of the harmonic amplitudes of the Complex Ideal Oscillator.**

In a simplified notation with a single resonant frequency, instead of expression (6) we have:

$$\mathrm{i}\gamma x'[t]+x[t]=\sin[t],\quad x'[0]=0 \tag{8}$$

and we obtain the relative change in the harmonics of the Complex Ideal Oscillator), similar to formula (2):

$$\mathrm{x}=\mathrm{i}\left(-\gamma\cos[t]/\left(1-\gamma^2\right)+\gamma\cos\left[\frac{t}{\gamma}\right]/\left(1-\gamma^2\right)\right)+\sin[t]/\left(1-\gamma^2\right)-\gamma\sin\left[\frac{t}{\gamma}\right]/\left(1-\gamma^2\right) \tag{9}$$

For Real harmonics this change, similar to Fig.4, is shown in Fig.7.

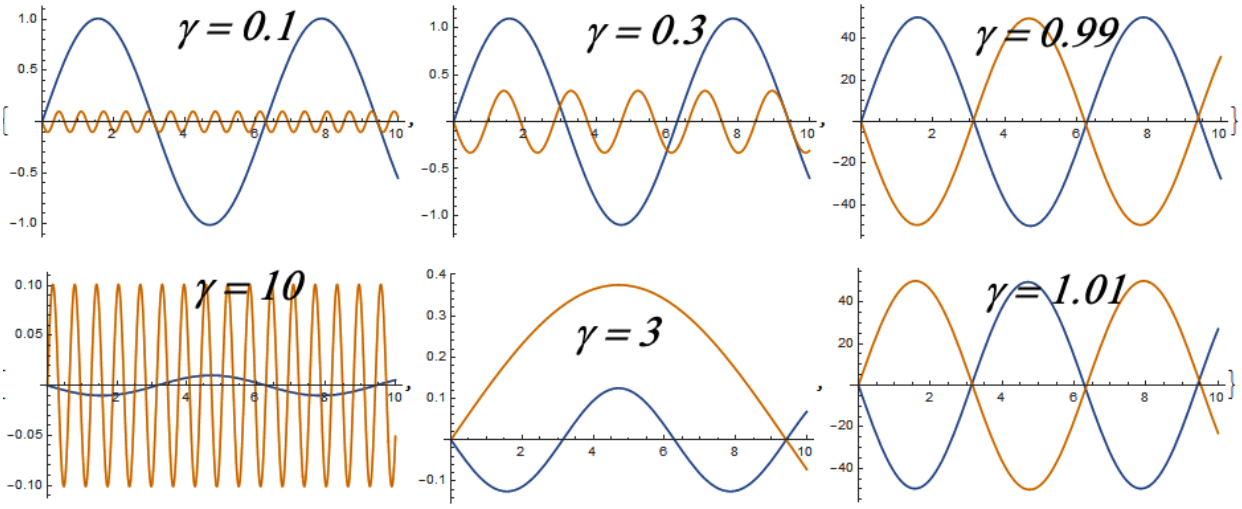


**Fig.7: Relative change in the Real harmonics of the Complex Oscillator.**

Changes in the Imaginary (shifted by a quarter of the period relative to the Real) harmonics of the Complex Oscillator are also obtained similar to those shown in Fig. 7.

Thus, we obtain for the Ideal Complex Oscillator and under the influence of the driving force of the pair, exchanging oscillation energy. Moreover, each of these two pairs consists of a Real oscillation along the Oscillator axis and an "Imaginary" oscillation orthogonal to the Real oscillation, phase-shifted by a quarter of the period. And the "imaginary" arose earlier from orthogonality, and not due to the fact that the Magnetic Force is not the interaction of Descartes' "gimlets", simply mathematized by Maxwell.

## CONCLUSIONS

Purely technically, the analysis shows that the true "IMAGINARY" (in the sense of orthogonal) Solutions strictly correspond to the IMAGINARY term initially introduced into the differential equation, corresponding to the Magnetic Field, orthogonal to the Electric Field, but exchanging energy with it. Thus, a qualitatively described mechanism of the formation of the Magnetic Field can also be described on the basis of the ELEMENTARY OSCILLATOR Model, cleared of the husk of "Imaginary" solutions for the Real Oscillator, but supplemented with an imaginary term strictly corresponding to the ORTHOGONALITY of the Forces, the balance of which leads to a set of interconnected oscillations. Elimination of this confusion with IMAGINES allowed us to make a correct macroscopic Redefinition of the Magnetic Field.

## REFERENCES

1. Stanislav Ordin, "Exceptionality Exclusion: Bridging Quantization and Relativity ", Global Journal of Science Frontier Research: A, Physics and Space Science Volume 24 Issue 2 Version 1.0 Year 2024, p. 5-65. Publisher: Global Journals. Online ISSN: 2249-4626 & Print ISSN: 0975-5896. DOI: 10.17406/GJSFR, GJSFR-A Classification: LCC: QC174.12 https://globaljournals.org/GJSFR_Volume24/5-EXCEPTIONALITY-EXCLUSION.pdf

2. Stanislav Ordin, "Reasons for Redefining the Magnetic Field ", the Journal of Electromagnetic Analysis and Applications (JEMAA), Vol.15 No.5, May 31, 2023. DOI: 10.4236/jemaa.2023.155005, ISSN Print: 1942-0730, ISSN Online: 1942-0749, Scientific Research an Academic Publisher, Manuscript ID: 9801938, Submission Time: 2024-02-01 09:27:44, DOI: 10.4236/jemaa.2023.156006

3. Stanislav Ordin, Review Article, "Non-Elementary Elementary Harmonic Oscillator", American Journal of Materials & Applied Science (AJMAS), Volume 3 Issue 1, Published date: 03/08/2021, Pages: 003-008/, https://www.scireslit.com/MaterialScience/AJMAS-ID14.pdf

4. Stanislav Ordin, "Comprehensive Analysis of the ELEMENTARY Oscillator", the Journal of Electromagnetic Analysis and Applications (JEMAA), ISSN Print: 1942-0730, ISSN Online: 1942-0749, Scientific Research An Academic Publisher, Manuscript ID: 9801939, Submission Time: 2024-02-01 09:36:26, DOI: 10.4236/jemaa.2023.156006
Stanislav Ordin, manuscript "ID: MTT24FEB002, Title: «Comprehensive Analysis of the ELEMENTARY Oscillator» has been "Accepted for Publication" in SSRG-International Journal of Mathematics Trends and Technology – (IJMTT)", ISSN: 2231-5373.

5. Ordin S.V., "Impedance of Skin-Plasma Effect", International Journal of Research Studies in Electrical and Electronics Engineering (IJRSEEE), Volume 6, Issue 3, 2020, PP 25-39, ID 2120011, ISSN 2454-9436 (Online), ISSN: 2301-380X (print). DOI: http://dx.doi.org/10.20431/2454-9436.0603003

6. Stanislav Ordin, "Planckian Expansion of the Heaviside Impedance", website of the Nanotechnological Society of Russia, published 12/14/2020, - http://rusnor.org/pubs/articles/18085.htm

7. S.V. Ordin, in Book: Optical Lattices: Structures, Atoms and Solitons, "Giant spatial dispersion in the region of plasmon-phonon interaction in one-dimensional- incommensurate crystal the higher silicide of manganese (HSM)", Editors: Benjamin J. Fuentes, Nova Sc. Publ. Inc., 2011, pp. 101-130. ISBN: 978-1-61324-937-6, Series: Lasers and Electro-Optics Research and Technology, Physics Research and Technology, Binding: Hardcover, Pages: 241.pp, Status: AV

8. Ordin S.V., «Newton's Coulomb Laws», Global Journal of Science Frontier Research- Physics & Space Science (GJSFR-A), 2019 Vol.19 Issue 1 Version 1.0, p. 145-155.
https://globaljournals.org/GJSFR_Volume19/E,Journal_GJSFR_(A)_Vol_19_Issue_1.pdf

9. Ordin, S.V., «Parametrically excited Anharmonic Oscillator», Global Journal of Science Frontier Research - Physics & Space Science, GJSFR-A Volume 19 Issue 3 Version 1.0 p.133-144,
https://globaljournals.org/GJSFR_Volume19/7-Parametrically-Excited.pdf

10. Ordin S.V., Sokolov I.A, Zjuzin A.J., «Parametrical Interaction of Normal Oscillations in anisotropic crystals», the Physico-Technical institute of A.F. Ioffe of the Russian Academy of Sciences, St.-Petersburg, Russia, Proceedings of X interstate seminar: Thermoelectrics and their application, on November, 14-15th 2006, p.144-149.

Applied Sciences Research Periodicals – ISSN 3033-330X
May 2024, Vol. 2, No. 5, pp. 11-42.

# Feedback Functions in Problems Minimax Search

A. E. Umnov & E.A. Umnov

1. Moscow Institute of Physics and Technology (National Research University) 9 Institutskiy per., Dolgoprudny, Moscow Region, 141701, Russian Federation

**Abstract:**
This paper considers a method for obtaining a smooth approximation of the maximum function. Some generalizations of this approach are suggested, including formulas for minimax, maximin and their combinations. The resulting error is estimated and ways to reduce it are indicated. The proposed method uses functions that establish feedback links between primary and dual variables of the Lagrange function. These links are similar to the Karush-Kuhn-Tucker theorem, but without conditions of non-negativity or complementary non-rigidity. To illustrate the proposed method, task of searching for global extremum, estimation of the minimax value and an example from game theory are considered.

*Keywords: maximum function, multiple extremum, minimax, feedback function method, modified Lagrange function, game theory problems.*

## INTRODUCTION

This article discusses the tasks the basis of which is the search for minimax:

$$\begin{aligned} &\text{find} \quad \min_{y\in \mathrm{Y}} \max_{x\in\Theta_y} F(x,y)\,, \\ &\text{where} \quad x=(x_1x_2,\ldots,x_n)^{\mathrm{T}}\in E^n, \quad \Theta_y:\ (\,x\mid f_i(x,y)\le 0 \ \ \forall i=\overline{1,m}\,) \\ &\text{and} \quad y=(y_1y_2,\ldots,y_K)^{\mathrm{T}}\in \mathrm{Y}\subseteq E^K. \end{aligned} \tag{1.1}$$

This problem obviously comes down to a two-level system of tasks. At the lower level the problem is solved parametric programming of the form:

$$\begin{aligned} &\text{maximized} \quad F(x,y) \quad by\ x=(x_1x_2,\ldots,x_n)^{\mathrm{T}}\in E^n \\ &\text{for a fixed vector of parameters}\ \ y=(y_1y_2,\ldots,y_K)^{\mathrm{T}}\in \mathrm{Y}\subseteq E^K \\ &\text{under conditions} \quad x\in\Theta_y: \quad (\,x\mid f_i(x,y)\le 0 \ \ \forall i=\overline{1,m}\,). \end{aligned} \tag{1.2}$$

At the lower level the problem is solved

$$\text{minimized} \quad F(x_y^*,y) \quad by \ \ y=(y_1y_2,\ldots,y_K)^{\mathrm{T}}\in \mathrm{Y}. \tag{1.3}$$

Where vector $x_y^*$ is dependence of $\arg\max_{x\in\Theta_y} F(x,y)$ on $y$.

We will also assume that the functions $F(x,y)$, $f_i(x,y)\le 0 \ \ \forall i=\overline{1,m}$ have continuous derivatives with respect to all to its arguments up to the second order inclusive.

Problems (1.2) --- (1.3), as well as those reducible to them, were considered in large numbers research. A detailed overview of these works can be found, for example, in [Izmailov, 2006].

The main obstacles complicating the decision problem (1.3), are created by the following properties dependencies $x_y^*$

- domain of definition for the dependence $x_y^*$ may *be narrower* (by *y*) than domains for functions $F(x,y)$, $f_i(x,y) \le 0 \ \ \forall i = \overline{1,m}$ ;
- dependency $x_y^*$ may be *ambiguous*, i.e., *non-functional*;
- dependency $x_y^*$ maybe function, but *non-differentiable*.

It is clear that all these properties arise from inequalities in the constraints of problem (1.2).

A large number of algorithms are known solving problems (1.2) --- (1.3) using non-differentiable optimization methods and tools of sensitivity theory, e.g. [Danskin, 1967], [Fiacco, 1983], [Rockafellar, 1970], [Demyanov, Vasiliev, 1972], [Nurminsky, 1991], [Izmailov, 2006]. Such algorithms make it possible to overcome computational difficulties caused by features of the dependence $x_y^*$.

At the same time, there are methods for solving problems (1.2) --- (1.3), based on classical Taylor expansions. To date, options such algorithms have been proposed, for example, in [Fiacco, McCormic, 1968], [Germeyer, 1969], [Umnov, 2018]. This article discusses an approach related to the second direction.

Suggested method is based on smooth function $\bar{x}(\tau, y)$, which approximates the dependence $x_y^*$ . That is, such a function for which equality $\lim\limits_{\tau \to +0} F\left(\bar{x}(\tau, y), y\right) = F(x_y^*, y)$ is valid $\forall y \in \mathrm{Y}$ . If $x_y^*$ is unambiguous the last equality is replaced by $\lim\limits_{\tau \to +0} \bar{x}(\tau, y) = x_y^*$. Moreover, the proposed approximation allows to overcome all the computational difficulties noted above. Specifically, as $\bar{x}(\tau, y)$ it is proposed to use saddle point, modified in a special way, Lagrange functions for problem (1.2). This specificity is such that existence, functionality and smoothness for $\bar{x}(\tau, y)$ are guaranteed $\forall y \in \mathrm{Y}$ .

The proposed function $\bar{x}(\tau, y)$ is defined implicitly. However, the use the classical theorem on the system of implicit functions allows us to overcome this difficulty and build for $\bar{x}(\tau, y)$ Taylor polynomials of the required orders.

In what follows, for brevity, the procedure for modifying the Lagrange function and searching for its saddle points is called as a *method of feedback functions*.

For linear problem (1.2) this method described and justified in [Umnov, 2019]. The nonlinear case is considered in [Umnov, 2022, 2023]. Here is the use of this approach demonstrated by examples:

- searching for the global extremum of functions of several variables,
- calculations of minimax and/or maximin,
- solving some types of game theory problems.

## FEEDBACK FUNCTIONS: DEFINITION AND PROPERTIES

For greater clarity First let's demonstrate the use feedback function method for the linear case. Let's consider the problem

$$F(x)=\sum_{j=1}^{n}\sigma_j x_j \to \max \quad x\in E_+^n \qquad \text{under conditions} \qquad f_i(x)=-\beta_i+\sum_{j=1}^{n}\alpha_{ij}x_j\le 0 \quad \forall i=\overline{1,m}, \tag{2.1}$$

where $\sigma_j,\beta_i,\alpha_{ij}\ \forall j=\overline{1,n},\forall i=\overline{1,m}$ are constants. Here $E_+^n$ is non-negative orthant of the Euclidean space $E^n$. Then the dual problem to (2.1) looks like

$$G(\lambda)=\sum_{i=1}^{m}\beta_i\lambda_i \to \min \quad \lambda\in E_+^m \quad \text{under conditions} \qquad g_j(\lambda)=-\sigma_j+\sum_{i=1}^{m}\alpha_{ij}\lambda_i\ge 0 \quad \forall j=\overline{1,n}, \tag{2.2}$$

where $\lambda=(\lambda_1,\lambda_2,\ldots,\lambda_m)^{\mathrm{T}}$. The solution of (2.2) we will denote by $\lambda^*=(\lambda_1^*,\lambda_2^*,\ldots,\lambda_m^*)^{\mathrm{T}}$.

Feedback function method to solve problems (2.1) --- (2.2) consists in replacing them with a system of equations

$$\begin{cases} -\beta_i+\sum_{j=1}^{n}\alpha_{ij}\bar{x}_j=Q\left(\tau,\bar{\lambda}_i(\tau)\right) & \forall i=\overline{1,m}, \\ \sigma_j-\sum_{i=1}^{m}\alpha_{ij}\bar{\lambda}_i=Q\left(\tau,\bar{x}_j(\tau)\right) & \forall j=\overline{1,n}. \end{cases} \tag{2.3}$$

Here the function $Q(\tau,s)$ has the following properties.

- 2–1°. $Q(\tau,s)$ defined for $\tau>0$, strictly monotonically increases in *s* and at the same time for any fixed $\tau$ $\lim\limits_{s\to+0}Q(\tau,s)=-\infty$, $\lim\limits_{s\to+\infty}Q(\tau,s)=+\infty$.
- 2–2°. $\forall s>0$ $\lim\limits_{\tau\to+0}Q(\tau,s)=0$ and this passage to the limit uniform by s on $s\in[\varepsilon_0,+\infty)\ \forall\varepsilon_0>0$.
- 2–3°. In the area of definition function $Q(\tau,s)$ is continuously differentiable with respect to the totality of all its arguments.

In [Umnov, 2019] it is shown that with such properties of the function $Q(\tau,s)$, system (2.3) has a unique solution $\left\{\bar{x}(\tau),\bar{\lambda}(\tau)\right\}$ for any fixed $\tau>0$. Structure of the system (2.3) justifies the use for $Q(\tau,s)$ term feedback function.

Moreover, if $\left|F^*\right|<+\infty$, then for vector functions $\left\{\bar{x}(\tau)\right\}$ and $\left\{\bar{\lambda}(\tau)\right\}$ equalities are valid $\lim\limits_{\tau\to+0}F\left(\bar{x}(\tau)\right)=F^*=\lim\limits_{\tau\to+0}G\left(\bar{\lambda}(\tau)\right)$. In the case when the vectors $x^*$ and $\lambda^*$ are *unique*, then $\lim\limits_{\tau\to+0}\bar{x}(\tau)=x^*$ and $\lim\limits_{\tau\to+0}\bar{\lambda}(\tau)=\lambda^*$. Note also that the system of equations (2.3) due to the condition 2---1° can also be written as

$$\begin{cases} \overline{\lambda}_i(\tau) = \mathrm{inv}Q\left(\tau, -\beta_i + \sum_{j=1}^{n} \alpha_{ij}\overline{x}_j\right) & \forall i = \overline{1,m}, \\ \overline{x}_j(\tau) = \mathrm{inv}Q\left(\tau, \ \sigma_j - \sum_{i=1}^{m} \alpha_{ij}\overline{\lambda}_i\right) & \forall j = \overline{1,n}. \end{cases}$$

The function $\mathrm{inv}Q(\tau,s)$ is inverse to the function $Q(\tau,s)$. $\mathrm{inv}Q(\tau,s)$ is defined $\forall \tau > 0$ positive and increases monotonically in *s* on the entire real axis. All together this means that the vector functions $\overline{x}(\tau)$ and $\overline{\lambda}(\tau)$ can be used as an approximation of solutions to problems (2.1) and (2.2) at $\tau \to +0$.

Let us illustrate this statement with the following example.

**Example 2.1. For Tasks**

- Direct Problem: maximize in $E^2$ the function $2x_1 + 3x_2$ , under conditions $x_1 \geq 0, \quad x_2 \geq 0$ and $x_1 + 2x_2 \leq 6, \quad 2x_1 + x_2 \leq 6$ ;
- Dual Problem: minimize in $E^2$ the function $6\lambda_1 + 6\lambda_2$ , under conditions $\lambda_1 \geq 0, \quad \lambda_2 \geq 0$ and $\lambda_1 + 2\lambda_2 \geq 2, \quad 2\lambda_1 + \lambda_2 \geq 3$ .

Their solutions will be $x_1^* = 2, \quad x_2^* = 2, \quad F^* = 10$ and $\lambda_1^* = \frac{4}{3}, \quad \lambda_2^* = \frac{1}{3}, \quad G^* = 10$ .

If you use $Q(\tau,s) = \tau \ln s$ then system (2.3) will have the form

$$\begin{cases} -6 + \overline{x}_1 + 2\overline{x}_2 = \quad \tau \ln \overline{\lambda}_1, \\ -6 + 2\overline{x}_1 + \overline{x}_2 = \quad \tau \ln \overline{\lambda}_2, \\ -2 + \overline{\lambda}_1 + 2\overline{\lambda}_2 = -\tau \ln \overline{x}_1, \\ -2 + 2\overline{\lambda}_1 + \overline{\lambda}_2 = -\tau \ln \overline{x}_2. \end{cases}.$$

Its solutions for different values of the parameter $\tau$ are given in Table. 2.1.[1]

**Table 2.1.**

| $\tau$ | $\overline{x}_1(\tau)$ | $\overline{x}_2(\tau)$ | $F(\overline{x}(\tau))$ | $\overline{\lambda}_1(\tau)$ | $\overline{\lambda}_2(\tau)$ | $G(\overline{\lambda}(\tau))$ |
|---|---|---|---|---|---|---|
| $10^{-1}$ | 1.91387303 | 2.05644660 | 9.99708585 | 1.30690566 | 0.31409072 | 9.72597830 |
| $10^{-2}$ | 1.99167722 | 2.00559101 | 10.0001275 | 1.33099033 | 0.33105995 | 9.97230168 |
| $10^{-3}$ | 1.99917130 | 2.00055811 | 10.0000169 | 1.33310196 | 0.33310265 | 9.99722768 |
| $10^{-4}$ | 1.99991717 | 2.00005580 | 10.0000017 | 1.33331023 | 0.33331023 | 9.99972274 |
| $10^{-5}$ | 1.99999172 | 2.00000558 | 10.0000002 | 1.33333102 | 0.33333102 | 9.99997227 |
| $10^{-6}$ | 1.99999917 | 2.00000056 | 10.0000000 | 1.33333310 | 0.33333310 | 9.99999723 |

[1] To check the results, the authors recommend using formula (6.1) given in the Conclusion. In this case, the calculations will depend less on the choice of initial approximations.

Let us now move on to the nonlinear case. It is easy to verify that system (2.3) gives stationarity conditions auxiliary function

$$U(\tau,x,\lambda)=\left(\sum_{j=1}^{n}\sigma_j x_j - R\left(\tau,x_j\right)\right)+\left(\sum_{i=1}^{m}\beta_i\lambda_i + R\left(\tau,\lambda_i\right)\right)-\sum_{j=1}^{n}\sum_{i=1}^{m}\alpha_{ij}x_j\lambda_i\,, \qquad (2.4)$$

Where $R(\tau,s)=\int_{\kappa(\tau)}^{s}Q(\tau,v)\,dv$ and the value of $\kappa(\tau)$ is found from the equation $Q(\tau,\kappa(\tau))=0$. This equation has (and, moreover, the only) solution $\forall\tau>0$. Indeed, the function $Q(\tau,s)$ strictly monotonically increasing in *s* and not limited both below and above $\forall s\in\left(0,+\infty\right)$.

Function (2.4) can be interpreted like some modification of the Lagrange function. Really,

$$U(\tau,x,\lambda)=L\left(x,\lambda\right)-\sum_{j=1}^{n}R\left(\tau,x_j\right)+\sum_{i=1}^{m}R\left(\tau,\lambda_i\right), \qquad (2.5)$$

where $L\left(x,\lambda\right)$ – regular Lagrange function of problem (2.1) [*Bazaraa*, 2006], [*Bertsekas*, 2016], having the form

$$L(x,\lambda)=\sum_{j=1}^{n}\sigma_j x_j-\sum_{i=1}^{m}\lambda_i\left(-\beta_i+\sum_{j=1}^{n}\alpha_{ij}x_j\right)\qquad\Rightarrow\qquad L(x,\lambda)=F(x)-\sum_{i=1}^{m}\lambda_i f_i(x)\,.$$

This form of recording Lagrange functions for problem (2.1) does not depend on whether the functions are linear $F(x)$, $f_i(x)\ \forall i=\overline{1,m}$ or not. Therefore (2.5) can be used as definition auxiliary function $U\left(\tau,x,\lambda\right)$ for a nonlinear problem.

$$F(x)\to\max\quad x\in E_+^n\qquad\text{under conditions}\qquad f_i(x)\le 0\quad\forall i=\overline{1,m}. \qquad (2.6)$$

In what follows we will assume that the functions $F(x)$ and $f_i(x)\ \forall i=\overline{1,m}$ have continuous derivatives with respect to all their arguments up to the second order inclusive.

Let's consider the conditions of applicability feedback functions to find a local solution to problem (2.6) with finite value $F^*$ and maybe with not a single point $x^*$ such that that $F^*=F(x^*)$. We will also assume that in the problem under consideration the Lagrange function is regular, and there are also compact, with non-empty interior of the set $\Omega_x\subset E^n$ and $\Omega_\lambda\subset E^m$, for which there is at least one pair of vectors $x^*\in\Omega_x$ and $\lambda^*\in\Omega_\lambda$, such that $L\left(x^*,\lambda^*\right)=F^*$.

Let the function feedbacks $Q\left(\tau,s\right)$ defined $\forall\tau>0$ and $\forall s\in\left(0,+\infty\right)$ and has the properties 2-1°, 2-2° and 2-3°. From the definition of $R\left(\tau,s\right)$ it also follows that $Q(\tau,s)=\frac{\partial R}{\partial s}\left(\tau,s\right)$.

In the future it will be convenient to use a more general formulation of the problem (2.6). We will assume that the conditions $x_j\ge 0$ are not available for all $\forall j=\overline{1,n}$, but only for the first $q\le n$ or

are absent altogether. In addition, let us assume that in formulation (2.6) there are only $p \le m$ restrictions type <<inequality>> and the rest are of the <<equality>> type.

That is, the nonlinear programming problem is considered:

$$\begin{array}{lll} F(x) \to \max & x \in E^n & \\ \text{under conditions} & x_j \ge 0 & \forall j = \overline{1,q}, \\ & f_i(x) \le 0 & \forall i = \overline{1,p}, \\ & f_i(x) = 0 & \forall i = \overline{p+1,m}. \end{array} \tag{2.7}$$

Then, taken by definition, the auxiliary function will look like

$$U(\tau, x, \lambda) = L(x, \lambda) - \sum_{j=1}^{q} R(\tau, x_j) + \sum_{i=1}^{p} R(\tau, \lambda_i), \tag{2.8}$$

where case $q = 0$ or $p = 0$ means the absence of corresponding terms in (2.8).

In [Umnov, 2022] it is shown that under the assumptions made above the following statements are true.

***Theorem 2.1:***
If the function $U(\tau, x, \lambda)$ has saddle point $\{\bar{x}(\tau), \bar{\lambda}(\tau)\}$ inside $\Omega_x \otimes \Omega_\lambda$ then the vectors $\bar{x}(\tau)$ and $\bar{\lambda}(\tau)$ are solutions to the system of equations

$$\begin{cases} \operatorname{grad}_x U(\tau, \bar{x}, \bar{\lambda}) = o, \\ \operatorname{grad}_\lambda U(\tau, \bar{x}, \bar{\lambda}) = o. \end{cases} \tag{2.9}$$

In coordinates system (2.9) has the form

$$\begin{cases} \dfrac{\partial F}{\partial x_j} - \sum\limits_{i=1}^{m} \bar{\lambda}_i(\tau) \dfrac{\partial f_i}{\partial x_j} = Q(\tau, \bar{x}_j(\tau)) & \forall j = \overline{1,q}, \\ \dfrac{\partial F}{\partial x_j} - \sum\limits_{i=1}^{m} \bar{\lambda}_i(\tau) \dfrac{\partial f_i}{\partial x_j} = 0 & \forall j = \overline{q+1,n}, \\ f_i(\bar{x}_j(\tau)) = -Q(\tau, \bar{\lambda}_i(\tau)) & \forall i = \overline{1,p}, \\ f_i(\bar{x}_j(\tau)) = 0 & \forall i = \overline{p+1,m}. \end{cases} \tag{2.10}$$

The structure of system (2.10) is similar to the conditions of the Karush-Kuhn-Tucker theorem, but does not contain explicit conditions non-negativity of Lagrange multipliers and conditions of complementary non-rigidity.

Vector functions $\bar{x}(\tau)$ and $\bar{\lambda}(\tau)$ set parametrically in $\Omega_x \otimes \Omega_\lambda$ a line, which we will call saddle point trajectory of the problem (2.7).

***Theorem 2.2:***
On the saddle-point trajectory of the problem (2.7) we have $\lim_{\tau\to+0} U\left(\tau,\bar{x}(\tau),\bar{\lambda}(\tau)\right)=F^*$, and in the case of local uniqueness solution to problem (2.7) the equalities are also valid $\lim_{\tau\to+0}\bar{x}(\tau)=x^*$ and $\lim_{\tau\to+0}\bar{\lambda}(\tau)=\lambda^*$.

***Theorem 2.3:***
On a saddle trajectory, the vector functions $\bar{x}(\tau)$ and $\bar{\lambda}(\tau)$ continuously differentiable according to your arguments $\forall\tau>0$.

**Example 2.2**
maximize by $x\in E^1$ function $F(x)=(x-2)^2$ under the conditions and $f_1(x)=x\le 4$, $f_2(x)=-x\le -1$ illustrates the statements of these theorems.

This example has two local solutions $x^*=1,\quad F^*=1$ and $x^*=4,\quad F^*=4$. To solve this problem, we use the feedback function $Q(\tau,s)=\frac{\tau}{2}\left(s-\frac{1}{s}\right)$ with $R(\tau,s)=\frac{\tau}{2}\left(\frac{s^2}{2}-\ln s-\frac{1}{2}\right)$. Then the *U*-function (since $q=1$ and $p=2$) will look like

$$U(\tau,x,\lambda_1,\lambda_2)=(x-2)^2-\lambda_1(-4+x)-\lambda_2(1-x)-\frac{\tau}{2}\left(\frac{x^2}{2}-\ln x-\frac{1}{2}\right)+\frac{\tau}{2}\left(\frac{\lambda_1^2}{2}-\ln\lambda_1-\frac{1}{2}\right)+\frac{\tau}{2}\left(\frac{\lambda_2^2}{2}-\ln\lambda_2-\frac{1}{2}\right)$$

and the conditions for its stationarity are correspondingly

$$\begin{cases} 2(\bar{x}-2)-\bar{\lambda}_1+\bar{\lambda}_2 &= \dfrac{\tau}{2}\left(\bar{x}-\dfrac{1}{\bar{x}}\right), \\ 4-\bar{x} &= -\dfrac{\tau}{2}\left(\bar{\lambda}_1-\dfrac{1}{\bar{\lambda}_1}\right), \\ -1_1+\bar{x} &= -\dfrac{\tau}{2}\left(\bar{\lambda}_2-\dfrac{1}{\bar{\lambda}_2}\right). \end{cases} \qquad (2.11)$$

Properties of the *U*-function for Example 2.2 are illustrated in Fig. 2.1–2.4. Fig. 2.1 shows the system of isolines of the function $U(\tau,x,\lambda_1,\lambda_2)$ for fixed $\tau=0.01$ and $\lambda_1=0.001$.

Figures 2.2, 2.3 and 2.4 present (at three different vertical scales) graphical solution of the equation $\bar{x}=\Phi(\tau,\bar{x})$. This equation is obtained by excluding the unknowns $\lambda_1$ and $\lambda_2$ from (2.11) for values $\tau=0.025,0.1$ and 0.250.

Figures 2.2 – 2.4 show that the function $U(\tau,x,\lambda_1,\lambda_2)$ for small positive values of $\tau$ has three isolated stationary points, correspondingly belonging to the neighborhoods of the points:

$$\{\ x^*_{(1)}=1,\ \lambda^*_{1(1)}=0,\ \lambda^*_{2(1)}=2\ \},\quad \{\ x^*_{(2)}=2,\ \lambda^*_{1(2)}=0,\ \lambda^*_{2(2)}=0\ \},\quad \{\ x^*_{(3)}=4,\ \lambda^*_{1(3)}=4,\ \lambda^*_{2(3)}=0\ \}.$$

According to the data given in table 2.2 (obtained by the same algorithm), we can also conclude that convergence point depends both on the starting points and on the value of the parameter $\tau$ .

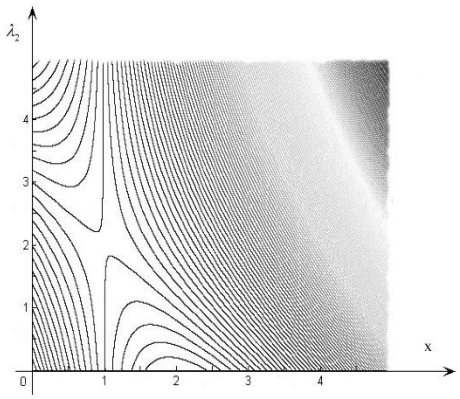


**Fig. 2.1. System of isolines for a function** $U(0.01, x, 0.001, \lambda_2)$.

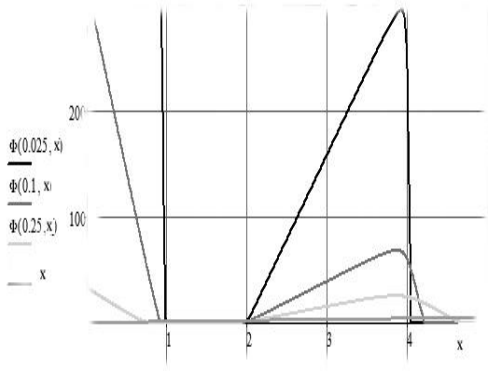


**Fig. 2.2. Graphical solution of the equation** $\bar{x} = \Phi(\tau, \bar{x})$**. Vertical scale is 1.00.**

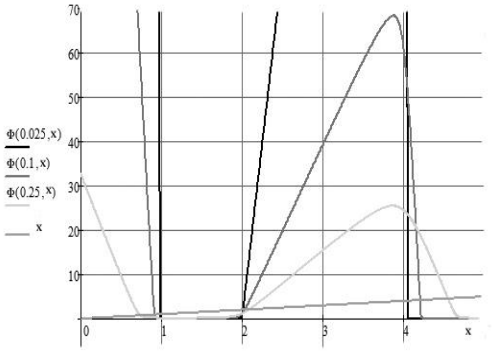


**Fig. 2.3 Graphical solution of the equation** $\bar{x} = \Phi(\tau, \bar{x})$**. Vertical scale is 0.20.**

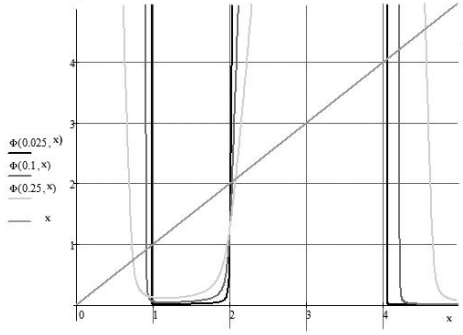


**Fig. 2.4. Graphical solution of the equation $\bar{x} = \Phi(\tau, \bar{x})$. Vertical scale is 0.02.**

**Table 2.2.**

**Starting Points**

| | | | | | | | | |
|---|---|---|---|---|---|---|---|---|
| 3.0000 | 0.0001 | 1.0000 | 3.0000 | 2.0000 | 1.0000 | 3.0000 | 0.0001 | 0.0001 |

**Solutions to system (2.11)**

| $\tau$ | $\bar{x}$ | $\bar{\lambda}_1$ | $\bar{\lambda}_2$ | $\bar{x}$ | $\bar{\lambda}_1$ | $\bar{\lambda}_2$ | $\bar{x}$ | $\bar{\lambda}_1$ | $\bar{\lambda}_2$ |
|---|---|---|---|---|---|---|---|---|---|
| 0.1 | 0.91398 262 | 0.01619 786 | 2.17922 612 | 4.19890 911 | 4.21540 712 | 0.01562 651 | 2.02670 086 | 0.02532 203 | 0.04858 472 |
| 0.03 | 0.97654 558 | $4.96\ 10^{-3}$ | 2.05115 786 | 4.05724 084 | 4.06222 643 | $4.91\ 10^{-3}$ | 2.00764 433 | $7.53\ 10^{-3}$ | 0.01488 291 |
| 0.01 | 0.99239 520 | $1.66\ 10^{-3}$ | 2.01679 571 | 4.01885 900 | 4.02052 410 | $1.66\ 10^{-3}$ | 2.00251 576 | $2.50\ 10^{-3}$ | $4.99\ 10^{-3}$ |
| 0.003 | 0.99774 061 | $5.00\ 10^{-4}$ | 2.00501 162 | 4.00563 478 | 4.00613 464 | $4.99\ 10^{-4}$ | 2.00075 141 | $7.50\ 10^{-4}$ | $1.50\ 10^{-3}$ |
| 0.001 | 0.99924 896 | $1.67\ 10^{-4}$ | 2.00166 796 | 4.00187 609 | 4.00204 2746 | $1.67\ 10^{-4}$ | 2.00025 016 | $2.50\ 10^{-4}$ | $5.00\ 10^{-4}$ |
| 0.000 3 | 0.99977 491 | $5.00\ 10^{-5}$ | 2.00050 012 | 4.00056 260 | 4.00061 260 | $5.00\ 10^{-5}$ | 2.00007 501 | $7.50\ 10^{-5}$ | $1.50\ 10^{-4}$ |
| 0.000 1 | 2.00002 500 | $2.50\ 10^{-5}$ | 2.00501 162 | 4.00018 751 | 4.00020 418 | $1.67\ 10^{-5}$ | 2.00002 500 | $2.50\ 10^{-5}$ | $5.00\ 10^{-5}$ |
| 0.000 07 | 2.00001 750 | $1.75\ 10^{-5}$ | $3.50\ 10^{-5}$ | 4.00013 126 | 4.00014 292 | $1.17\ 10^{-5}$ | 2.00001 750 | $1.75\ 10^{-5}$ | $3.50\ 10^{-5}$ |
| 0.000 03 | 4.00005 625 | 4.00006 125 | $5.00\ 10^{-6}$ | 4.00005 625 | 4.00006 125 | $5.00\ 10^{-6}$ | 2.00000 750 | $7.50\ 10^{-6}$ | $1.50\ 10^{-5}$ |
| 0.000 01 | 4.00001 875 | 4.00002 042 | $1.67\ 10^{-6}$ | 4.00001 875 | 4.00002 042 | $1.67\ 10^{-6}$ | 4.00001 875 | 4.00002 042 | $1.67\ 10^{-6}$ |

## USING FEEDBACK FUNCTIONS IN PROBLEMS OF SEARCHING FOR A GLOBAL EXTREMUM

Let us now describe the scheme for applying method feedback functions in tasks, which are reduced to mathematical programming problems. First, consider the problem of finding an extremum on a finite set of numbers.

The value of the maximum number in the set $\{v_1, v_2, \ldots, v_K\}$ there is a solution to the following linear programming problems:

$$f \to \min \qquad \text{under conditions} \qquad f \geq v_i \quad \forall i = \overline{1, K}. \tag{3.1}$$

The variable $f$ can have any sign. Therefore, we take the auxiliary function in the form

$$U(\tau, f, \lambda, v) = -f - \sum_{i=1}^{K} \lambda_i (v_i - f) + \sum_{i=1}^{K} R(\tau, \lambda_i).$$

If feedback function $Q(\tau, s) = \tau \ln s$ is selected, then the system of equations (2.9) will be

$$\begin{cases} -1 + \sum_{i=1}^{K} \overline{\lambda}_i = o, \\ v_i - \overline{f} = \tau \ln \overline{\lambda}_i \quad \forall i = \overline{1, K} \end{cases} \Rightarrow \begin{cases} \overline{\lambda}_i = \exp \dfrac{v_i - \overline{f}}{\tau} \qquad \forall i = \overline{1, K}, \\ \overline{f} = \tau \ln \left( \sum_{i=1}^{K} \exp \dfrac{v_i}{\tau} \right). \end{cases} \tag{3.2}$$

The maximum and minimum of the numbers in the set $\{v_1, v_2, \ldots, v_K\}$ will be equal respectively to

$$f^*_{\max} = \lim_{\tau \to +0} \tau \ln \left( \sum_{i=1}^{K} \exp \frac{v_i}{\tau} \right) \qquad \text{and} \qquad f^*_{\min} = -\lim_{\tau \to +0} \tau \ln \left( \sum_{i=1}^{K} \exp \left( -\frac{v_i}{\tau} \right) \right) \tag{3.3}$$

Now let's evaluate the difference between $f^*_{\max}$ and $\overline{f} = \tau \ln \left( \sum_{i=1}^{K} \exp \frac{v_i}{\tau} \right)$. We will assume that the numbers in the set $\{v_1, v_2, \ldots, v_K\}$ sorted in descending order and the first $M < K$ of them are equal to $f^*$. Then we have

$$\overline{f} - f^* = \tau \ln \left( \sum_{i=1}^{K} \exp \frac{v_i}{\tau} \right) - \tau \ln \exp \frac{f^*}{\tau} = \tau \ln \left( \sum_{i=1}^{K} \exp \frac{v_i - f^*}{\tau} \right) = \tau \ln \left( M + \sum_{i=M+1}^{K} \exp \frac{v_i - f^*}{\tau} \right) \leq$$

$$\leq \tau \ln \left( M + (K - M) \exp \frac{A - f^*}{\tau} \right) = \tau \ln M + \tau \ln \left( 1 + \frac{K - M}{M} \exp \frac{A - f^*}{\tau} \right) = \tau \ln M + \tau \exp \frac{A - f^*}{\tau},$$

where $A = v_{M+1}$.

The resulting inequality means that the order of smallness of the error is equal to $\tau \ln M$ in the case when $M > 1$. If $M = 1$, then for $\tau \to +0$ the order of error is noticeably smaller, since it is determined by the term $\tau \cdot \exp \dfrac{A - f^*}{\tau}$.

If you use the feedback function $Q(\tau, s) = \dfrac{\tau}{2} \left( s - \dfrac{1}{s} \right)$, then the system of equations (2.9) will have the form

$$\begin{cases} -1 + \sum_{i=1}^{K} \overline{\lambda}_i = o, \\ v_i - \overline{f} = \dfrac{\tau}{2} \left( \overline{\lambda}_i - \dfrac{1}{\overline{\lambda}_i} \right) \quad \forall i = \overline{1, K}, \end{cases} \tag{3.4}$$

for which only a numerical solution is possible.

For illustration in Table 3.1 shows the results of solving system (3.2) for a set of numbers $\{5, -2, 4, 7, 0\}$ for different values of the parameter $\tau$ .

**Table 3.1.**

| $\tau$ | $\overline{f}(\tau)$ | $\overline{\lambda}_1(\tau)$ | $\overline{\lambda}_2(\tau)$ | $\overline{\lambda}_3(\tau)$ | $\overline{\lambda}_4(\tau)$ | $\overline{\lambda}_5(\tau)$ |
|---|---|---|---|---|---|---|
| $10^{-0.00}$ | 7.170719212 | 0.114095529 | $1.0404\ 10^{-4}$ | 0.041973399 | 0.843058261 | $7.687710^{-4}$ |
| $10^{-0.25}$ | 7.018454440 | 0.027615558 | $1.0841\ 10^{-7}$ | $4.6651\ 10^{-3}$ | 0.967715479 | $3.7990\ 10^{-6}$ |
| $10^{-0.50}$ | 7.000590038 | $1.7884\ 10^{-3}$ | $4.355\ 10^{-13}$ | $7.5703\ 10^{-5}$ | 0.998135874 | $2.430\ 10^{-10}$ |
| $10^{-0.75}$ | 7.000002329 | $1.3048\ 10^{-5}$ | $4.355\ 10^{-13}$ | $4.7135\ 10^{-8}$ | 0.999986904 | 0.000000000 |
| $10^{-1.00}$ | 7.000000000 | $2.0612\ 10^{-9}$ | 0.000000000 | $9.358\ 10^{-14}$ | 0.999999998 | 0.000000000 |
| $10^{-1.25}$ | 7.000000000 | 0.000000000 | 0.000000000 | 0.000000000 | 1.000000000 | 0.000000000 |

In Table 3.2 are given for comparison numerical solutions of system (3.4) for a set of numbers $\{5, 5, 4, 5, 0\}$ also for the parameter $\tau$ .

**Table 3.2.**

| $\tau$ | $\overline{f}(\tau)$ | $\overline{\lambda}_1(\tau)$ | $\overline{\lambda}_2(\tau)$ | $\overline{\lambda}_3(\tau)$ | $\overline{\lambda}_4(\tau)$ | $\overline{\lambda}_5(\tau)$ |
|---|---|---|---|---|---|---|
| $10^{-1.00}$ | 5.109862742 | 0.333328289 | 0.333328289 | $1.5133\ 10^{-5}$ | 0.333328289 | 0.000000000 |
| $10^{-1.20}$ | 5.069317752 | 0.333333319 | 0.333333319 | $4.3629\ 10^{-8}$ | 0.333333319 | 0.000000000 |
| $10^{-1.50}$ | 5.034741173 | 0.333333333 | 0.333333333 | 0.000000000 | 0.333333333 | 0.000000000 |
| $10^{-2.00}$ | 5.010986124 | 0.333333333 | 0.333333333 | 0.000000000 | 0.333333333 | 0.000000000 |
| $10^{-4.00}$ | 5.000109861 | 0.333333333 | 0.333333333 | 0.000000000 | 0.333333333 | 0.000000000 |
| $10^{-7.00}$ | 5.000000110 | 0.333333333 | 0.333333333 | 0.000000000 | 0.333333333 | 0.000000000 |

From Theorem 3.2 it follows that the error of the feedback function method decreases when $\tau \to +0$. However, sometimes for a specific value $\tau$ it may be unacceptably large. In this case, we can apply the implicit function theorem to system (2.9) to reduce the approximation error.

Really, if we consider system (2.9) as an implicit definition of vector functions $\overline{x}(\tau)$ and $\overline{\lambda}(\tau)$, then their refined values can be obtained for example, according to the formulas

$$\hat{x}_j = \overline{x}_j - \tau \frac{d\overline{x}_j}{d\tau} \quad \forall j = \overline{1,n} \text{ and } \hat{\lambda}_i = \overline{\lambda}_i - \tau \frac{d\overline{x}_i}{d\tau} \quad \forall i = \overline{1,m} \tag{3.5}$$

A detailed look at this procedure is beyond the scope of this article. We only note that in [Umnov, 2022]

it is shown that, the point $\{\hat{x}, \hat{\lambda}\}$ no longer belongs to the saddle trajectory. However, using formulas (3.5) can be performed iteratively in several steps. To do this, it is enough to replace scalar parameter $\tau$ to a vector, turning the saddle path into a beam such trajectories.

Let us now consider the problem of finding extreme values for numerical sets of cardinality continuum. Let $\Omega \subset E^n$ is a compact with not empty inside. Replacing the operation of summation by integration in formulas (3.3), we obtain an estimate of the value global maximum of a function $f(x)$ of several variables

$$f^*_{\max} = \lim_{\tau \to +0} \tau \ln \int_{\Omega} \exp \frac{f(x)}{\tau} dx. \tag{3.6}$$

Validity (3.6) follows from conditions $f(x) \le f^* \ \forall x \in \Omega$ and estimates:

$$f^*_{\max} = \lim_{\tau \to +0} \tau \ln \int_{\Omega} \exp \frac{f(x)}{\tau} dx = \lim_{\tau \to +0} \tau \ln \left( \left( \exp \frac{f^*}{\tau} \right) \left( \int_{\Omega} \exp \frac{f(x) - f^*}{\tau} dx \right) \right) = f^* + \lim_{\tau \to +0} \tau \ln \int_{\Omega} \exp \frac{f(x) - f^*}{\tau} dx.$$

$$0 \le \lim_{\tau \to +0} \tau \ln \int_{\Omega} \exp \frac{f(x) - f^*}{\tau} dx \le \lim_{\tau \to +0} \tau \ln \operatorname{mes} \Omega.$$

Relationship between integration operations and extremum search was previously used for solving problems of different classes: in the pass method, described, for example, in [Fedoryuk, 1977] or when searching for maximin in game problems [Fedorov, 1979].

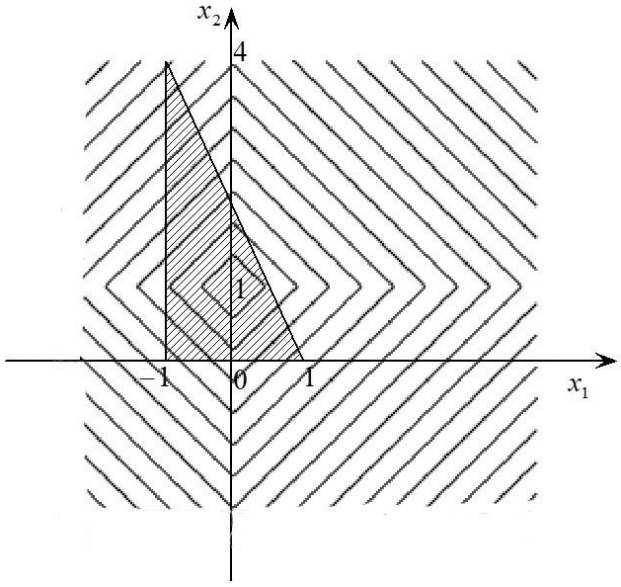


**Fig. 3.1. System of isolines for a function $f(x) = |x_1| + |x_2 - 1|$.**

The following example illustrates application of formula (3.7).

**Example 3.1**

Find global extremes by $x \in \Omega \subseteq E^2$ functions $f(x) = |x_1| + |x_2 - 1|$, where $\Omega = \begin{Bmatrix} -1 \le x_1 \le 1, \\ 0 \le x_2, \\ 2x_1 + x_2 \le 2 \end{Bmatrix}$.

**Solution:**
For the global maximum we have:

$$f^*_{\max} = \lim_{\tau\to+0} \tau \ln \iint\limits_{\Omega} \exp \frac{|x_1| + |x_2 - 1|}{\tau} dx_1 dx_2 =$$
$$= \lim_{\tau\to+0} \tau \ln \exp \frac{2}{\tau} \left( 5 - 10\exp\left( -\frac{1}{\tau} \right) + \exp \frac{2}{\tau} - 8\exp\left( -\frac{3}{2\tau} \right) + 12\exp\left( -\frac{2}{\tau} \right) \right) = 4.$$

It is achieved on the boundary of the region $\Omega$ with $x_1 = -1$ and $x_2 = 4$ (Fig. 3.1).

Global minimum is internal, non-smooth, at point $x_1 = 0$ and $x_2 = 1$:

$$f^*_{\min} = -\lim_{\tau\to+0} \tau \ln \iint\limits_{\Omega} \exp\left( -\frac{|x_1| + |x_2 - 1|}{\tau} \right) dx_1 dx_2 =$$
$$= -\lim_{\tau\to+0} \tau \ln \exp \frac{2}{\tau} \left( 5\exp\left( -\frac{2}{\tau} \right) - 10\exp\left( -\frac{1}{\tau} \right) + \exp \frac{4}{\tau} - 8\exp\left( -\frac{1}{2\tau} \right) + 12 \right) = 0.$$

Note also that the optimal value of the objective function in a mathematical programming problem

$$F(x) \to \max \qquad \text{under conditions} \qquad x \in \Omega \subseteq E^n.$$

can be represented (under appropriate assumptions about the properties of $F(x)$ and $\Omega$) as

$$F^*_{\max} = \lim_{\tau\to+0} \tau \ln \int\limits_{\Omega} \exp \frac{F(x)}{\tau} dx.$$

## USING FEEDBACK FUNCTIONS IN PROBLEMS OF SEARCHING FOR MULTIPLE EXTREMUM AND MINIMAX

Feedback function method can be used to solve optimization tasks, whose objective functions are superpositions of extremum search operators.

For example, consider the discrete problem finding *minimax* and *maximin* for a matrix

$$\left\| A_{ij} \right\| = \begin{Vmatrix} 5 & 2 & 8 & 4 \\ 12 & 3 & 11 & 9 \\ 1 & 6 & 7 & 10 \end{Vmatrix},$$

in which you need to find $A_{\max\min} = \max\limits_{j=\overline{1,n}} \left( \min\limits_{i=\overline{1,m}} A_{ij} \right)$ and $A_{\min\max} = \min\limits_{i=\overline{1,m}} \left( \max\limits_{j=\overline{1,n}} A_{ij} \right)$, where $n = 4$ and $m = 3$.

Let us use equalities (3.3), from which follows that

$$A_{\max\min} = \lim_{\tau\to+0} \tau \ln\left(\sum_{i=1}^{m} \exp\frac{A_{i,\min}}{\tau}\right), \qquad \text{where} \qquad A_{i,\min} = -\lim_{\tau\to+0} \tau \ln\left(\sum_{j=1}^{n} \exp\left(-\frac{A_{ij}}{\tau}\right)\right).$$

Or, after simplifications,

$$A_{\max\min} = \lim_{\tau\to+0} \tau \ln \sum_{i=1}^{m}\left(\sum_{j=1}^{n} \exp\left(-\frac{A_{ij}}{\tau}\right)\right)^{-1} = 7. \qquad (4.1)$$

Similarly, we find

$$A_{\min\max} = -\lim_{\tau\to+0} \tau \ln \sum_{i=1}^{m}\left(\sum_{j=1}^{n} \exp\left(\frac{A_{ij}}{\tau}\right)\right)^{-1} = 8. \qquad (4.2)$$

In Table 4.1 shows for various $\tau$ the values of the functions from which the limits in (4.1) and (4.2) are taken.

**Table 4.1.**

| $\tau$ | 0300 | 0.250 | 0.200 | 0.150 | 0.125 | 0.100 | 0.075 | 0.050 |
|---|---|---|---|---|---|---|---|---|
| minmax ($\tau$) | 7.999631605 | 7.999917657 | 7.999990981 | 7.999999757 | 7.999999986 | 8 | 8 | 8 |
| maximin($\tau$) | 6.989497444 | 6.995464027 | 6.998656991 | 6.999809227 | 6.999958074 | 6.99999546 | 6.999999879 | 7 |

Now we consider the discrete-continuous minimax problem:

$$\begin{gathered} \text{find the minimum by } x\text{: } F(x) = \max_{k=\overline{1,K}} f_k(x) \\ \text{subject to: } x \in \Omega\text{, where } \Omega \subseteq E^n \text{ is compact,} \end{gathered} \qquad (4.3)$$

assuming that the functions $f_k(x) \quad \forall k = \overline{1,K}$ continuously differentiable on $\Omega$.

In the case when the set $\Omega$ is specified by a system of inequalities of the form $y_i(x) \quad \forall i = \overline{1,m}$ problem (4.3) is equivalent to the mathematical programming problem:

$$\begin{gathered} \text{maximize by: } \{x, w\} \ -w \\ \text{subject to: } f_k(x) - w \le 0 \quad \forall k = \overline{1,K}\text{,} \\ y_i(x) \le 0 \quad \forall i = \overline{1,m} \end{gathered} \qquad (4.4)$$

Here we also assume that the functions $y_i(x) \quad \forall i = \overline{1,m}$ continuously differentiable on the set $\Omega$ .

The dependence $w_x^*$ under the assumptions made is a continuous but non-differentiable function. Therefore, to solve problem (4.4), we apply the method of feedback functions with the auxiliary function (2.5)

$$U(\tau, x, \Lambda, w) = -w - \sum_{k=1}^{K} \mu_k \left( f_k(x) - w \right) - \sum_{i=1}^{m} \lambda_i y_i(x) + \sum_{k=1}^{K} R(\tau, \mu_k) + \sum_{i=1}^{m} R(\tau, \lambda_i) \qquad (4.5)$$

Stationarity conditions for function (4.5) can be written in the form of a system of equations:

$$\begin{cases} \sum_{k=1}^{K} \overline{\mu}_k \operatorname*{grad}_x f_k(\overline{x}) + \sum_{i=1}^{m} \overline{\lambda}_i \operatorname*{grad}_x y_i(\overline{x}) = o, \\ -f_k(\overline{x}) + \overline{w} + Q(\tau, \overline{\mu}_k) = 0 \quad \forall k = \overline{1, K}, \\ -y_i(\overline{x}) + Q(\tau, \overline{\lambda}_i) = 0 \quad \forall i = \overline{1, m}, \\ -1 + \sum_{k=1}^{K} \overline{\mu}_k = 0. \end{cases}$$

If the task the search for minimax has no restrictions and the feedback function is defined as $Q(\tau, s) = \tau \ln s$, then the stationarity conditions auxiliary functions are simplified

$$\begin{cases} \sum_{k=1}^{K} \overline{\mu}_k \operatorname*{grad}_x f_k(\overline{x}) = o, \\ \overline{\mu}_k = \exp\left( \frac{f_k(\overline{x}) - \overline{\mu}_k}{\tau} \right) \quad \forall k = \overline{1, K}, \\ -1 + \sum_{k=1}^{K} \overline{\mu}_k = 0. \end{cases} \qquad (4.6)$$

The last two conditions of system (4.6) give us a smoothed approximation of the dependance $w_x^*$ $\overline{w}(x) = \tau \ln \sum_{k=1}^{K} \exp\left( \frac{f_k(\overline{x})}{\tau} \right)$. In this case, the first equality in (4.6) is necessary condition for stationarity $\overline{w}(x)$ by $x$.

The smoothness of the $\overline{w}(x)$ function allows us to use standard analytical tools. We can check whether both necessary and sufficient classical optimality conditions are met. Let's take a problem as an example.

***Problem 4.1***:
Find the minimum value of the maximum function

$$f(x_1, x_2) = \max_{\{x_1, x_2\}} \left\{ x_1^2 + x_2^2 ; \quad 25 - (x_1 + 1)^2 - (x_2 - 2)^2 \right\}$$

**Solution**:
The formulation of task (4.4) in this case has the form

$$\text{maximize by } \{x_1, x_2, w\} : -w$$
$$\text{subject to: } x_1^2 + x_2^2 - w \le 0,$$

$$25-(x_1+1)^2-(x_2-2)^2-w\le 0.$$

Auxiliary function (4.5) in this task there will be

$$U(\tau,x_1,x_2,\mu_1,\mu_2,w)=-w-\mu_1(x_1^2+x_2^2-w)-\mu_2(25-(x_1+1)^2-(x_2-2)^2-w)+R(\tau,\mu_1)+R(\tau,\mu_2) \tag{4.7}$$

Stationarity conditions for function (4.7) by variables $x_1,x_2,\mu_1,\mu_2,w$ are

$$\begin{cases} -2\bar{\mu}_1\bar{x}_1+2\bar{\mu}_2(\bar{x}_1+1)= & 0,\\ -2\bar{\mu}_1\bar{x}_2+2\bar{\mu}_2(\bar{x}_2-2)= & 0,\\ x_1^2+x_2^2-w= & Q(\tau,\bar{\mu}_1),\\ 25-(x_1+1)^2-(x_2-2)^2-w= & Q(\tau,\bar{\mu}_2),\\ -1+\bar{\mu}_1+\bar{\mu}_2= & 0, \end{cases} \tag{4.8}$$

where $Q(\tau,s)=\tau\ln s$.

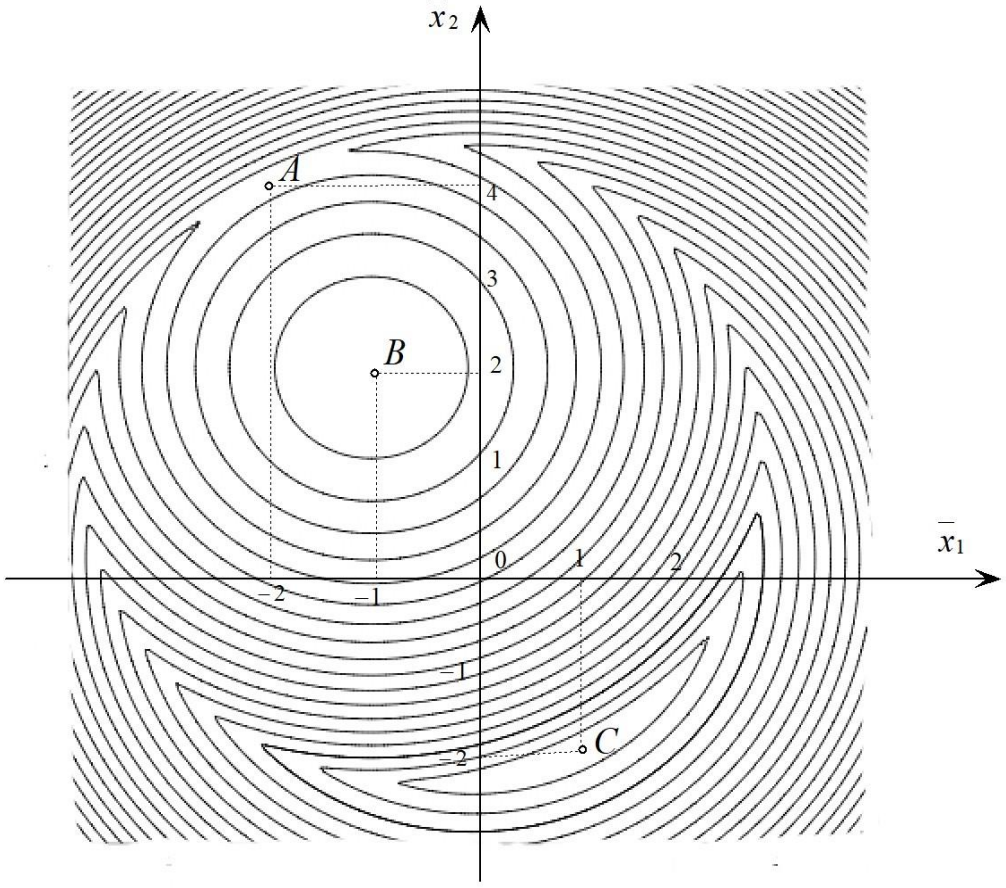


**Fig. 4.1. System of isolines of function (4.9).**

Let us briefly explain the scheme for solving system (4.8). From the first two equations we have $\bar{x}_2=-2\bar{x}_1$. From the last three – it follows that as smoothed approximation of the maximum function $f(x_1,x_2)$ you can take

$$\overline{w}(\tau, x_1, x_2) = \tau \ln\left( \exp\frac{x_1^2 + x_2^2}{\tau} + \exp\frac{25-(x_1+1)^2-(x_2-2)^2}{\tau} \right) \quad (4.9)$$

system of isolines of which for $\tau = 0.1$ is shown in Fig. 4.1.

Based on the form of the isoline of function (4.9), we can expect that this function has stationary points: $\{\overline{x}_{1(A)}; \overline{x}_{2(A)}\}$, $\{\overline{x}_{1(B)}; \overline{x}_{2(B)}\}$ and $\{\overline{x}_{1(C)}; \overline{x}_{2(C)}\}$, belonging respectively to the surrounding areas for points *A*, *B* and *C*.

Coordinates of points *A*, *B* and *C* can be found by considering the maximum function $f(x_1, x_2)$. Point *B* is local maximum of the function $f(x_1, x_2)$. It has coordinates $\{-1;2\}$. Points *A* and *C* are solutions to the extremum problem of the form:

$$\text{maximize by: } \{x_1, x_2\} \quad x_1^2 + x_2^2,$$
$$\text{subject to: } 25-(x_1+1)^2-(x_2-2)^2 = x_1^2 + x_2^2.$$

It is easy to check that A$\{-2;4\}$ and C$\{1;-2\}$.

Table 4.2 shows numerical estimates of the coordinates of stationary points for smoothing function $\overline{w}(\tau, x_1, x_2)$ for different values of the parameter $\tau$.

**Table 4.2**

| | **Starting point solution search procedures** | | | | | | | | |
|---|---|---|---|---|---|---|---|---|---|
| | -1.5 | 3.5 | 22.5 | -0.6 | 2.3 | 24.8 | 3.0 | 1.0 | 10.0 |
| | **Solutions of system (4.8) in the vicinity of the point:** | | | | | | | | |
| | **A** | | | **B** | | | **C** | | |
| $\tau$ | $\overline{x}_1$ | $\overline{x}_2$ | $\overline{w}$ | $\overline{x}_1$ | $\overline{x}_2$ | $\overline{w}$ | $\overline{x}_1$ | $\overline{x}_2$ | $\overline{w}$ |
| 1.00 | -1.976305906 | 3.952611813 | 20.63559463 | -1.000000002 | 2.000000004 | 25 | 1.022565341 | -2.045130681 | 5.63737652 |
| 0.95 | -1.977519843 | 3.955039686 | 20.60385998 | -1.000000001 | 2.000000001 | 25 | 1.021461696 | -2.042923391 | 5.60546 7921 |
| 0.90$ | -1.978730572 | 3.957461144 | 20.57212044 | -1 | 2 | 25 | 1.020355555 | -2.040711109 | 5.57356 3393 |
| 0.85 | -1.979938116 | 3.959876232 | 20.54037603 | -1 | 2 | 25 | 1.019246903 | -2.038493805 | 5.54166 2957 |
| 0.80 | -1.981142498 | 3.962284995 | 20.50862678 | -1 | 2 | 25 | 1.018135724 | -2.036271447 | 5.50976 6630 |
| Sol. | -2 | 4 | 20 | -1 | 2 | 25 | 1 | -2 | 5 |

To illustrate the smoothing property of feedback functions we may use equality $\overline{x}_2 = -2\overline{x}_1$. In this case the dependence of $\overline{w}$ on $\overline{x}_1$ can be represented by the function

$$\Phi(\tau, x_1) = \tau \ln\left( \exp\frac{5x_1^2}{\tau} + \exp\frac{25 - 5(x_1+1)^2}{\tau} \right)$$

Graph of this function, as well as its fragments in the vicinity of stationary points for different values of the parameter $\tau$, are shown in Fig. 4.2, 4.3, 4.4 and 4.5.

Note that in the neighborhood of point *B* (see Fig. 4.4) differences in smoothing function values for different $\tau$ are small and practically invisible on the chart. This effect can be explained by specific properties of the feedback function $Q(\tau, s) = \tau \ln s$.

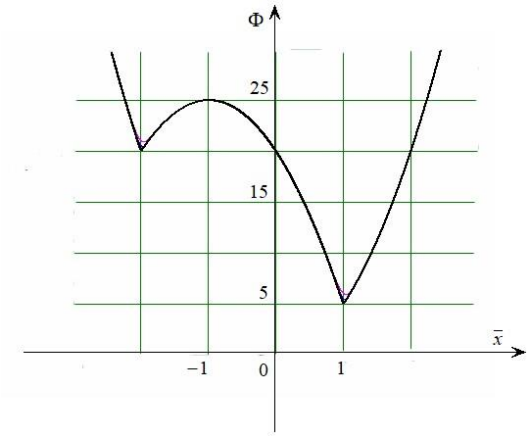


**Fig. 4.2. Function graphs $\Phi(\tau, x_1)$**

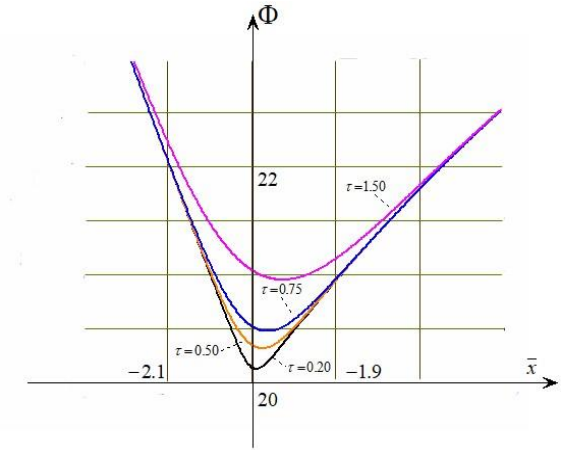


**Fig. 4.3. Function graphs $\Phi(\tau, x_1)$ at *A***

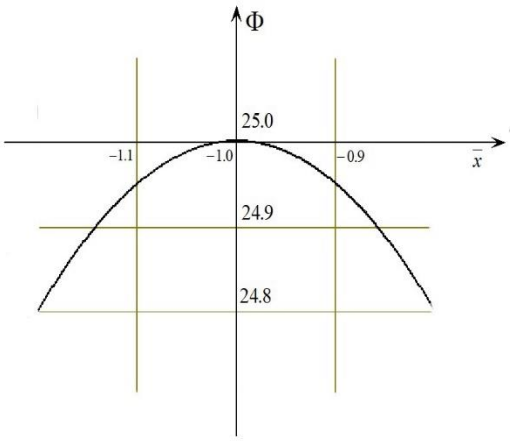


**Fig. 4.4. Function graphs $\Phi(\tau, x_1)$ at *B***

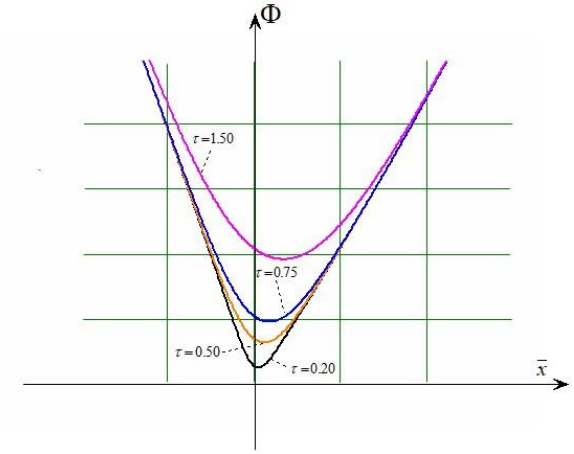


**Fig. 4.5. Function graphs $\Phi(\tau, x_1)$ at *C***

To study the behavior of the function $\overline{w}(\tau, x_1, x_2)$ we may use standard sufficient conditions classification of stationary points, based on Sylvester's criterion. For this purpose, we first present the formulas for partial derivatives of this function up to the second order inclusive.

Let

$$\Delta = \exp\frac{x_1^2 + x_2^2}{\tau} + \exp\frac{25-(x_1+1)^2-(x_2-2)^2}{\tau}\ .$$

Then

$$\frac{\partial \overline{w}}{\partial x_1} = -\frac{2}{\Delta}\left((1+x_1)\exp\frac{25-(x_1+1)^2-(x_2-2)^2}{\tau} - x_1\exp\frac{x_1^2+x_2^2}{\tau}\right)$$

And

$$\frac{\partial \overline{w}}{\partial x_2} = 2x_2 + \frac{4(1-x_2)}{\Delta}\exp\frac{25-(x_1+1)^2-(x_2-2)^2}{\tau}.$$

Similarly, for second derivatives we have

$$\frac{\partial^2 \overline{w}}{\partial x_1^2} = \frac{2}{\Delta^2}\left( \frac{2(1+2x_1)}{\tau}\exp\frac{-2x_1+4x_2+20}{\tau} - \exp\frac{2}{\tau}\left(25-(x_1+1)^2-(x_2-2)^2\right) + \exp\frac{2}{\tau}\left(x_1^2+x_2^2\right)\right),$$

$$\frac{\partial^2 \overline{w}}{\partial x_1 \partial x_2} = \frac{8(2x_1+1)(x_2-1)}{\tau\Delta^2}\exp\frac{-2x_1+4x_2+20}{\tau},$$

$$\frac{\partial^2 \overline{w}}{\partial x_2^2} = \frac{2}{\Delta^2}\left( \frac{8(1-x_2)^2}{\tau}\exp\frac{-2x_1+4x_2+20}{\tau} - \exp\frac{2}{\tau}\left(25-(x_1+1)^2-(x_2-2)^2\right) + \exp\frac{2}{\tau}\left(x_1^2+x_2^2\right)\right).$$

At points $\{\overline{x}_{1(A)};\overline{x}_{2(A)}\}$, $\{\overline{x}_{1(B)};\overline{x}_{2(B)}\}$ and $\{\overline{x}_{1(C)};\overline{x}_{2(C)}\}$ Hessian matrices for functions $\overline{w}(\tau,x_1,x_2)$ at $\tau = 0.85$ there will be

$$\|\mathrm{Hess}(A)\| = \begin{Vmatrix} 8.45472820\mathbf{3} & -18.26086423 \\ -18.26086423 & 35.84602459\mathbf{7} \end{Vmatrix},$$

$$\|\mathrm{Hess}(B)\| = \begin{Vmatrix} -1.99999999\mathbf{9} & -5.688\cdot 10^{-10} \\ -5.688\cdot 10^{-10} & -1.99999999\mathbf{9} \end{Vmatrix}$$

$$\text{and } \|\mathrm{Hess}(C)\| = \begin{Vmatrix} 10.3434498\mathbf{02} & -19.37045787\mathbf{6} \\ -19.37045787\mathbf{6} & 39.3991366\mathbf{01} \end{Vmatrix}.$$

From mathematical analysis it is known that that to use Sylvester's criterion, as a sufficient condition for the presence or absence of an extremum, the following values are required: gradient norm $N_{\text{grad}} = \sqrt{\left(\frac{\partial \overline{w}}{\partial x_1}\right)^2 + \left(\frac{\partial \overline{w}}{\partial x_2}\right)^2}$, as well as the principal minors of the Hessian matrix: $M_{(1)} = \frac{\partial^2 \overline{w}}{\partial x_1^2}$ and $M_{(2)} = \frac{\partial^2 \overline{w}}{\partial x_1^2}\frac{\partial^2 \overline{w}}{\partial x_2^2} - \left(\frac{\partial^2 \overline{w}}{\partial x_1 \partial x_2}\right)^2$.

These values for points $\{\overline{x}_{1(A)};\overline{x}_{2(A)}\}$, $\{\overline{x}_{1(B)};\overline{x}_{2(B)}\}$ and $\{\overline{x}_{1(C)};\overline{x}_{2(C)}\}$ as well as classification of the points according to Sylvester's criterion are given in Table 4.3.

Note that the rather large value relative error of the obtained solutions is caused by the properties of the feedback function $Q(\tau,s) = \tau \ln s$. It was used because allows you to find solutions in the form of formulas.

**Table 4.3**

| | **Solutions of system (4.8) in the vicinity of the point:** | | |
|---|---|---|---|
| | *A* | *B* | *C* |
| $\overline{x}_1$ | -1.979938116 | -1.000000000 | 1.019246903 |
| $\overline{x}_2$ | 3.959876232 | 2.000000000 | -2.038493805 |
| $\overline{w}$ | 20.540376029 | 25.000000000 | 5.541662957 |
| $N_{\text{grad}}$ | $3.2095\cdot 10^{-9}$ | $0.2418\cdot 10^{-9}$ | $9.4269\cdot 10^{-9}$ |
| $M_{(1)}$ | 8.454728203 | -1.999999999 | 10.343449802 |
| $M_{(2)}$ | -30.390768491 | 3.999999996 | 32.308353346 |

| *Point type*: | *No extremum* (*saddle point*) | *Local maximum* | *Local minimum* |
|---|---|---|---|

If we limit ourselves to a numerical search stationary point, then we may use the function feedback $Q(\tau,s)=\frac{\tau}{2}\left(s-\frac{1}{s}\right)$ in system (4.8). It allows us to obtain solutions with significantly less error only by decreasing the value parameter $\tau$. Results of solving this system at points $\{\bar{x}_{1(A)};\bar{x}_{2(A)}\}$, $\{\bar{x}_{1(B)};\bar{x}_{2(B)}\}$ and $\{\bar{x}_{1(C)};\bar{x}_{2(C)}\}$ for this case are given in tables 4.4(*A*), 4.4(*B*) and 4.4(C).

Now suppose that the feedback function used does not produce a solution with an acceptable error. In this case we can apply the procedure of iterative refinement of the solution using formulas similar to (3.5):

$$\bar{x}_{j(T+1)}=\bar{x}_{j(T)}-\tau\frac{d\bar{x}_j}{d\tau}\qquad\forall j=\overline{1,2}\qquad\forall T=0,1,2,...,$$

where *T* is the iteration number.

Since $\tau$ is now fixed, then for the clarifying vector you may enter a designation $\delta\bar{x}_{(T)}$. Then, according to the implicit function theorem, the components of this vector satisfy system of linear equations of the form:

$$\begin{cases}\dfrac{\partial^2\bar{w}}{\partial x_1^2}\delta\bar{x}_{1(T)}+\dfrac{\partial^2\bar{w}}{\partial x_1\partial x_2}\delta\bar{x}_{2(T)}=-\tau\dfrac{\partial^2\bar{w}}{\partial x_1\partial\tau},\\ \dfrac{\partial^2\bar{w}}{\partial x_1\partial x_2}\delta\bar{x}_{1(T)}+\dfrac{\partial^2\bar{w}}{\partial x_2^2}\delta\bar{x}_{2(T)}=-\tau\dfrac{\partial^2\bar{w}}{\partial x_2\partial\tau},\end{cases}$$

Where,

$$\frac{\partial^2\bar{w}}{\partial x_1\partial\tau}=-\frac{4(2x_1+1)(x_1^2+x_1+x_2^2-2x_2-10)}{\tau^2\Delta^2}\exp\frac{-2x_1+4x_2+20}{\tau},$$

$$\frac{\partial^2\bar{w}}{\partial x_2\partial\tau}=-\frac{8(x_2-1)(x_1^2+x_1+x_2^2-2x_2-10)}{\tau^2\Delta^2}\exp\frac{-2x_1+4_2+20}{\tau}.$$

**Table 4.4(*A*)}**

| $\tau$ | $\bar{x}_1$ | $\bar{x}_2$ | $\bar{\mu}_1$ | $\bar{\mu}_2$ | $\bar{w}$ |
|---|---|---|---|---|---|
| 1.00 | -1.934001409 | 3.868002818 | 0.325662654 | 0.674337346 | 21.44680679 |
| $10^{-1}$ | -1.993845902 | 3.987691805 | 0.332646728 | 0.667353272 | 20.14446196 |
| $10^{-2}$ | -1.999388464 | 3.998776928 | 0.333265357 | 0.666734643 | 20.01444462 |
| $10^{-3}$ | -1.999938885 | 3.999877769 | 0.333326542 | 0.666673458 | 20.00144445 |
| $10^{-4}$ | -1.999993889 | 3.999987778 | 0.333332654 | 0.666667346 | 20.00014444 |
| $10^{-5}$ | -1.999999389 | 3.999998778 | 0.333333265 | 0.666666735 | 20.00001444 |
| $10^{-6}$ | -1.999999939 | 3.999999878 | 0.333333327 | 0.666666673 | 20.00000144 |
| $10^{-7}$ | -1.999999994 | 3.999999988 | 0.333333333 | 0.666666667 | 20.00000014 |

| | | | | | |
|---|---|---|---|---|---|
| $10^{-8}$ | -1.999999999 | 3.999999999 | 0.333333333 | 0.666666667 | 20.00000001 |
| $10^{-9}$ | -2 | 4 | 0.333333333 | 0.666666667 | 20 |
| $10^{-10}$ | -2 | 4 | 0.333333333 | 0.666666667 | 20 |
| *Solution*: | -2 | 4 | $\frac{1}{3}$ | $\frac{2}{3}$ | 20 |

**Table 4.4(*B*)}**

| $\tau$ | $\overline{x}_1$ | $\overline{x}_2$ | $\overline{\mu}_1$ | $\overline{\mu}_2$ | $\overline{w}$ |
|---|---|---|---|---|---|
| 1.00 | -1.056966891 | 2.113933783 | 0.051140285 | 0.948859715 | 25.08881072 |
| $10^{-1}$ | -1.005063133 | 2.010126265 | $5.0124\cdot10^{-3}$ | 0.994987624 | 25.00087682 |
| $10^{-2}$ | -1.000500626 | 2.001001251 | $5.0012\cdot10^{-4}$ | 0.999499875 | 25.00000875 |
| $10^{-3}$ | -1.000050006 | 2.000100013 | $5.0001\cdot10^{-5}$ | 0.999949999 | 25.00000009 |
| $10^{-4}$ | -1.000005000 | 2.000010000 | $5.0000\cdot10^{-6}$ | 0.999995000 | 25 |
| $10^{-5}$ | -1.000000500 | 2.000001000 | $5.0000\cdot10^{-7}$ | 0.999999500 | 25 |
| $10^{-6}$ | -1.000000050 | 2.000000100 | $5.0000\cdot10^{-8}$ | 0.999999950 | 25 |
| $10^{-7}$ | -1.000000005 | 2.000000010 | $5.0000\cdot10^{-9}$ | 0.999999995 | 25 |
| $10^{-8}$ | -1.000000001 | 2.000000001 | $5.0000\cdot10^{-10}$ | 0.999999999 | 25 |
| $10^{-9}$ | -1 | 2 | $5.0000\cdot10^{-11}$ | 1 | 25 |
| $10^{-10}$ | -1 | 2 | $5.0000\cdot10^{-12}$ | 1 | 25 |
| *Solution*: | -1 | 2 | 0 | 1 | 25 |

Let the assumption of continuity second derivatives of the function $\overline{w}(\tau, x_1, x_2)$ according to all its arguments is valid in some compact space containing the point *C*. Then we can assume that process (4.10) will converge to point *C* for a sufficiently small positive $\tau$ due to the principle of contraction operator.

Results of the corresponding calculations for the problem being solved are given in table. 4.5, in which the following notations are used: $\overline{F} = \overline{x}_1^2 + \overline{x}_2^2$ and $\overline{G} = 25 - (\overline{x}_1 + 1)^2 - (\overline{x}_2 - 2)^2$.

**Table 4.4(*C*)}**

| $\tau$ | $\overline{x}_1$ | $\overline{x}_2$ | $\overline{\mu}_1$ | $\overline{\mu}_2$ | $\overline{w}$ |
|---|---|---|---|---|---|
| 1.00 | 1.057334324 | -2.114668648 | 0.660530720 | 0.339469280 | 6.443182771 |
| $10^{-1}$ | 1.006069204 | -2.012138408 | 0.665995028 | 0.334004972 | 5.144427985 |
| $10^{-2}$ | 1.000610687 | -2.001221375 | 0.666598840 | 0.333401160 | 5.014444275 |
| $10^{-3}$ | 1.000061107 | -2.000122214 | 0.666659877 | 0.333340123 | 5.001444443 |
| $10^{-4}$ | 1.000006111 | -2.000012222 | 0.666665988 | 0.333334012 | 5.000144444 |
| $10^{-5}$ | 1.000000611 | -2.000001222 | 0.666666599 | 0.333333401 | 5.000014444 |
| $10^{-6}$ | 1.000000061 | -2.000000122 | 0.666666660 | 0.333333340 | 5.000001444 |
| $10^{-7}$ | 1.000000006 | -2.000000012 | 0.666666666 | 0.333333334 | 5.000000144 |
| $10^{-8}$ | 1.000000001 | -2.000000001 | 0.666666667 | 0.333333333 | 5.000000014 |
| $10^{-9}$ | 1 | -2 | 0.666666667 | 0.333333333 | 5.000000001 |
| $10^{-10}$ | 1 | -2 | 0.666666667 | 0.333333333 | 5 |

| | | | | | |
|---|---|---|---|---|---|
| *Solution*: | 1 | -2 | $\frac{2}{3}$ | $\frac{1}{3}$ | 5 |

**Table 4.5.**

| $T$ | $\bar{x}_{1(T)}$ | $\bar{x}_{2(T)}$ | $\delta\bar{x}_{1(T)}$ | $\delta\bar{x}_{2(T)}$ | $\bar{x}_{1(T+1)}$ | $\bar{x}_{2(T+1)}$ | $\bar{F}_{(T+1)}$ | $\bar{G}_{(T+1)}$ |
|---|---|---|---|---|---|---|---|---|
| 0 | 1.019246 903 | -2.038493 805 | -0.018868 520 | 0.037737 040 | 1.000378 383 | -2.000756 765 | 5.003784 542 | 4.992431 632 |
| 1 | 1.000378 383 | -2.000756 765 | $-3.7824\cdot 10^{-4}$ | $7.5648\cdot 10^{-4}$ | 1.000000 143 | -2.000000 286 | 5.000001 431 | 4.999997 138 |
| 2 | 1.000000 143 | -2.000000 286 | $-1.4321\cdot 10^{-7}$ | $2.8612\cdot 10^{-7}$ | 1 | -2 | 5 | 5 |
| 3 | 1 | -2 | … | … | … | … | … | … |
| $\infty$ | 1 | -2 | 0 | 0 | 1 | -2 | 5 | 5 |

## FEEDBACK FUNCTIONS IN GAME THEORY PROBLEMS

One of the areas of mathematical modeling that uses the minimax (or maximin) operator is game theory.

Since the feedback function method there is a tool for searching minimax values, then the main features of its application can be considered for the case of a standard game problem [Fudenberg, 1991]. However, we complicate the condition of the tasks so to demonstrate the capabilities feedback method in full.

Suppose we need to find optimal strategies opposing players for a known zero-sum payment matrix. We consider the following version of the task.

Let we have two players: first *A* and second *B*. Each of them has its own set of strategies with numbers $j=\overline{1,n}$ and $i=\overline{1,m}$ respectively. The elements of the payment matrix are numbers $\alpha_{ij}$. Here $\alpha_{ij}$ equal to the winning values for player *A* and loss for *B*, subject to the first player's choice of strategy is *j* and for the second is *i*. We will also assume that the elements of the payment matrix are fairly smooth functions of a parameter vector $p=(p_1,p_2,\ldots,p_K)^{\mathrm{T}}\in \mathrm{T},$ where $\mathrm{T}$ is a domain in $E^K$.

We denote the vector of mixed strategy of player *A* as $x=(x_1,x_2,\ldots,x_n)^{\mathrm{T}}$, where $x_j$ is the probability of choice the first player of the strategy with number *j*. The optimal payoff of the first player $v$ is the solution to the linear parametric programming problem:

$$\begin{aligned} &\text{maximize by } \{x,v\}: \text{ function } v \\ &\text{under conditions: } x_j\ge 0 \quad \forall j=\overline{1,n}; \qquad \sum_{j=1}^{n} x_j=1; \\ &\sum_{j=1}^{n}\alpha_{ij}(p)x_j\ge v \qquad \forall i=\overline{1,m}. \end{aligned} \tag{5.1}$$

As noted in the introduction, the solution to problem (5.1) is the dependence $\left\{x_p^*, v_p^*\right\}$. The dependence may not be defined in everything $E^{n+1}$, may not be a function of *p*, and (in the case of functionality) have no derivatives with respect to the components of *p*. A detailed description of the use of feedback functions to solve parametric problems is given in [Umnov, 2023].

The value $\sum_{j=1}^{n} \alpha_{ij}(p) x_j$ is a mathematical expectation player's winnings *A*, when player B chooses strategy *i*. It is also known from game theory that optimal mixed strategy of player *B* $\lambda = (\lambda_1, \lambda_2, \ldots, \lambda_m)^{\mathrm{T}}$ is a solution to the problem dual to problem (5.1):

$$\begin{gathered} \text{minimize by } \{\lambda, \mu\} \quad \textit{function } \mu \\ \text{under conditions: } \lambda_i \geq 0 \quad \forall i = \overline{1,m}; \qquad \sum_{i=1}^{m} \lambda_i = 1; \\ \sum_{i=1}^{m} \alpha_{ij}(p) \lambda_i \leq \mu \quad \forall j = \overline{1,n}\,. \end{gathered} \tag{5.2}$$

The quantity $\sum_{i=1}^{m} \alpha_{ij}(p) \lambda_i$ is a mathematical expectation loss of player *B*, when player *A* chooses strategy *j*. The solution to problem (5.2) will be denoted by $\left\{\lambda_p^*, \mu_p^*\right\}$. Let also the components of the vector *p* and parameter $\tau > 0$ be fixed.

We use the method of feedback functions as a search for stationary points auxiliary function

$$U(\tau, x, \lambda, v, \mu, p) = v - \sum_{i=1}^{m} \lambda_i \left( v - \sum_{j=1}^{n} \alpha_{ij}(p) x_j \right) - \mu \left( -1 + \sum_{j=1}^{n} x_j \right) - \sum_{j=1}^{n} R(\tau, x_j) + \sum_{i=1}^{m} R(\tau, \lambda_i)\,. \tag{5.3}$$

The stationarity conditions for (5.3) are determined by the following system of equations

$$\begin{cases} \sum_{i=1}^{m} \alpha_{ij}(p) \bar{\lambda}_i - \bar{\mu} - Q(\tau, \bar{x}_j) = 0 & \forall j = \overline{1,n}, \\ 1 - \sum_{i=1}^{m} \lambda_i = 0, \qquad 1 - \sum_{j=1}^{n} x_j = 0, & \\ \sum_{j=1}^{n} \alpha_{ij}(p) \bar{x}_j - \bar{v} + Q(\tau, \bar{\lambda}_i) = 0 & \forall i = \overline{1,m}. \end{cases} \tag{5.4}$$

In [Umnov, 2019] it is shown that $\forall p \in E^K$ system (5.4) is uniquely solvable. In this case, the equalities are true for $\bar{v}(\tau, p)$ and $\bar{\mu}(\tau, p)$: $\lim_{\tau \to +0} \bar{v}(\tau, p) = v_p^*$ and $\lim_{\tau \to +0} \bar{\mu}(\tau, p) = \mu_p^*$.

Theorem 2.3 remains valid if parameter $\tau$ is replaced with any of the components of the vector *p*. Therefore, functions $\bar{v}(\tau, p)$ and $\bar{\mu}(\tau, p)$ can be used as smooth approximations of dependencies $v_p^*$ and $\mu_p^*$.

Let, say, the second-order derivatives of $\alpha_{ij}(p)$ be continuous. Then to solve problems we can use Taylor approximations of functions $\bar{v}(\tau, p)$ and $\overline{\mu}(\tau, p)$ up to the second order inclusive. For example, as it was done in [Umnov, 2023], let's apply to system (5.4) both rule for differentiating a composite function and theorem about implicit functions. This will allow us to get

$$\overline{U}'_{p_t} = \frac{\partial U}{\partial p_t}\left(\tau, \bar{x}, \bar{\lambda}, \bar{v}, \overline{\mu}, p\right) = \sum_{i=1}^{m}\sum_{j=1}^{n} \bar{x}_j \bar{\lambda}_i \frac{\partial \alpha_{ij}(p)}{\partial p_t} \qquad \forall t = \overline{1, K}. \tag{5.5}$$

Function (5.5) is a smooth approximation of $\operatorname{grad}_p \bar{v}(\tau, p)$.

Let us now demonstrate the use of feedback functions to solve a minimax problem with a payment matrix, depending on two scalar parameters *p* and *q*,

$$\left\| D_{ij}(p,q) \right\| = \begin{Vmatrix} 1 & 25-p-q & 3 & 4 \\ 5 & p & 7 & 8 \\ 9 & q & 11 & 12 \end{Vmatrix}, \tag{5.6}$$

where $p \in [0,15]$ and $q \in [0,15]$.

It is clear that values $D_{\min\max}(p,q) = \min\limits_{i=\overline{1,3}}\left( \max\limits_{j=\overline{1,4}} D_{ij}(p,q) \right)$ and $D_{\max\min}(p,q) = \max\limits_{j=\overline{1,4}}\left( \min\limits_{i=\overline{1,3}} D_{ij}(p,q) \right)$ are continuous, piecewise linear functions of *p* and *q*. To explore other properties of $D_{\min\max}(p,q)$ and $D_{\min\max}(p,q)$, we use their smooth approximations obtained by the method of feedback functions. From (4.1) and (4.2) we have $\overline{D}_{\min\max}(\tau, p, q) = -\tau \ln \sum\limits_{j=1}^{4}\left( \sum\limits_{i=1}^{3} \exp \frac{D_{ij}(p,q)}{\tau} \right)^{-1}$,

$\overline{D}_{\max\min}(\tau, p, q) = \tau \ln \sum\limits_{i=1}^{3}\left( \sum\limits_{j=1}^{4} \exp\left( -\frac{D_{ij}(p,q)}{\tau} \right) \right)^{-1}$.

Isoline systems for functions $\overline{D}_{\min\max}(\tau, p, q)$ and $\overline{D}_{\max\min}(\tau, p, q)$ at value $\tau = 0.05$ are shown in Fig. 5.1 and 5.2 respectively. These pictures also show their meanings at some characteristic points.

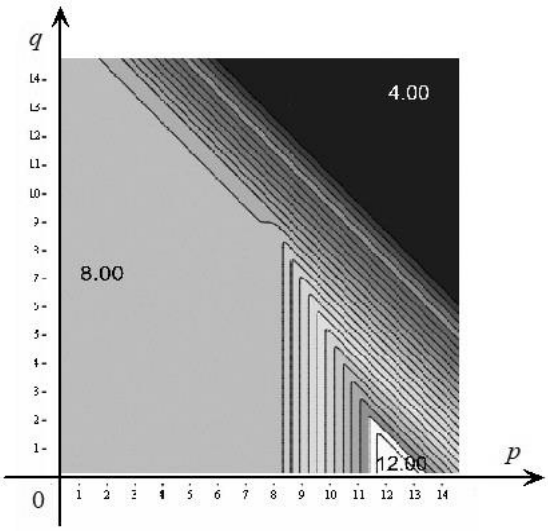


**Fig. 5.1. System of isolines for function** $\overline{D}_{\min\max}(\tau, p, q)$

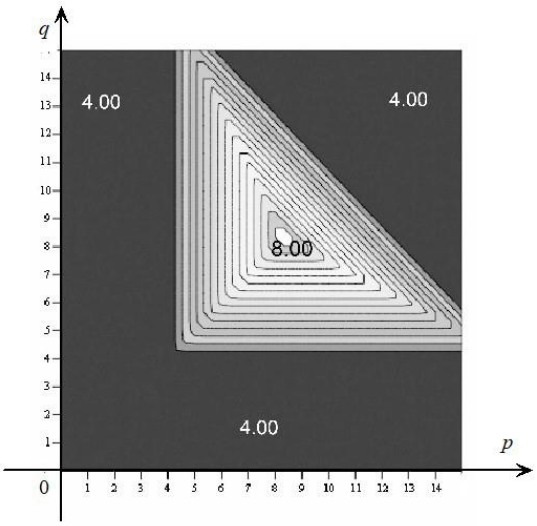


**Fig. 5.2. System of isolines for function** $\overline{D}_{\max\min}(\tau, p, q)$

It is known that a solution to the pair of problems (5.1) – (5.2) in mixed strategies exists for any payment matrix. However, solutions in pure strategies} are of particular interest. Recall that solutions in pure strategies have all components equal to zero, except one, equal to 1.

The condition for the existence of solutions in pure strategies is the following fact. The payment matrix has a saddle element, that is, the element $\alpha_{ij}^{*}$, for which $\alpha_{ij}^{*} = D_{\min\max} = D_{\max\min}$. The fulfillment of this condition is obvious depends on the values of the parameters *p* and *q*. In Fig. 5.3 is shown isoline system for a function $\overline{D}_{\min\max}(\tau, p, q) - \overline{D}_{\max\min}(\tau, p, q)$ at $\tau = 0.05$. Points where a saddle element exists are marked here in black.

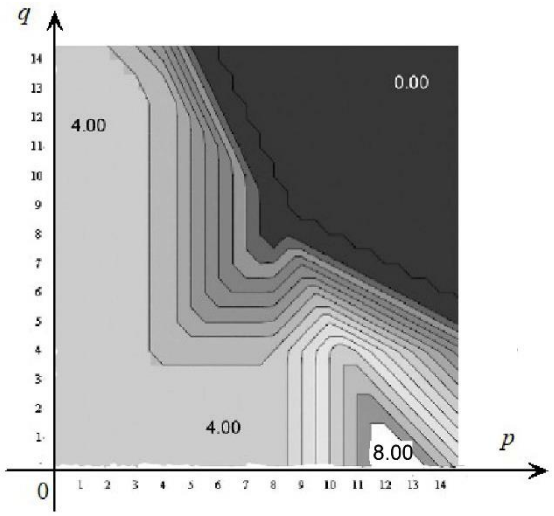


**Fig. 5.3 System of isolines for function** $\overline{D}_{\min\max}(\tau, p, q) - \overline{D}_{\max\min}(\tau, p, q)$

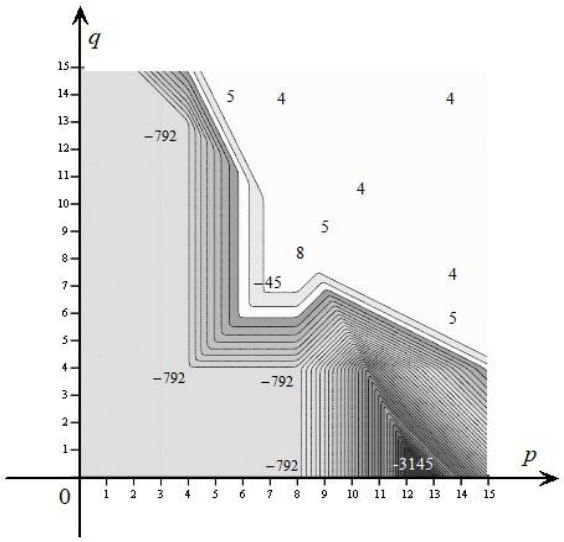


**Fig. 5.4. System of isolines for function** $\Omega(\Theta, p, q)$ **at scall 1.00**

A detailed study of the properties auxiliary function *U* may require its numerical characteristics with higher accuracy. To get this we can use in (5.4) feedback function $Q(\tau, s) = \frac{\tau}{2}\left(s - \frac{1}{s}\right)$ instead of function $Q(\tau, s) = \tau \ln s$. As an illustration in Table 5.1*a* and 5.1*b* show the values of the argument's stationary points auxiliary function (5.3) at $p = 10, q = 9$ for different $\tau$. Note also that in this example derivatives (5.5) are found according to the formulas $\overline{U}'_p = -\bar{x}_2\bar{\lambda}_1 + \bar{x}_2\bar{\lambda}_2$ and $\overline{U}'_q = -\bar{x}_2\bar{\lambda}_1 + \bar{x}_2\bar{\lambda}_3$.

**Table 5.1*a***

| $\tau$ | $\bar{x}_1$ | $\bar{x}_2$ | $\bar{x}_3$ | $\bar{x}_4$ | $\bar{v}$ | $U(\tau, \bar{x}, \bar{\lambda}, \bar{v}, \bar{\mu}, p, q)$ |
|---|---|---|---|---|---|---|
| $10^{-1}$ | 0.010143028 | 0.946888255 | 0.017065774 | 0.025902943 | 5.843463575 | 5.783467242 |
| $10^{-2}$ | 1.0016 $\cdot 10^{-3}$ | 0.994816832 | 1.6712 $10^{-3}$ | 2.5103 $\cdot 10^{-3}$ | 5.984928431 | 5.966469792 |

| | | | | | | |
|---|---|---|---|---|---|---|
| $10^{-3}$ | 1.0002 $\cdot 10^{-4}$ | 0.999483166 | 1.6671 $\cdot 10^{-4}$ | 2.5010 $\cdot 10^{-4}$ | 5.998499278 | 5.995491834 |
| $10^{-4}$ | 1.0000 $\cdot 10^{-5}$ | 0.999948332 | 1.6667 $\cdot 10^{-5}$ | 2.5001 $\cdot 10^{-5}$ | 5.999849993 | 5.999434015 |
| $10^{-5}$ | 1.0000 $\cdot 10^{-6}$ | 0.999994833 | 1.6667 $\cdot 10^{-6}$ | 2.5000 $\cdot 10^{-6}$ | 5.999985000 | 5.999931888 |
| $10^{-6}$ | 1.0000 $\cdot 10^{-7}$ | 0.999999483 | 1.6667 $\cdot 10^{-7}$ | 2.5000 $\cdot 10^{-7}$ | 5.999998500 | 5.999992038 |
| $10^{-7}$ | 1.0000 $\cdot 10^{-8}$ | 0.999999948 | 1.6667 $\cdot 10^{-8}$ | 2.5000 $\cdot 10^{-8}$ | 5.999999850 | 5.999999089 |
| *Solution*: | 0 | 1 | 0 | 0 | 6 | 6 |

**Table 5.1*b***

| $\tau$ | $\overline{\lambda}_1$ | $\overline{\lambda}_2$ | $\overline{\lambda}_3$ | $\overline{\mu}$ | $\overline{U}'_p$ | $\overline{U}'_q$ |
|---|---|---|---|---|---|---|
| $10^{-1}$ | 0.972216214 | 0.012489251 | 0.015294535 | 6.101300739 | -0.908754189 | -0.906097899 |
| $10^{-2}$ | 0.997097639 | $1.2500 \cdot 10^{-3}$ | $1.6524 \cdot 10^{-3}$ | 6.010009038 | -0.990686004 | -0.990285707 |
| $10^{-3}$ | 0.999708477 | $1.2500 \cdot 10^{-4}$ | $1.6652 \cdot 10^{-4}$ | 6.001000087 | -0.999066859 | -0.999025357 |
| $10^{-4}$ | 0.999970835 | $1.2500 \cdot 10^{-5}$ | $1.6665 \cdot 10^{-5}$ | 6.000100001 | -0.999906669 | -0.999902504 |
| $10^{-5}$ | 0.999997083 | $1.2500 \cdot 10^{-6}$ | $1.6667 \cdot 10^{-6}$ | 6.000010000 | -0.999990667 | -0.999990250 |
| $10^{-6}$ | 0.999999708 | $1.2500 \cdot 10^{-7}$ | $1.6667 \cdot 10^{-7}$ | 6.000001000 | -0.999999067 | -0.999999025 |
| $10^{-7}$ | 0.999999971 | $1.2500 \cdot 10^{-8}$ | $1.6667 \cdot 10^{-8}$ | 6.000000100 | -0.999999907 | -0.999999903 |
| *Solution*: | 1 | 0 | 0 | 6 | -1 | -1 |

The values of parameters *p* and *q* for which saddle elements exist are not unique. This allows us to generalize the formulation of the problem under consideration. For example, you can consider the following problem.

**Example 5.1**

For the game with payoff matrix (5.6) find parameter values *p* and *q*, at which the value $D_{\min\max}$ has a maximum on the set of pure strategies.

**Solution.**

1°: Since the existence of a solution in pure strategies requires the existence of a saddle element in the payment matrix, the formulation of this problem can look like: maximize by $\{p,q\}$ function $D_{\min\max}(p,q)$ under conditions $0 \le p \le 15, \quad 0 \le q \le 15, \; D_{\min\max}(p,q) - D_{\max\min}(p,q) = 0.$

2°. Let's use the method penalty functions [Fiacco, McCormick, 1968] to estimate the required values of *p* and *q*. This method may consist of unconditionally maximizing the auxiliary function of the form

$\Omega(\Theta, p, q) = \overline{D}_{\min\max}(p,q) - \frac{1}{2\Theta}\left(\overline{D}_{\min\max}(p,q) - \overline{D}_{\max\min}(p,q)\right)^2$ for a small positive value of $\Theta$.

The smoothing property of the penalty function method is illustrated in Fig. 5.4–5.6. These figures show a system of isolines of the function $\Omega(\Theta, p, q)$ at three different scales. These figures also show the values of the function $\Omega(\Theta, p, q)$ at $\Theta = 0.01$.

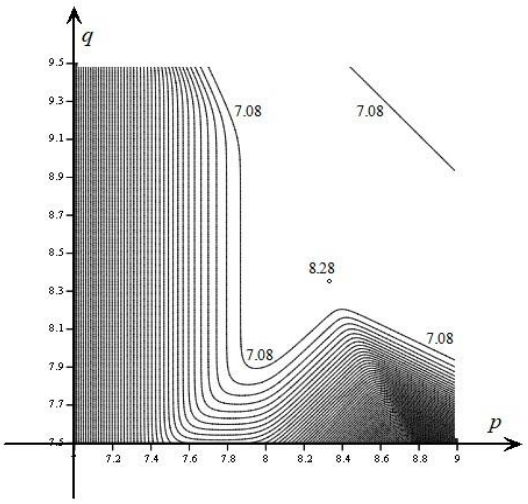


**Fig. 5.5. System of isolines for a function $\Omega(\Theta, p, q)$ at scale 0.10**

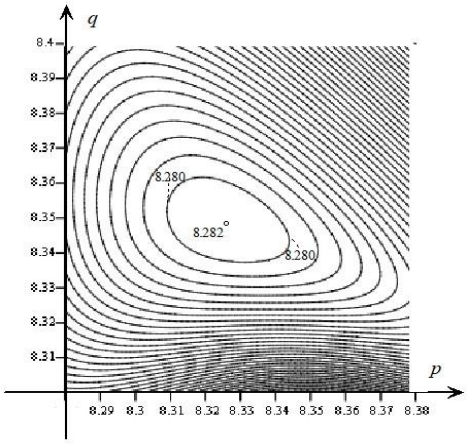


**Fig. 5.6. System of isolines for a function $\Omega(\Theta, p, q)$ at scale 0.01**

The maximum of function $\Omega(\Theta, p, q)$ is 8.28158929. It is with $\Theta = 0.01$ at $p$=8.325815949 and $q$=8.348452929. The norm of the gradient of the function $\Omega(\Theta, p, q)$ at this point is equal to $1.4541 \cdot 10^{-6}$.

3°. To obtain an exact solution in the example 5.1 it is convenient to use the method linear extrapolation. This method has already been considered in detail for problem 4.1. Therefore, here we will limit ourselves to discussing the final estimates obtained using formulas similar to (4.12): $p^* = 8.33333333$ and $q^* = 8.33333333$. Table 5.2*a* and 5.2*b* show solution of system (5.4) for these values of $p$ and $q$ at different $\tau$.

**Table 5.2*a***

| $\tau$ | $\bar{x}_1$ | $\bar{x}_2$ | $\bar{x}_3$ | $\bar{x}_4$ | $\bar{v}$ | $U(\tau, \bar{x}, \bar{\lambda}, \bar{v}, \bar{\mu}, p, q)$ |
|---|---|---|---|---|---|---|

| | | | | | | |
|---|---|---|---|---|---|---|
| $10^{-1}$ | 9.1459 $\cdot 10^{-3}$ | 0.956169686 | 0.014420881 | 0.020263533 | 8.058310734 | 7.755364268 |
| $10^{-2}$ | 9.1515 $\cdot 10^{-4}$ | 0.995611686 | 1.4436 $10^{-3}$ | 2.0296 $\cdot 10^{-3}$ | 8.305809423 | 8.241009057 |
| $10^{-3}$ | 9.1516 $\cdot 10^{-5}$ | 0.999561163 | 0.000144361 | 2.0296 $\cdot 10^{-4}$ | 8.330580921 | 8.320647039 |
| $10^{-4}$ | 9.1516 $\cdot 10^{-6}$ | 0.999956116 | 1.4436 $\cdot 10^{-5}$ | 2.0296 $\cdot 10^{-5}$ | 8.333058092 | 8.331719316 |
| $10^{-5}$ | 9.2730 $\cdot 10^{-7}$ | 0.999995508 | 1.4740 $\cdot 10^{-6}$ | 2.0903 $\cdot 10^{-6}$ | 8.333306242 | 8.333137414 |
| $10^{-6}$ | 1.3369 $\cdot 10^{-7}$ | 0.999998903 | 2.8735 $\cdot 10^{-7}$ | 6.7565 $\cdot 10^{-7}$ | 8.333330906 | 8.333311038 |
| $10^{-7}$ | 1.5512 $\cdot 10^{-8}$ | 0.999999720 | 4.0876 $\cdot 10^{-8}$ | 2.2400 $\cdot 10^{-7}$ | 8.333333009 | 8.333330847 |
| *Solution*: | 0 | 1 | 0 | 0 | $\frac{25}{3}$ | $\frac{25}{3}$ |

**Table 5.2*b***

| $\tau$ | $\overline{\lambda}_1$ | $\overline{\lambda}_2$ | $\overline{\lambda}_3$ | $\overline{\mu}$ | $\overline{U}'_p$ | $\overline{U}'_q$ |
|---|---|---|---|---|---|---|
| $10^{-1}$ | 0.657125682 | 0.217912820 | 0.124961498 | 8.337816823 | -0.419962024 | -0.508839261 |
| $10^{-2}$ | 0.657393186 | 0.217761533 | 0.124845281 | 8.333377313 | -0.437702412 | -0.530210918 |
| $10^{-3}$ | 0.657395820 | 0.217760043 | 0.124844137 | 8.333333772 | -0.439442849 | -0.532317980 |
| $10^{-4}$ | 0.657395847 | 0.217760028 | 0.124844125 | 8.333333338 | -0.439616526 | -0.532528351 |
| $10^{-5}$ | 0.640002794 | 0.234666153 | 0.125331054 | 8.333333333 | -0.405334820 | -0.514669428 |
| $10^{-6}$ | 0.410689714 | 0.280293397 | 0.309016889 | 8.333333334 | -0.130396173 | -0.101672713 |
| $10^{-7}$ | 0.257461958 | 0.457547439 | 0.284990604 | 8.333333333 | 0.200085425 | 0.027528638 |
| *Solution*: | *** | *** | *** | $\frac{25}{3}$ | *** | *** |

Note that for $p^* = \frac{25}{3}$ and $q^* = \frac{25}{3}$ saddle elements of matrix (5.6) exist. These are elements $D_{12}, D_{22}$ and $D_{32}$. But the solution in Table 5.2*b* is not a solution in pure strategies to problem (5.2).

The point is that the solution to problem (5.2) is ambiguous, while the solution to problem (5.1) is overdetermined. The solution to problem (5.2) is any ordered triple of non-negative numbers $\{\lambda_1^*, \lambda_2^*, \lambda_3^*\}$ such that $\lambda_1^* + \lambda_2^* + \lambda_3^* = 1$.

Among them, there are three in pure strategies. One such solution with $\lambda_1^* = 0, \lambda_2^* = 1, \lambda_3^* = 0$ shown in Table 5.3*a* and 5.3*b*.

For example, this solution can be obtained by adding to system (5.4) the inequality $x_2 \geq 1$. It has the same optimal objective function value, as the solution in table. 5.2*a* and 5.2*b*. Other solutions in pure strategies $\lambda_1^* = 0, \lambda_2^* = 1, \lambda_3^* = 0$ and $\lambda_1^* = 0, \lambda_2^* = 1, \lambda_3^* = 0$ are found similarly.

**Table 5.3*a***

| $\tau$ | $\bar{x}_1$ | $\bar{x}_2$ | $\bar{x}_3$ | $\bar{x}_4$ | $\bar{v}$ | $U(\tau, \bar{x}, \bar{\lambda}, \bar{v}, \bar{\mu}, p, q)$ |
|---|---|---|---|---|---|---|
| $10^{-15}$ | 0 | 1 | 0 | $1.5000 \cdot 10^{-15}$ | 8.333333314 | 8.333333333 |
| *Solution*: | 0 | 1 | 0 | 0 | $\frac{25}{3}$ | $\frac{25}{3}$ |

**Table 5.3*b***

| $\tau$ | $\bar{\lambda}_1$ | $\bar{\lambda}_2$ | $\bar{\lambda}_3$ | $\bar{\mu}$ | $\bar{U}'_p$ | $\bar{U}'_q$ |
|---|---|---|---|---|---|---|
| $10^{-15}$ | $1.6928 \cdot 10^{-8}$ | 0.999999979 | $1.7177 \cdot 10^{-8}$ | 8.337816823 | 0.999999962 | $2.4870 \cdot 10^{-10}$ |
| *Solution*: | 0 | 1 | 0 | $\frac{25}{3}$ | *** | *** |

## CONCLUSION

This article discusses methods for searching for multiple extrema, as well as minimax (maximin) values.

Suggested method consists in constructing a smooth approximation of saddle points modified Lagrange function. This modification uses functions that implement feedback within optimality conditions. The stationarity conditions for the modified Lagrange function are similar to the conditions of the Karush-Kuhn-Tucker theorem. But they do not contain both non-negativity restrictions for variables and conditions of complementary non-rigidity. This article also formulates the properties of feedback functions, which provide the required smoothness for approximations. A possible direction of development of the proposed method is increasing its efficiency. According to the authors, this is the subject of special research. However, some ideas can be formulated here already.

For example, you can reduce the dependence of the calculation process on initial approximations. To do this, it is enough to replace the non-negative variables in (2.9) with their absolute values. That is, instead of system (2.9), we will solve the system

$$\begin{cases} \operatorname{grad}\limits_{x} U\left(\tau, |\bar{x}_1|, |\bar{x}_2|, \ldots, |\bar{x}_q|, \bar{x}_{q+1}, \ldots, \bar{x}_n, |\bar{\lambda}_1|, |\bar{\lambda}_2|, \ldots, |\bar{\lambda}_p|, \bar{\lambda}_{p+1}, \ldots, \bar{\lambda}_m\right) = o, \\ \operatorname{grad}\limits_{\lambda} U\left(\tau, |\bar{x}_1|, |\bar{x}_2|, \ldots, |\bar{x}_q|, \bar{x}_{q+1}, \ldots, \bar{x}_n, |\bar{\lambda}_1|, |\bar{\lambda}_2|, \ldots, |\bar{\lambda}_p|, \bar{\lambda}_{p+1}, \ldots, \bar{\lambda}_m\right) = o. \end{cases} \quad (6.1)$$

The solution process to (6.1) can end in any orthant of $E^n \otimes E^m$. But the solution to system (2.9) will obviously be obtained from the solution to (6.1) replacing the found component values $\bar{x}$ and $\bar{\lambda}$ with their absolute values. Note that this technique was used to solve all the problems discussed above. Also, according to the authors, it would be interesting to investigate convergence of solution of system (2.9). Especially in case when one of the problems of the dual pair is ill-conditioned, and the second is overdetermined. This situation, for example, occurs for problems (5.1) – (5.2).

## REFERENCES

1. Bazaraa M.S., Sherali H.D., Shetty C.M. Nonlinear programming: Theory and Algorithms. New Jersey, John Wiley \& Sons, Inc., 2006.

2. Dimitri P. Bertsekas. Nonlinear Programming. Athena Scientific, Belmont MA, 2016.

3. Danskin J. The theory of Max-Min and its application to weapons allocation problems. // N.Y. Springer. 1967.

4. Demyanov V.F., Vasiliev L.V. Nondifferentiable optimization. // M. Nauka. 1981, 384~P.

5. Dem'yanov V.F., Vasil'yev L.V. Nedifferentsiruyemaya optimizatsiya. // M. Nauka. 1981, 384~S. (in Russian)

6. Germeier Yu.B. Approximate reduction using penalty functions of the problem of determining the maximin to the problem of determining the maximum. // ZhVM-MF. 1969. V. 9, No. 3. P. 730-731.

7. Germeyyer YU.B. Priblizhennoye svedeniye s pomoshch'yu shtrafnykh funktsiy zadachi opredeleniya maksimina k zadache opredeleniya maksimuma. // ZHVM-MF. 1969. T. 9, № 3. S. 730-731. (in Russian)

8. Izmailov A.F. Sensitivity in optimization. // - M.: Fizmatlit, 2006. - 245 p.

9. Izmailov A.F. Chuvstvitel'nost' v optimizatsii. // -- M.: Fizmatlit, 2006. -- 245 S.(in Russian)

10. Fedorov V.V. Numerical methods of maximin. // M. Science. 1979. 279 p.

11. Fedorov V.V. Chislennyye metody maksimina. // M. Nauka. 1979. 279 S. (in Russian)

12. Fedoryuk M.V. Pass method. // M. Science. 1977. 368 p.

13. Fedoryuk M.V. Metod perevala. // M. Nauka. 1977. 368 S. (in Russian)

14. Fiacco A.V. Introduction to Sensitivity and Stability Analysis in Nonlinear Programming. // N.Y.: Academic Press, 1983.

15. Fiacco A.V., McCormickG.P. Nonlinear Programming: Sequential Unconstrained Minimization Techniques. N.Y.: John Wiley and Sons, 1968. – 210 P.

16. Fudenberg Dr., Tirole J. Game Theory. The MIT Press. : Cambridge, Massachusetts, 1991. -- 604 P.

17. Nurminsky E.A. Numerical methods of convex optimization. // ~M.: Science, 1991. - 168 p.

18. Nurminskiy E.A. Chislennyye metody vypukloy optimizatsii. // ~M.: Nauka, 1991. - 168 S. (in Russian)

19. Rockafellar T. Convex Analysis. // Prinseton University Press. 1970. v.3.

20. Umnov A.E., Umnov E.A. Using feedback functions in linear programming problems. Computational Mathematics and Mathematical Physics, 2019, Volume 59, Issue 10, PP. 1626–1638. DOI: https://doi.org/10.1134/S0965542519100142

21. Umnov A.E., Umnov E.A. Feedback Functions in Problems of Nonlinear Programming. // SCIREA Journal of Mathematics, 2022, Volume 7, Issue 5, PP 67-82, DOI: 10.54647/mathematics11348

21. Umnov A.E., Umnov E.A. Using feedback functions to solve parametric programming problems // Computer Research and Modeling, 2023, vol. 15, no. 5, PP. 1125-1151. DOI: 10.20537/2076-7633-2023-15-5-1125-1151

22. Umnov E.A., Umnov A.E. Parametric problems in mathematical programming. M.: MIPT, 2018. – 297 P. //www.umnov.ru

23. Umnov E.A., Umnov A.E. Parametricheskiye zadachi v matematicheskom programmirovanii. M.: MFTI, 2018. – 297 S. //www.umnov.ru (in Russian)

Applied Sciences Research Periodicals – ISSN 3033-330X
May 2024, Vol. 2, No. 5, pp. 43-49.

# Biotope Distribution of The Common Fox in The Steppe Zone of Ukraine

Anatoly M. Volokh[1] & Nikolai V. Rozhenko[2]

1. Department of the Geoecology and Land management Dmytro Motornyi Tavria State Agrotechnological University, Melitopol: Ukraine
2. National Natural Park "Nizhnednestrovsky", Odessa: Ukraine

**Abstract:**
In the steppe zone, foxes use fields, meadows and steppe areas characterised by good visibility during daytime rest. A total of 37.8% of individuals were recorded in these areas, with the highest numbers on the coasts of the Dnipro (48.9%), Azov (43.3%) and Black (29.9%) Seas. In forested areas, foxes rested most often in deciduous (12.5%) and pine plantations (2.8%), while in field areas - in forest belts (6.7%), uncultivated fields (16.2%), and in orchards and vineyards (7.6%). However, the largest number of individuals (32.6%) was found in thickets of southern reeds (Phragmites australis) and other aquatic plants. In the Black Sea region, more than 45% of foxes spent the day in reed beds. This resulted in a high population density (26.6±1.37 individuals/10 ha or 4.4±0.18 per reed bed). The probability of encountering predators in such areas, which usually do not exceed 1-2 ha (49.4%), is very high - out of 231 surveyed sites, animals were absent only in 2. The location of foxes' dwellings, which they create to breed their young, is peculiar: the main number of dens (about 23%) was located on the forest margins, somewhat less - in the treeless valleys of small rivers, as well as on the banks of estuaries. In the Black Sea region, many burrows (18.5%) were found in floodplains of large rivers (Danube, Dniester, Southern Bug and Dnieper), and in the Azov region - on sea spits and islands (14.3%), as well as in numerous forest belts (11.5%). After the dust storms of 1969, many of these sites were covered with high earthen berms made of wind-blown black soil. This improved conditions for dens of all predatory animals, but especially for foxes. Already in the early 20th century in Ukraine, they began to avoid open steppes and fields, although they made holes in haystacks that had been stored for many years and used to feed sheep.

*Keywords: vox, steppe zone, Ukraine, population, dynamics, structure, biotopes.*

## INTRODUCTION

The most numerous predators of the steppe zone are undoubtedly the common fox. Since it is less picky than other animals in choosing places to rest and feed, the geographical variability of its biotope distribution is quite high. In Germany, most foxes rest in dense shrubs and meadows (Pielowski, 1976), in Denmark - in swamps (Jensen, 1968), in the mountainous regions of Azerbaijan - in rock crevices or small grottoes (Gidayatov, 1965), in Spain - in blackberry bushes (Blanco, 1986), etc. The fox can be found anywhere: in fields, meadows, forests, gardens, and even in settlements. There are cases of repeated visits of this predator to Odesa, Zaporizhzhia, Dnipro, Lviv and other large cities, and there is nothing to say about villages. In Western Europe, urban populations of foxes have formed, which are typical for Copenhagen (Jensen, 1968), Bristol, London (Harris and Smith, 1987), Berlin (Börner u. a., 2009) and other cities. Therefore, the purpose of our research was to study the biotopic distribution of the common fox in the steppe regions of Ukraine, which are characterised by regular intensive agricultural development.

## MATERIALS AND METHODS

In 1978-2014, during hunting (12.X - 22.I) in the southern districts of Zaporizhzhia and Kherson (Azov Sea), Mykolaiv and Odesa (Black Sea), northern districts of Zaporizhzhia, Dnipro, Donetsk (Dnipro) regions, more than 3000 individuals of the common fox were recorded. In most cases, the animals were taken by hunters using different hunting dogs. In the Black Sea region, these were hunting hounds, in the Azov Sea region - Foxterriers and Jagdterriers, in the Dnipro River region - Siberian huskies. In those years, the fur of 1 common fox was worth 100-150 USD, and therefore its extraction was economically very profitable for a hunter. This contributed to keeping the number and density of the predator population at a low and stable level (1-2 individuals/ 1 thousand hectares), as defined by the World Health Organisation. In addition, several tens of thousands of foxes were counted in the hunting grounds of the steppe regions of Ukraine during special surveys during the time prohibited for hunting. The collected scientific material was processed, if necessary, by regression and correlation analyses using the CSS software package (Microsoft-Corpiring). In most cases, the 95% confidence level (P = 0.05) was used when comparing fox population densities.

## DISCUSSION

In the steppe zone, the first category includes fields, meadows and steppe areas characterised by very good visibility. In such places, foxes build their dens both on flat surfaces and on small elevations, which can be piles of stalks of various crops, earthen blocks, mounds, straw piles, etc. These animals often rest on the ground in open areas during the rut. At the time of high prices for fox fur, there was even a specialisation of hunters who used binoculars to track down animals resting in the open, carefully approach them within shooting distance and often kill them. The location of daytime fox dens in open areas is very typical for steppe reserves (Askania Nova, Chornomorskyi, Ukrainian Steppe). It is also typical for other regions, including the forest-steppe (Polushina, 1967) and forest zones, taiga and even tundra (Geptner et al., 1967). In Prydniprovia, 37.8% of foxes were recorded in fields, meadows and steppe areas (Table 1).

**Table 1: Biotopic distribution of foxes in 1978-2014**

| B i o t o p s | Dnieper region* | | Black Sea region | | Azov Sea region | | Total: | |
|---|---|---|---|---|---|---|---|---|
| | Abs. | % | Abs. | % | Abs. | % | Abs. | % |
| Meadows | 76 | 9.4 | 275 | 17.5 | 150 | 22.7 | 501 | 16.5 |
| Reed thickets | 98 | 12.1 | 737 | 46.9 | 155 | 23.6 | 990 | 32.6 |
| Deciduous forests | 93 | 11.5 | 221 | 14.0 | 64 | 9.7 | 378 | 12.5 |
| Coniferous forests | 10 | 1.2 | 58 | 3.7 | 18 | 2.7 | 86 | 2.8 |
| Gardens, vineyards | 109 | 13.5 | 45 | 2.9 | 77 | 11.7 | 231 | 7.6 |
| Fields | 194 | 24.1 | 195 | 12.4 | 103 | 15.7 | 492 | 16.2 |
| Forest belts | 103 | 12.8 | 41 | 2.6 | 59 | 9.0 | 203 | 6.7 |
| Steppe areas | 124 | 15.4 | – | – | 32 | 4.9 | 156 | 5.1 |
| Total: | 807 | 100.0 | 1572 | 100.0 | 658 | 100.0 | 3037 | 100.0 |

Data from: *N. Lebedeva, V. Domnich (1998)

The reason for this is the high density of their population in this region, which led to the frequent appearance of predators in field areas where animals hunt and rest. The second group of habitats chosen by foxes for daytime rest includes dense thickets of grass, woody shrubs and hygrophytes. In forest areas, foxes often rest in unsparse pine saplings and bushes, in field areas - in forest belts, uncleared or abandoned fields and in gullies. However, most often the fox spends the night in reed beds (Figure 1), and then in cattails and other aquatic plants that line the banks of all steppe

rivers. According to our data, when hounds were used in studies, more than 45% of foxes in the Black Sea region rested during the day mainly in reed beds (Rozhenko, 2007).


**Figure 1: Reedbeds near Zaporizhzhia (A); a hunter with foxes harvested near Odesa (B)**

Moreover, several animals rested in these places side by side, having come here independently of each other (Gursky, 1979). This creates a very high density of foxes in reed beds (26.6±1.37 individuals/10 ha or 4.4±0.18 per 1 bed with a maximum number of 17 individuals). The probability of encountering predators in such places is very high, as out of 231 surveyed plots, animals were absent in only 2! The area of such plots usually does not exceed 1-2 ha (49.4%), although, of course, foxes use larger reed beds for rest (Rozhenko, 2006). It is interesting to note that in areas of frequent hunting with hunting dogs, which used to be very popular in the Ukrainian Black Sea region, foxes rarely stayed for a day in dense reed beds of less than 0.5 ha.

This selectivity is not well understood, but it is possible that it is the result of learning from the experience of animals that have survived hunting. In other regions, where animals are not disturbed much, their resting places can be not only small reed beds, but also small islands of grass in meadows and fields. The reason for the significant dynamics in the use of habitats by foxes is the large area of individual plots, which is generally characteristic of predatory animals, and the significant dispersion of individuals. For example, in Denmark, based on the tagging of almost 500 animals, it was found that during the first year of life, 85% of young females and 75% of males travelled within ~15 km of their birthplace, and 5 individuals (3 males and 2 females) were captured at a distance of 55-140 km (Jensen, 1968). Similar results were obtained in the Kyiv region, where within 1-2 years most of the tagged foxes dispersed within a radius of 15-30 km, a few within a radius of 2-5 km, and only one travelled over 120 km (Heptner et al., 1967).

In the Voronezh Reserve, out of 123 foxes, most travelled to different habitats within 1-6 km, although one young male travelled 50 km in one year (Sapelnikov 1999). In Norway, several animals migrated up to 30 km in 9 years (Lund and Munthe-Kaas, 1967). At the same time, in the United States, cases were recorded when one female moved 16 km away from the tagging site in more than 8 years (Tular, 1983), and another young female travelled 395 km in one year (Ables, 1965). However, when there is a high concentration of animal prey, the area of an individual fox's territory may be small. For example, in Central Spain, in an area with many wild rabbits and a household waste dump, the home range of an adult male fox over 7 months of observations was only 113 ha, and the length of a daily walk was ~5 km. The predator used only ~35% of the occupied territory per day (Blanco, 1986).

The territorial distribution of foxes' dens, which they create for breeding, is quite peculiar and differs significantly from the biotopic distribution of adult animals, as the majority of dens (about 23%) were located on the edges of natural forests, somewhat less in the treeless valleys of small rivers, as well as on the banks of estuaries (Table 2).

**Table 2: Territorial distribution of fox burrows in 1978-2013**

| B i o t o p s | Black Sea region | | Azov Sea region | | Total: | |
|---|---|---|---|---|---|---|
| | Abs. | % | Abs. | % | Abs. | % |
| Sea coast | 31 | 6.4 | 64 | 14.3 | 95 | 10.2 |
| Shores of estuaries | 111 | 23.0 | 68 | 15.1 | 179 | 19.2 |
| Valleys of small rivers | 46 | 9.6 | 136 | 30.3 | 182 | 19.6 |
| Valleys of large rivers | 89 | 18.5 | – | – | 89 | 9.6 |
| Deciduous forests | 133 | 27.6 | 76 | 16.9 | 209 | 22.5 |
| Coniferous forests | 32 | 6.6 | 12 | 2.7 | 44 | 4.7 |
| Gardens, vineyards | 11 | 2,3 | 6 | 1.3 | 17 | 1.8 |
| Fields | 6 | 1.2 | 3 | 0.7 | 9 | 0.9 |
| Forest belts | 23 | 4.8 | 84 | 18.7 | 107 | 11.5 |
| Total: | 482 | 100.0 | 449 | 100.0 | 931 | 100.0 |

In the Black Sea region, many burrows (18.5%) were found in floodplains of large rivers (Danube, Dniester, Southern Bug and Dnieper), whereas in the Azov region – on sea spits and islands (14.3%), as well as in numerous forest belts (11.5%). In many of them, after the dust storms of 1969, high earth ramparts of wind–borne black soil were formed.This improved the conditions for burrowing by all species of predatory animals, but especially for foxes.

Regular use of dens as resting shelters was observed only in adult females during the breeding season and also in their pups. The latter visit their birthplaces for some time after brood separation and often hide in dens. As it is more comfortable and safe underground, this is observed both during inclement weather and very hot summer days. In winter, foxes very rarely rest in their burrows - usually in rainy or snowy weather. They are mostly avoided by predators when not needed. Fox dens can vary greatly in their structure due to the landscape features of the area and their purpose.

Both simple and complex burrows are very common, but are used in different ways. For example, in the steppe zone of Ukraine, 24.2% of the 219 burrows detected were classified as brood burrows. Of these, 1.8 % were simple straight or slightly branched tunnels, while 22.4 % were complex multi-storey structures (Table 3), covering an area of up to 130 sq m.

**Table 3: Characteristics of common fox burrows (%)* 1 – brood, 2 – visited, 3 – unvisited**

| Study areas | n | Simple burrows | | | Complex burrows | | |
|---|---|---|---|---|---|---|---|
| | | 1 | 2 | 3 | 1 | 2 | 3 |
| Biryuchiy Peninsula (Sea of Azov) | 101 | – | 25.8 | 24.7 | 18.8 | 19.8 | 10.9 |
| Khortitsa Island (Dnieper River) | 46 | 4.4 | 15.2 | 13.0 | 21.7 | 26.1 | 19.6 |
| Deciduous forests (Zaporizhzhya region) | 45 | – | 11.1 | 8.9 | 33.3 | 28.9 | 17.8 |
| Kinburn Spit (Black Sea) | 27 | 7.4 | 25.9 | 14.8 | 18.5 | 18.6 | 14.8 |
| Total: | 219 | 1.8 | 20.6 | 17.8 | 22.4 | 22.8 | 14.6 |

*Data from V. Domnich, N. Lebedeva (2000)

Complex burrows, although very common, were found with almost equal frequency in different study areas, while simple burrows were more typical of sea spits and sandy islands (Domnich and Lebedeva 2000). In the south of Ukraine, where agrocenoses dominate, quite a few adult and juvenile animals settle in straw haystacks, regardless of their location. And, of course, in the flat terrain, predators use all the ancient mounds, which are called "graves" in the south. In Odesa and Mykolaiv regions, foxes often dig burrows in gully forests, on the slopes of beams, in forest belts, in thorns, and in dams of former ponds (Gursky, 1979). In western Ukraine, they typically use ravines, gullies, valleys, hollows, gullies, karst hollows and shrubs (Polushyna, 1967). In the Mordovian Reserve, which is located in the taiga zone, foxes prefer burrows in pine forests (70%), less often in mixed forests (15%), old clearings (10%) and deciduous stands (5%) (Borodin, 1976).

The swarming activity of large rodents has a great influence on the location of fox dens. In 1975, we even found a fox litter in a burrow occupied by a family of beavers (Volokh, 1979). On the territory of Askania Nova Reserve, 62.5 % of fox dens (n = 49) were located in steppe marmot colonies (Dumenko, 2001). We observed many such cases in many northern districts of the Luhansk region (Fig. 2), where this rodent is quite numerous. Naturally, on the eve of birth and during the rearing of young foxes, they try not to stray far from their dwellings. Usually, during this period of life, the size of their individual territory decreases to 0.31-2.33 sq. km (Kolb, 1986), although the number of habitats visited by adult animals can be quite large. At this time, the fox population is characterised by an uneven distribution of individuals, which is associated with its sedentary lifestyle.

**Figure 2: Fox cubs at the steppe marmot hole (Lugansk region, «Streltsovskaya Steppe nature reserve», 2009). Photo by A. Volokh**

The distance between brood burrows in the Ukrainian steppe can reach 2.7±0.14 km (Dumenko, 2001), whereas, for example, in the south of Western Siberia – 7.0±0.8 km (Poleshchuk & Sidorov, 2007). Interestingly, in the latter case, the distance between dens with single animals was significantly greater (11.1±2.0 km) than between brood dwellings. Occupancy of the same den by foxes occurs irregularly. It is known that in Siberia one burrow was used by these predators 1–2 and only once – 4 years in a row. Even during one reproductive period in Askania Nova Reserve,

these animals moved broods to a distance of 52.6±10.3 m in 94.7% of cases, using 2.6±0.22 dens (Dumenko, 2001).

In general, red foxes prefer frequent changes of dwellings, regardless of their biotopic habitat. For example, in the Azov region, burrows located on sea spits are rarely used again – within 2-3 months they crumble and become small holes. Even such very comfortable places in the steppe zone as ancient burial mounds and forest tracts are not used by foxes for burrowing every year. As early as the early 20th century, it was noted that as the steppe biota in Ukraine was transforming, the red fox began to change the places used for breeding (Brauner, 1914).

It began to avoid open steppes and fields, although it had previously willingly burrowed in haystacks that had been stored for many years and used to feed sheep. In the 1960s, this predator began to make frequent burrows in the precipices of ravines, among rocks, as well as in dense bushes and forest tracts (Formozov, 1962). Very few fox dens are now also found in fields, as all agrocenoses undergo regular structural changes. Usually, animals create dwellings in such places only in case of very high intraspecific competition, using even insignificant elevations or depressions of the ground surface for this purpose.

## CONCLUSIONS

1. In the steppe zone of Ukraine the common fox most often uses reed thickets for daytime rest, and then - meadows and fields.
2. This predator prefers forested areas for making dens, although it often makes them in steppe and meadow areas located on the slopes of river valleys.
3. Despite the scarcity of dwelling sites, old burrows are rarely reused.

## REFERENCES

Ables E. (1965). An exceptional fox movement. J. Mammal. 46. N 1: 102.

Blanco C. (1986). On the diet, size and use of home range and activity patterns of a red fox in Central Spain. Acta theriologica. 31. N 27–41: 547–556.

Borodin, P. L. (1976). Distribution of burrows and shelters of badger, fox and raccoon dog in the Mordovian Nature Reserve. Bull. MOIP. T. 81. № 6: 133-135 [in Russian].

Brauner, A. (1914). Mammals of Bessarabian, Kherson and Tauride provinces. Fox. Notes of Novoross. Society of Natural Sciences. Odessa: Kommer. printing house. Issue. 1: 10–36 [in Russian].

Börner R., and Schneider R., & Wittstatt U. (2009). Untersuchung zur Populationsökologie des Rotfuchses (Vulpes vulpes L.). Beiträge zur Jagd & Wild forschung. Bd. 34: 307–313.

Harris, S., and Smith G. C. (1987) Demography of two urban fox (Vulpes vulpes) populations. J. Appl. Ecol. 24. N 1: 75–86.

Geptner, V. G., and Naumov N. P., Yurgenson P. B., Sludsky A. A., Chirkova A. F., Bannikov A. G. 1967. Mammals of the Soviet Union. (Sea cows and carnivores). Moscow: Higher School. T. 2. Part 1: 1–1002 [in Russian].

Gidayatov, Yu. Kh. (1965). Burrow biotopes of foxes in Azerbaijan. Proceedings of the Institute of Zoology of the Academy of Sciences of the Azerbaijan SSR. 25: 165–174 [in Russian].

Gursky, I. G. (1979). Fox in the North-Western Black Sea region. Ecological foundations of the protection and rational use of predatory mammals: Materials of the All-Union Meeting. Moscow: 181–182 [in Russian].

Domnich, V. I. & Lebedeva, N. I. (2000). Types and structural features of burrows of the common fox (Vulpes vulpes) of the Lower Dnieper. Bulletin of the Zaporizhzhya National University. Phys.-math. and biol. Sciences. Zaporizhzhya. No. 14: 124–128 [in Russian].

Dumenko, V. P. (2001). Spatial structure and topical connections of the fox population during the reproductive period on the territory of the Askania-Nova Biosphere Reserve. Structure and functional role of the animal. population in natural and transform. ecosystems: Proc. report I international scientific conf. Dnepropetrovsk: 137–139 [in Russian].

Kolb, H. H. (1986). Some observations on the home randes of vihens (Vulpes vulpes) in the suburs of Edinbyrgh. J. Zool. A 210. N 4: 636–639.

Lebedeva, N. I. & Domnich, V. I. (1998). Biotopic distribution of the common fox (Vulpes vulpes) in the Lower Dnieper region. Bulletin of Zaporizhzhya State University. № 2: 187–194 [in Russian].

Lund, Hj., and Munthe-Kaas, L. (1967). Om merking av rev. Fauna. 20. N 1: 7–17.

Pielowski Z. (1976). The role of foxes in the reduction of the European hare populations. Ecol. and manag. Europ. hare populations. Warszawa: 135–148.

Poleshchuk, E. M. & Sidorov G. N. (2007). Spatial differentiation of fox and corsac populations in the south of Western Siberia. Theriofauna of Russia and adjacent territories: Materials of the 8th Congress of the Theriological Society. Moscow: 386 [in Russian].

Polushina, N. A. (1967). Ecology and practical importance of the fox in the Western regions of Ukraine. Bulletin of the Lviv State University. Series of biol. Vol. 3: 13–18 [In Ukrainian].

Jensen|, B. (1968). Preliminary results from the marking of foxes (Vulpes vulpes L.) in Denmark. Dan. Rrev. Game Biol. Vol. 5. N 4: 131–139.

Rozhenko, M. V. (2006). Carnivorous mammals of the North-Western Black Sea region (fauna, population dynamics and morphology): Dissertation of candidate of biological sciences. Kyiv: 1–209 [In Ukrainian].

Rozhenko, M. V. (2008). Biotope distribution and dynamics of the number of foxes (Vulpes vulpes) in the North-Western Black Sea region. Herald of Zaporizhzhya State University. Phys.-math. and biol. Science. No. 1: 211–219 [In Ukrainian].

Sapelnikov, S. F. (1999). Methods of capturing and results of tagging fox cubs in the Voronezh Nature Reserve. Abstracts of reports of the VI Congress of the Theriological Society of the Russian Academy of Sciences. Moscow: 225 [in Russian].

Tular, B. F. (1983). An unusually long-lived red fox. N.Y. Fish and Game J. 30. N 2: 227.

Formozov, A. N. (1962). Changes in the natural conditions of the steppe south of the European part of the USSR over the last hundred years and some features of the modern fauna of the steppes. Study of natural geography. resources of flora and fauna. Moscow: Publishing House of the USSR Academy of Sciences: 114–161 [in Russian].

Volokh, A. M. (1979). River beaver of the Middle Dnieper region and prospects for its economic use. Dissertation of a candidate of biological sciences. Kyiv: 1–205 [in Russian].

Applied Sciences Research Periodicals – ISSN 3033-330X
May 2024, Vol. 2, No. 5, pp. 50-50.

# The Foundation of a Dark Energy Theory

Friedhelm M. Jöge

**Abstract:**
Based on the article „Calculation of Dark Energy and Dark Matter "[1] the article „Commentary about Calculation of Dark energy and Dark Matter "emerged [2]. The Foundation of a Dark Energy Theory is formulated there.

*Keywords: Dark Energy, Dark Matter, Calculation, Foundation, Theory*

## INTRODUCTION

Nobody knows what Dark Energy actually is. Dark Energy and Dark Matter cannot be observed directly. It is thought to be responsible for the accelerated expansion of the universe. Some considerations have been made; however, they have not yet produced fruitful results to date. In particular, it was not possible to carry out an exact calculation of the Dark Energy. With the present approach, this goal has probably been achieved.

## DERIVATION

The exact calculation of Dark Energy can be achieved in particular using the formula

$$E_d = h\, t_u / t_p^2 \qquad (1)$$

It is derived in the article „Calculation of Dark Energy and Dark Matter "[1]. The theoretical result is confronted with the numerical value calculated from the MAX PLANCK Institute for radio Astronomy. Excellent matching of numerical values resulting in three independent paths makes the approach plausible.

## CONCLUSION

Thus, the Foundation of a Dark Energy Theory is laid.

## DEFINITION OF SYMBOLS USED IN THE FORMULA (1)

$E_d$ = Dark Energy
$t_u$ = age of the universe
h = PLANCK quantum of action
$t_p$ = PLANCK time

## REFERENCES

[1] JÖGE, F.M.: Calculation of Dark Energy and Dark Matter. International Journal of Physics and Astronomy June 2019, Vol.7, No.1, pp.1-7

[2] JÖGE, F.M.: Commentary about Calculation of Dark Energy and Dark Matter. Journal of Physics and Astronomy 2023 Vol.11 Issue 5; 346

Applied Sciences Research Periodicals – ISSN 3033-330X
May 2024, Vol. 2, No. 5, pp. 51-70.

# Forced KdV Equation for Tsunamis Generation: How to Choose the External Forces and Corresponding Solutions

Bogning, Jean Roger [1,2]

1. Department of Physics, Higher Teacher Training College, University of Bamenda, PO Box 39, Bamenda, Cameroon
2. African optical fiber family, Po. Box 2042, Campost Kamkop, Bafoussam, Cameroon

**Abstract:**
The artificial triggering of tsunamis is increasingly modeled by the forced Korteveg de Vries (KdV) equation. But beyond this modeling, the biggest problem is knowing how to choose the excitations or external forces so that the solutions obtained are exact. In this article, we show how to choose the external force in the forced KdV equation. We also show that all the exact solutions obtained depend closely on the external force. Beyond all these demonstrations, we offer some solutions as well as their profiles.

*Keywords: KdV equation, tsunamis, solitary wave, solutions, external forces*

## INTRODUCTION

Since the discovery of the solitary wave by the Scottish engineer John Scott Russell, his first analytical sequences began to emerge in 1895, through the modeling of the KdV equation. This is how the KdV equations were at the center of the first beginnings of solitary wave theory [1-5]. Subsequently, the solitary wave theory became generalized in other transmission media such as optical fibers, atomic chains, electrical lines, plasmas, Bose-Einstein condensate, etc. [6-11]. The equations which most often generate solitary wave solutions being very complicated nonlinear partial differential equations, the development of the theory of solitons was carried out with mathematics theories. Numerous works have established mathematical techniques dedicated to the search for solitary wave solutions [11-18]. For some time, the solitary wave theory has been increasingly used to try to explain certain complex natural phenomena such as hurricanes, earthquakes, certain types of clouds and especially tsunamis. But as the ultimate goal of physics is to study natural phenomena to better understand them in order to use them to improve the living conditions of beings living on earth, researchers are on a permanent quest for tools to control these natural phenomena.

But if we know that the KdV equation in its original form describes the dynamics of free propagation of solitary waves, we want to know how to artificially cause a tsunami. Thus, E. Pelinovsky was one of the very first researchers to use a forced KdV equation to describe the artificial or forced generation of seabed sliding and tsunamis [19]. To date, we have seen very little work that has been done in the sense of integrating the external force into the KdV equations [20,24]. But before returning to the forced KdV equation which is the subject of this article, it should be noted that this equation has attracted the attention of many researchers to this day. Numerous articles have been produced in this direction [25-27]. This article is part of the large list of works which are interested in marine waves and more precisely in solitary waves seen from the angle of KdV equations. Thus, the originality of this work rests on the construction of exact solutions of the forced KdV equations at the same time as the corresponding external forces. It is

not only a question of constructing simple solutions, but above all of obtaining solutions whose profiles are close to the profiles of the giant waves that can be observed during tsunamis. We specifically use ansatz solutions based on iB-functions [28-32] which have already shown their effectiveness in finding solutions in other studies. Thus, our work is organized as follows: In section 2, we present the model of the forced KdV equation which will be at the center of our analyses. In section 3, we present the method to be used to obtain the results; we will use the main iB-functions to construct the first series of solutions and the external forces in section 4. Section 5 will use the secondary forms of the iB-functions to construct the second series of solutions and the external forces. Section 6 analyzes the profiles of the solutions and external forces obtained in the case where the main forms of the iB-functions are used. Section 7 analyzes the solutions and the external forces in the case where secondary forms of iB-functions are used. We end the work with a conclusion and some perspectives.

## FORCED KDV EQUATION MODEL

As we mentioned in the introduction, one of the first models was made by E. Pelnovsky. This model is defined as follows

$$\frac{\partial \eta}{\partial t}+C\frac{\partial \eta}{\partial x}+\alpha\eta\frac{\partial \eta}{\partial x}+\beta\frac{\partial^3 \eta}{\partial x^3}=\frac{\partial f\left(x,t\right)}{\partial x}, \tag{1}$$

where $\eta(x,t)$ represents the elevation of the water surface, $\alpha$ the coefficient of nonlinearity dependent on the water depth and the speed of the wave, $C$ represents the speed of the wave, $\beta$ the dispersion coefficient and $\frac{\partial f}{\partial x}$ the external force where excitement. In this article, we adopt a more general model given by

$$\frac{\partial \eta}{\partial t}+C\frac{\partial \eta}{\partial x}+\alpha\eta\frac{\partial \eta}{\partial x}+\beta\frac{\partial^3 \eta}{\partial x^3}=\frac{\partial f\left(x,t\right)}{\partial x}=F\left(x,t\right), \tag{2}$$

where $F(x,t)$ represents the external force or excitation. We pass into the proper reference frame of the wave by setting the change of variable $\xi=\lambda x-\lambda_0 t$ where $\lambda$ is equivalent to the spatial frequency of the wave and $\lambda_0$ the angular frequency of the wave. The KdV equation becomes the equation with a single variable $\xi$ and given by

$$-\lambda_0\frac{\partial \eta}{\partial \xi}+C\lambda\frac{\partial \eta}{\partial \xi}+\alpha\lambda\eta\frac{\partial \eta}{\partial \xi}+\beta\lambda^3\frac{\partial^3 \eta}{\partial \xi^3}=F\left(\xi\right). \tag{3}$$

The free propagation equation of KdV, that is to say its basic equation without a second member, is given by

$$-\lambda_0\frac{\partial \eta}{\partial \xi}+C\lambda\frac{\partial \eta}{\partial \xi}+\alpha\lambda\eta\frac{\partial \eta}{\partial \xi}+\beta\lambda^3\frac{\partial^3 \eta}{\partial \xi^3}=0. \tag{4}$$

In the following, we construct the general solution of (2) and (3) supported by some particular solutions.

## METHOD USED

The ansatz solutions used come from the two forms of iB-functions, notably the main form and the secondary form. The main and secondary form are defined respectively in dimension one by [30-32]

$$J_{n,m}(\xi)=\frac{\sinh^m(\xi)}{\cosh^n(\xi)},, \tag{5}$$

and

$$T_{n,m}(\xi)=\frac{\sin^m(\xi)}{\cos^n(\xi)}. \tag{6}$$

The two previous functions are linked by relationships

$$J_{n,m}(i\xi)=(i)^m T_{n,m}(\xi), i^2=-1, \tag{7}$$

and

$$T_{n,m}(i\xi)=(i)^m J_{n,m}(\xi), i^2=-1. \tag{8}$$

In the following, we use these two forms of iB-functions to constitute our ansatz solutions to construct.

## FIRST SERIES OF SOLUTIONS: USE OF IB-MAIN FUNCTIONS

In this section we propose to construct the solutions of (3). To do this, we first start by solving this equation without a second member to get an idea of the general solution to equation (3) to construct. Thus, by seeking the solution of equation (4) in the form:

$$\eta(\xi)=aJ_{n,0}(\xi), \tag{9}$$

where $a$ and $n$ are real numbers to be determined. Thus, inserting (9) into (4) leads to the equation

$$-\left[an(C\lambda-\lambda_0)+\beta\lambda^3 an^3\right]J_{n+1,1}-\lambda\alpha a^2 nJ_{2n+1,1}+\beta\lambda^3 an(n+1)(n+2)J_{n+3,1}=0. \tag{10}$$

The search for values of $n$ for which certain terms of (10) come together gives $n=0$ and $n=2$. For $n=0$, we have a trivial solution. In the case where $n=2$, equation (10) becomes

$$2a\left[C\lambda-\lambda_0+4\beta\lambda^3\right]J_{n+1,1}+\lambda\left(\alpha a-12\beta\lambda^2\right)aJ_{3,1}=0. \tag{11}$$

Equation (11) is verified if for $a\neq 0$ ,we have $\lambda_0=C\lambda+4\beta\lambda^3$ and $a=12\beta\lambda^2/\alpha$. The solution to (4) under these conditions is given by

$$\eta(\xi)=\frac{12\beta\lambda^2}{\alpha}J_{2,0}(\xi)\equiv\frac{12\beta\lambda^2}{\alpha}\sec h^2(\xi). \tag{12}$$

Solution (12) serves as a guide for us to choose the general form of solution of equation (3) to construct. Thus, we propose to subsequently construct the solution to equation (3) in the form

$$\eta(\xi)=\frac{12\beta\lambda^2}{\alpha}J_{2,0}\left(f(\xi)\right), \tag{13}$$

where $f(\xi)$ is an arbitrary function continuously differentiable in its domain of definition. The insertion of (13) in (3) supposes the evaluation of its different terms. Thus, we have

$$\frac{\partial\eta}{\partial\xi}=\frac{-24\beta\lambda^2}{\alpha}f'J_{3,1}\left(f(\xi)\right), \tag{14}$$

$$\eta\frac{\partial\eta}{\partial\xi}=\frac{-288\beta^2\lambda^4}{\alpha^2}f'J_{5,1}(f), \tag{15}$$

$$\frac{\partial^2\eta}{\partial\xi^2}=\frac{-24\beta\lambda^2}{\alpha}\left[f''J_{3,1}(f)-2f'^2J_{2,0}(f)+3f'^2J_{4,0}(f)\right], \tag{16}$$

And

$$\frac{\partial^3\eta}{\partial\xi^3}=\frac{-24\beta\lambda^2}{\alpha}\left[-6f''f'J_{2,0}(f)+9f''f'J_{4,0}(f)+\left(f'''+4f'^2\right)J_{3,1}(f)-12f'^2J_{5,1}(f)\right]. \tag{17}$$

In expressions (14) to (17), $f'$, $f''$, $f'''$ denote respectively the first derivative of $f(\xi)$ with respect to $\xi$, the second derivative of $f(\xi)$ with respect to $\xi$ and the third derivative of $f(\xi)$ with respect to $\xi$. Insertion of terms (14) to (17) in the equation (3) allow us to have external strength under

$$F(\xi)=F_1(\xi)J_{2;0}(f)+F_2(\xi)J_{4,0}(f)+F_3(\xi)J_{3,1}(f)+F_4(\xi)J_{5,1}(f), \tag{18}$$

Where the functions $F_i(\xi), i=1,...,4$ are given

$$F_1(\xi)=\frac{144\beta^2\lambda^5}{\alpha}f''f', \tag{19}$$

$$F_2(\xi)=\frac{-216\beta^2\lambda^5}{\alpha}f''f', \tag{20}$$

$$F_3(\xi)=\frac{24\beta^2\lambda^5}{\alpha}\left(4f'-f'''-4f'^3\right), \tag{21}$$

And

$$F_4(\xi)=\frac{288\beta^2\lambda^5}{\alpha}\left(f'^3-f'\right). \tag{22}$$

The non-linear partial differential equation increasingly used to describe the generation of tsunamis is that of forced KdV, that is to say that of KdV subjected to an external force. The goal is to simulate an external force which can generate the tsunami which is embodied by the frenzied or brutal propagation of the solitary wave. This equation in this case will be corrected as follows

$$\begin{aligned}&-4\beta\lambda^3\frac{\partial\eta}{\partial\xi}+C\lambda\frac{\partial\eta}{\partial\xi}+\alpha\lambda\eta\frac{\partial\eta}{\partial\xi}+\beta\lambda^3\frac{\partial^3\eta}{\partial\xi^3}\\&=F_1(\xi)J_{2;0}(f)+F_2(\xi)J_{4,0}(f)+F_3(\xi)J_{3,1}(f)+F_4(\xi)J_{5,1}(f).\end{aligned} \tag{23}$$

The choice of external force is very important, it must be adequate for the reaction to produce the expected effects. Thus, any solitary wave solution of the form $\eta(\xi)=\left(12\beta\lambda^2/\alpha\right)J_{2,0}\left(f(\xi)\right)$, where $f(\xi)$ is a continuously differentiable function in its domain is always an exact solution to equation (23). Thus, we can generalize the exact solution of the forced KdV equation (23) as follows

$$\eta(\xi)=\frac{12\beta\lambda^2}{\alpha}J_{2,0}\left(f(\xi)+K\right)\equiv\frac{12\beta\lambda^2}{\alpha}\sec h^2\left(f(\xi)+K\right), \tag{24}$$

Where $\beta$ is the dispersion coefficient of order 3, $\alpha$ the nonlinearity coefficient, $K$ an arbitrary constant and $\xi=\lambda x-\lambda_0 t$.

**Some Exact Solutions and External Forces**

In this subsection, we propose some exact solutions as well as the forced KdV equations that they verify.

For $f(\xi)=\cos\xi$ the corresponding forced KdV equation is given by (23) as we have

$$F_1(\xi)=\frac{144\beta^2\lambda^5}{\alpha}\cos\xi\sin\xi, \tag{25}$$

$$F_2(\xi)=\frac{-216\beta^2\lambda^5}{\alpha}\cos\xi\sin\xi, \tag{26}$$

$$F_3(\xi)=\frac{24\beta^2\lambda^5}{\alpha}\left(-5\sin\xi+4\sin^3\xi\right), \tag{27}$$

And

$$F_4(\xi)=\frac{288\beta^2\lambda^5}{\alpha}\left(-\sin^3\xi+\sin\xi\right). \tag{28}$$

The exact general solution in this case is given by

$$\eta(\xi)=\frac{12\beta\lambda^2}{\alpha}J_{2,0}(\cos\xi+K)\equiv\frac{12\beta\lambda^2}{\alpha}\sec h^2(\cos\xi+K), \tag{29}$$

For $f(\xi)=\sec h\xi$ the corresponding forced KdV equation is given by (23) as we have

$$F_1(\xi)=\frac{-144\beta^2\lambda^5}{\alpha}\sec h^2\xi\sinh\xi\left(1-2\sec h^2\xi\right), \tag{30}$$

$$F_2(\xi)=\frac{216\beta^2\lambda^5}{\alpha}\sec h^3\xi\sinh\xi\left(1-2\sec h^2\xi\right), \tag{31}$$

$$F_3(\xi)=\frac{24\beta^2\lambda^5}{\alpha}\sec h^2\xi\sinh\xi\left(-3-6\sec h^2\xi+4\sec h^4\xi\sinh^2\xi\right), \tag{32}$$

And

$$F_4(\xi)=\frac{-288\beta^2\lambda^5}{\alpha}\sec h^3\xi\sinh\xi\left(\sec h^4\xi\sinh^2\xi-1\right). \tag{33}$$

The exact general solution in this case is given by

$$\eta(\xi)=\frac{12\beta\lambda^2}{\alpha}J_{2,0}(\sec h\xi+K)\equiv\frac{12\beta\lambda^2}{\alpha}\sec h^2(\sec h\xi+K). \tag{34}$$

For $f(\xi)=\tanh\xi$ the corresponding forced KdV equation is given by (23) as we have

$$F_1(\xi)=\frac{-288\beta^2\lambda^5}{\alpha}\sec h^5\xi\sinh\xi, \tag{35}$$

$$F_2(\xi)=\frac{432\beta^2\lambda^5}{\alpha}\sec h^5\xi\sinh\xi, \tag{36}$$

$$F_3(\xi)=\frac{48\beta^2\lambda^5}{\alpha}\sec h^4\xi\left(3-2\sec h^2\xi\right), \tag{37}$$

And

$$F_4(\xi)=\frac{288\beta^2\lambda^5}{\alpha}\sec h^2\xi\left(\sec h^4\xi-1\right). \tag{38}$$

The exact general solution in this case is given by

$$\eta(\xi)=\frac{12\beta\lambda^2}{\alpha}J_{2,0}(\tanh\xi+K)\equiv\frac{12\beta\lambda^2}{\alpha}\sec h^2(\tanh\xi+K). \tag{39}$$

For $f(\xi)=\xi^2$ the corresponding forced KdV equation is given by (23) as we have

$$F_1(\xi)=\frac{576\beta^2\lambda^5}{\alpha}\xi, \tag{40}$$

$$F_2(\xi)=\frac{-864\beta^2\lambda^5}{\alpha}\xi, \tag{41}$$

$$F_3(\xi)=\frac{192\beta^2\lambda^5}{\alpha}\left(\xi-4\xi^2\right), \tag{42}$$

And

$$F_4(\xi)=\frac{576\beta^2\lambda^5}{\alpha}\xi\left(4\xi^2-1\right). \tag{43}$$

The exact general solution in this case is given by

$$\eta(\xi)=\frac{12\beta\lambda^2}{\alpha}J_{2,0}\left(\xi^2+K\right)\equiv\frac{12\beta\lambda^2}{\alpha}\sec h^2\left(\xi^2+K\right). \tag{44}$$

For $f(\xi)=Arc\tan\xi$ the corresponding forced KdV equation is given by (23) as we have

$$F_1(\xi)=\frac{-288\beta^2\lambda^5}{\alpha}\frac{\xi}{\left(1+\xi^2\right)^3}, \tag{45}$$

$$F_2(\xi)=\frac{432\beta^2\lambda^5}{\alpha}\frac{\xi}{\left(1+\xi^2\right)^3}, \tag{46}$$

$$F_3(\xi)=\frac{96\beta^2\lambda^5}{\alpha}\frac{\left(2+\xi^4\right)}{\left(1+\xi^2\right)^3}, \tag{47}$$

And

$$F_4(\xi)=\frac{288\beta^2\lambda^5}{\alpha}\frac{\left(2\xi^2+\xi^4\right)}{\left(1+\xi^2\right)^3}. \tag{48}$$

The exact general solution in this case is given by

$$\eta(\xi)=\frac{12\beta\lambda^2}{\alpha}J_{2,0}\left(Arc\tan\xi+K\right)\equiv\frac{12\beta\lambda^2}{\alpha}\sec h^2\left(Arc\tan\xi+K\right), \tag{49}$$

We note that it is possible to construct as many exact solutions of the forced kdV equation knowing $f(\xi)$.

For $f(\xi)=\exp\xi$ the corresponding forced KdV equation is given by (23) as we have

$$F_1(\xi)=\frac{144\beta^2\lambda^5}{\alpha}\exp 2\xi, \tag{50}$$

$$F_2(\xi)=\frac{-216\beta^2\lambda^5}{\alpha}\exp 2\xi, \tag{51}$$

$$F_3(\xi)=\frac{24\beta^2\lambda^5}{\alpha}\left(4\exp\xi-\exp\xi-4\exp 3\xi\right), \tag{52}$$

And

$$F_4(\xi)=\frac{288\beta^2\lambda^5}{\alpha}\left(\exp 3\xi-\exp\xi\right). \tag{53}$$

The exact general solution in this case is given by

$$\eta(\xi)=\frac{12\beta\lambda^2}{\alpha}J_{2,0}\left(\exp\xi+K\right)\equiv\frac{12\beta\lambda^2}{\alpha}\sec h^2\left(\exp\xi+K\right). \tag{54}$$

for $f(\xi)=\cosh\xi$ the corresponding forced KdV equation is given by (23) as we have

$$F_1(\xi)=\frac{144\beta^2\lambda^5}{\alpha}\cosh\xi\sinh\xi, \tag{55}$$

$$F_2(\xi)=\frac{-216\beta^2\lambda^5}{\alpha}\cosh\xi\sinh\xi, \tag{56}$$

$$F_3(\xi)=\frac{192\beta^2\lambda^5}{\alpha}\sinh\xi\left(3-4\sinh^2\xi\right), \tag{57}$$

And

$$F_4(\xi)=\frac{288\beta^2\lambda^5}{\alpha}\sinh\xi\left(\sinh^2\xi-1\right). \tag{58}$$

The exact general solution in this case is given by

$$\eta(\xi)=\frac{12\beta\lambda^2}{\alpha}J_{2,0}\left(\cosh\xi+K\right)\equiv\frac{12\beta\lambda^2}{\alpha}\sec h^2\left(\cosh\xi+K\right). \tag{59}$$

## SECOND SERIES OF SOLUTIONS: USE OF IB-SECONDARY FUNCTIONS

In this section we propose to construct the solutions of (3). To do this we first start by solving this equation without a second member to get an idea of the general solution to equation (3) to construct. Thus, by looking for the solution to equation (4) in the form

$$\eta(\xi) = aT_{n,0}(\xi), \tag{60}$$

where $a$ and $n$ are real numbers to be determined. Thus, the insertion of (50) into (4) lead us to the equation

$$\left[an\left(C\lambda - \lambda_0\right) + \beta\lambda^3 an^3\right]T_{n+1,1} + \lambda\alpha a^2 nT_{2n+1,1} + \beta\lambda^3 an\left(n+1\right)\left(n+2\right)T_{n+3,1} = 0. \tag{61}$$

Looking for the values of $n$ for which certain terms in (61) group together gives us $n=0$ et $n=2$. For $n=0$, we have a trivial solution. In the case where $n=2$, equation (51) becomes

$$2a\left[C\lambda - \lambda_0 + 4\beta\lambda^3\right]J_{3,1} + 2\lambda\left(\alpha a + 12\beta\lambda^2\right)aJ_{3,1} = 0. \tag{62}$$

Equation (62) is verified if for $a \neq 0$, we have $\lambda_0 = C\lambda + 4\beta\lambda^3$ and $a = -12\beta\lambda^2/\alpha$. The solution to (4) under these conditions is given by

$$\eta(\xi) = \frac{-12\beta\lambda^2}{\alpha}T_{2,0}(\xi) \equiv \frac{-12\beta\lambda^2}{\alpha}\sec^2(\xi). \tag{63}$$

Solution (63) serves as a guide to choose the general form of solution of equation (3) to construct. Thus, we propose to subsequently construct the solution to equation (3) in the form

$$\eta(\xi) = \frac{-12\beta\lambda^2}{\alpha}T_{2,0}\left(f(\xi)\right), \tag{64}$$

where $f(\xi)$ is an arbitrary function continuously differentiable in its domain of definition. The insertion of (64) in (3) obliges to evaluate its different terms. Thus, we have

$$\frac{\partial\eta}{\partial\xi} = \frac{-24\beta\lambda^2}{\alpha}f'T_{3,1}\left(f(\xi)\right), \tag{65}$$

$$\eta\frac{\partial\eta}{\partial\xi} = \frac{288\beta^2\lambda^4}{\alpha^2}fT_{5,1}(f), \tag{66}$$

$$\frac{\partial^2\eta}{\partial\xi^2} = \frac{-24\beta\lambda^2}{\alpha}\left[f''T_{3,1}(f) - 2f'^2T_{2,0}(f) + 3f'^2T_{4,0}(f)\right], \tag{67}$$

And

$$\frac{\partial^3\eta}{\partial\xi^3}=\frac{-24\beta\lambda^2}{\alpha}\left[-6f''f'T_{2,0}(f)+9f''f'T_{4,0}(f)+\left(f'''-4f'^2\right)T_{3,1}(f)-12f'^2T_{5,1}(f)\right]. \quad (68)$$

In expressions (65) to (68), $f'$, $f''$, $f'''$ denote respectively the first derivative of $f(\xi)$ with respect to $\xi$, the second derivative of $f(\xi)$ with respect to $\xi$ and the third derivative of $f(\xi)$ with respect to $\xi$. The insertion of the terms (65) to (68) in the equation (3) allows us to have the external force under

$$F(\xi)=F_1(\xi)T_{2;0}(f)+F_2(\xi)T_{4,0}(f)+F_3(\xi)T_{3,1}(f)+F_4(\xi)T_{5,1}(f), \quad (69)$$

where the functions $F_i(\xi), i=1,...,4$ are given by

$$F_1(\xi)=\frac{144\beta^2\lambda^5}{\alpha}f''f', \quad (70)$$

$$F_2(\xi)=\frac{-216\beta^2\lambda^5}{\alpha}f''f', \quad (71)$$

$$F_3(\xi)=\frac{24\beta^2\lambda^5}{\alpha}\left(4f'-f'''+4f'^3\right), \quad (72)$$

And

$$F_4(\xi)=\frac{288\beta^2\lambda^5}{\alpha}\left(f'-f'^3\right). \quad (73)$$

The forced KdV equation in this case is corrected as follow

$$\begin{aligned}&-4\beta\lambda^3\frac{\partial\eta}{\partial\xi}+C\lambda\frac{\partial\eta}{\partial\xi}+\alpha\lambda\eta\frac{\partial\eta}{\partial\xi}+\beta\lambda^3\frac{\partial^3\eta}{\partial\xi^3}\\&=F_1(\xi)T_{2;0}(f)+F_2(\xi)T_{4,0}(f)+F_3(\xi)T_{3,1}(f)+F_4(\xi)T_{5,1}(f).\end{aligned} \quad (74)$$

The choice of external force is very important, it must be adequate for the reaction to produce the expected effects. Thus, any solitary wave solution of the form $\eta(\xi)=\left(-12\beta\lambda^2/\alpha\right)T_{2,0}(f(\xi))$, where $f(\xi)$ is a continuously differentiable function in its domain is always an exact solution to equation (23). Thus, we can generalize the exact solution of the forced KdV equation (23) as follows

$$\eta(\xi)=\frac{-12\beta\lambda^2}{\alpha}T_{2,0}(f(\xi)+K)\equiv\frac{-12\beta\lambda^2}{\alpha}\sec^2(f(\xi)+K), \quad (75)$$

where $\beta$ is the dispersion coefficient of order 3, $\alpha$ the nonlinearity coefficient, $K$ an arbitrary constant and $\xi = \lambda x - \lambda_0 t$. It should be noted that we can go from solution (24) to solution (75) and vice versa by making the following matches $\lambda \leftarrow i\lambda$ , $f(\xi) \leftarrow if(\xi)$ et $K \leftarrow iK$ .

**Some Exact Solutions and External Forces**

In this subsection, we propose some exact solutions as well as the forced KdV equations that they verify for $f(\xi) = \exp \xi$ the corresponding forced KdV equation is given by (23) such that we have

$$F_1(\xi) = \frac{144\beta^2\lambda^5}{\alpha} \exp 2\xi, \tag{76}$$

$$F_2(\xi) = \frac{-216\beta^2\lambda^5}{\alpha} \exp 2\xi, \tag{77}$$

$$F_3(\xi) = \frac{24\beta^2\lambda^5}{\alpha} \left(4\exp \xi - \exp \xi + 4\exp 3\xi\right), \tag{78}$$

And

$$F_4(\xi) = \frac{288\beta^2\lambda^5}{\alpha} \left(\exp \xi - \exp 3\xi\right). \tag{79}$$

The exact general solution in this case is given by

$$\eta(\xi) = \frac{-12\beta\lambda^2}{\alpha} T_{2,0}\left(\exp \xi + K\right) \equiv \frac{-12\beta\lambda^2}{\alpha} \sec^2\left(\exp \xi + K\right), \tag{80}$$

For $f(\xi) = \sec h\xi$ the corresponding forced KdV equation is given by (23) such that we have

$$F_1(\xi) = \frac{-144\beta^2\lambda^5}{\alpha} \sec h^2\xi \sinh \xi \left(1 - 2\sec h^2\xi\right), \tag{81}$$

$$F_2(\xi) = \frac{216\beta^2\lambda^5}{\alpha} \sec h^3\xi \sinh \xi \left(1 - 2\sec h^2\xi\right), \tag{82}$$

$$F_3(\xi) = \frac{24\beta^2\lambda^5}{\alpha} \sec h^2\xi \sinh \xi \left(-3 - 6\sec h^2\xi - 4\sec h^4\xi \sinh^2 \xi\right), \tag{83}$$

And

$$F_4(\xi) = \frac{-288\beta^2\lambda^5}{\alpha} \sec h^3\xi \sinh \xi \left(1 - \sec h^4\xi \sinh^2 \xi\right). \tag{84}$$

The exact general solution in this case is given by

$$\eta(\xi)=\frac{12\beta\lambda^2}{\alpha}T_{2,0}\left(\sec h\xi+K\right)\equiv\frac{12\beta\lambda^2}{\alpha}\sec^2\left(\sec h\xi+K\right). \tag{85}$$

For $f(\xi)=\tanh\xi$ the corresponding forced KdV equation is given by (23) such that we have

$$F_1(\xi)=\frac{-288\beta^2\lambda^5}{\alpha}\sec h^5\xi\sinh\xi, \tag{86}$$

$$F_2(\xi)=\frac{432\beta^2\lambda^5}{\alpha}\sec h^5\xi\sinh\xi, \tag{87}$$

$$F_3(\xi)=\frac{48\beta^2\lambda^5}{\alpha}\sec h^4\xi\left(3+2\sec h^2\xi\right), \tag{88}$$

And

$$F_4(\xi)=\frac{288\beta^2\lambda^5}{\alpha}\sec h^2\xi\left(1-\sec h^4\xi\right). \tag{89}$$

The exact general solution is given by

$$\eta(\xi)=\frac{12\beta\lambda^2}{\alpha}T_{2,0}\left(\tanh\xi+K\right)\equiv\frac{12\beta\lambda^2}{\alpha}\sec^2\left(\tanh\xi+K\right). \tag{90}$$

For $f(\xi)=\xi^2$ the corresponding forced KdV equation is given by (23) such that we have

$$F_1(\xi)=\frac{576\beta^2\lambda^5}{\alpha}\xi, \tag{91}$$

$$F_2(\xi)=\frac{-864\beta^2\lambda^5}{\alpha}\xi, \tag{92}$$

$$F_3(\xi)=\frac{192\beta^2\lambda^5}{\alpha}\left(\xi+4\xi^2\right), \tag{93}$$

And

$$F_4(\xi)=\frac{576\beta^2\lambda^5}{\alpha}\left(\xi-4\xi^3\right). \tag{94}$$

The exact general solution is given by

$$\eta(\xi)=\frac{12\beta\lambda^2}{\alpha}T_{2,0}\left(\xi^2+K\right)\equiv\frac{12\beta\lambda^2}{\alpha}\sec^2\left(\xi^2+K\right). \tag{95}$$

For $f(\xi) = Arc\tan\xi$ the corresponding forced KdV equation is given by (23) such that we have

$$F_1(\xi) = \frac{-288\beta^2\lambda^5}{\alpha}\frac{\xi}{\left(1+\xi^2\right)^3}, \tag{96}$$

$$F_2(\xi) = \frac{432\beta^2\lambda^5}{\alpha}\frac{\xi}{\left(1+\xi^2\right)^3}, \tag{97}$$

$$F_3(\xi) = \frac{24\beta^2\lambda^5}{\alpha}\frac{\left(4\xi^4+6\xi^2+10\right)}{\left(1+\xi^2\right)^3}, \tag{98}$$

and

$$F_4(\xi) = \frac{288\beta^2\lambda^5}{\alpha}\frac{\left(2\xi^2+\xi^4\right)}{\left(1+\xi^2\right)^3}. \tag{99}$$

The exact general solution in this case is given by

$$\eta(\xi) = \frac{12\beta\lambda^2}{\alpha}J_{2,0}\left(Arc\tan\xi+K\right) \equiv \frac{12\beta\lambda^2}{\alpha}\sec h^2\left(Arc\tan\xi+K\right), \tag{100}$$

For $f(\xi) = \cos h\xi$ the corresponding forced KdV equation is given by (23) such that we have

$$F_1(\xi) = \frac{144\beta^2\lambda^5}{\alpha}\cosh\xi\sinh\xi, \tag{101}$$

$$F_2(\xi) = \frac{-216\beta^2\lambda^5}{\alpha}\cosh\xi\sinh\xi, \tag{102}$$

$$F_3(\xi) = \frac{24\beta^2\lambda^5}{\alpha}\sinh\xi\left(3+4\sinh^2\xi\right), \tag{103}$$

And

$$F_4(\xi) = \frac{288\beta^2\lambda^5}{\alpha}\sinh\xi\left(1-\sinh^2\xi\right). \tag{104}$$

The exact general solution in this case is given by

$$\eta(\xi) = \frac{12\beta\lambda^2}{\alpha}T_{2,0}\left(\cos h\xi+K\right) \equiv \frac{12\beta\lambda^2}{\alpha}\sec^2\left(\cosh\xi+K\right). \tag{105}$$

For $f(\xi) = \cos\xi$ the corresponding forced kdV equation is given by (23) such that we have

$$F_1(\xi)=\frac{144\beta^2\lambda^5}{\alpha}\cos\xi\sin\xi, \tag{106}$$

$$F_2(\xi)=\frac{-216\beta^2\lambda^5}{\alpha}\cos\xi\sin\xi, \tag{107}$$

$$F_3(\xi)=\frac{24\beta^2\lambda^5}{\alpha}\left(-5\sin\xi+4\sin^2\xi\right), \tag{108}$$

And

$$F_4(\xi)=\frac{288\beta^2\lambda^5}{\alpha}\left(-\sin\xi+\sin^3\xi\right). \tag{109}$$

The exact general solution in this case is given by

$$\eta(\xi)=\frac{12\beta\lambda^2}{\alpha}T_{2,0}\left(\cos\xi+K\right)\equiv\frac{12\beta\lambda^2}{\alpha}\sec^2\left(\cos\xi+K\right). \tag{110}$$

## ANALYSIS OF SOLUTIONS PROFILES AND EXTERNAL EXCITATIONS: CASE OF THE FIRST SERIES OF SOLUTIONS

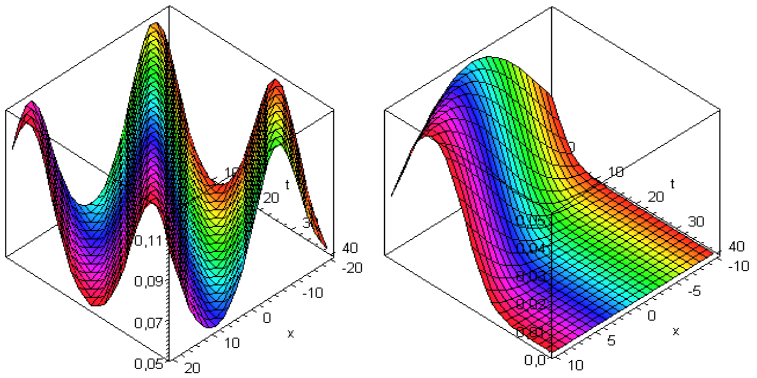


**Figure 1 : Curves representing the solution** $\eta(x,t)=\left(12\beta\lambda^2/\alpha\right)J_{2,0}\left(f\left(\lambda x-\lambda_0 t\right)\right)$ **for** $\beta=0.1$**,** $\lambda=0.1$**,** $\alpha=0.1$ **and** $\alpha_0=0.1$ **: the left curve is obtained for** $f\left(\lambda x-\lambda_0 t\right)=\cos\left(0.1x-0.t\right)$ **and the right curve for** $f\left(\lambda x-\lambda_0 t\right)=\cosh\left(0.1x-0.1t\right)$ **such that we have** $x\in[-10,10]$**,** $t\in[0,40]$**.**

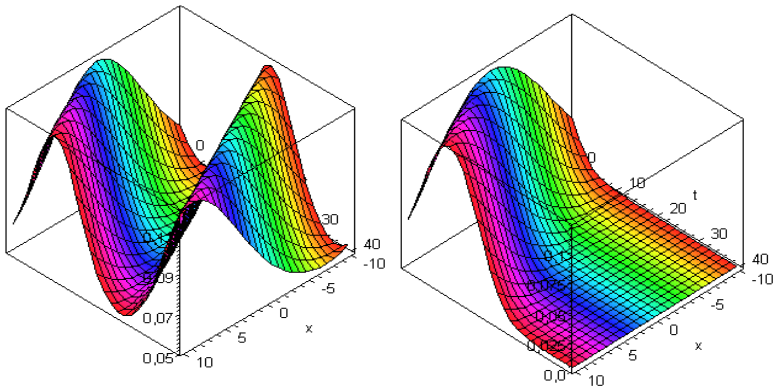

**Figure 2 : curves representing the solution** $\eta(x,t)=\left(12\beta\lambda^2/\alpha\right)J_{2,0}\left(f\left(\lambda x-\lambda_0 t\right)\right)$ **for** $\beta=0.1$**,** $\lambda=0.1$**,** $\alpha=0.1$ **and** $\alpha_0=0.1$ **: the left curve is obtained for** $f\left(\lambda x-\lambda_0 t\right)=\sin\left(0.1x-0.t\right)$ **and the right curve for** $f\left(\lambda x-\lambda_0 t\right)=\sinh\left(0.1x-0.1t\right)$ **suvh that we have** $x\in[-10,10]$**,** $t\in[0,40]$**.**

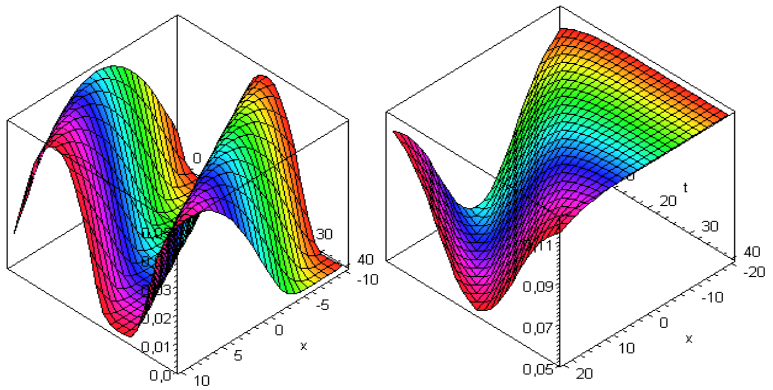


**Figure 3 : Curves representing the solution** $\eta(x,t)=\left(12\beta\lambda^2/\alpha\right)J_{2,0}\left(f\left(\lambda x-\lambda_0 t\right)\right)$ **for** $\beta=0.1$**,** $\lambda=0.1$**,** $\alpha=0.1$ **and** $\alpha_0=0.1$ **: the left curve is obtained for** $f\left(\lambda x-\lambda_0 t\right)=\sec\left(0.1x-0.t\right)$ **and the right curve for** $f\left(\lambda x-\lambda_0 t\right)=\operatorname{sech}\left(0.1x-0.1t\right)$ **such that we have** $x\in[-10,10]$**,** $t\in[0,40]$**.**

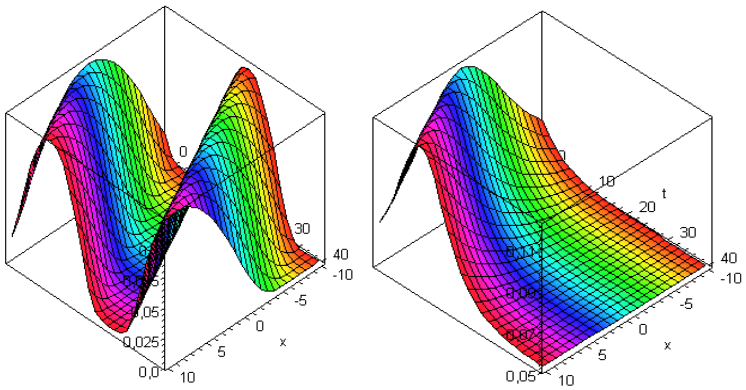


**Figure 4 : Curves representing the solution** $\eta(x,t)=\left(12\beta\lambda^2/\alpha\right)J_{2,0}\left(f\left(\lambda x-\lambda_0 t\right)\right)$ **for** $\beta=0.1$**,** $\lambda=0.1$**,** $\alpha=0.1$ **and** $\alpha_0=0.1$ **: the left curve is obtained for** $f\left(\lambda x-\lambda_0 t\right)=\tan\left(0.1x-0.t\right)$ **and the right curve for** $f\left(\lambda x-\lambda_0 t\right)=\tanh\left(0.1x-0.1t\right)$ **such that we have** $x\in[-10,10]$**,** $t\in[0,40]$**.**

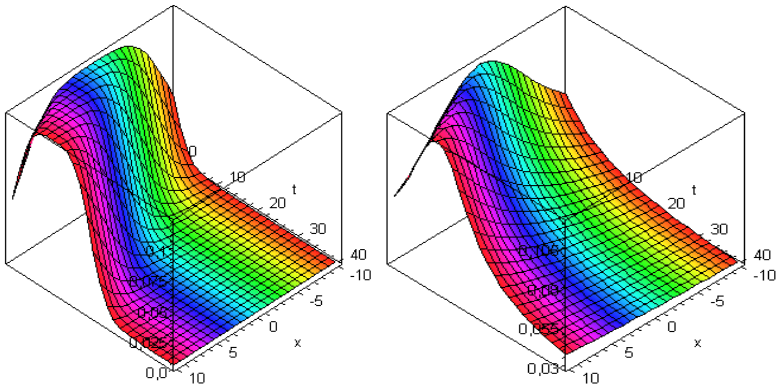


**Figure 5 : Curves representing the solution** $\eta(x,t)=\left(12\beta\lambda^2/\alpha\right)J_{2,0}\left(f\left(\lambda x-\lambda_0 t\right)\right)$ **for** $\beta=0.1$**,** $\lambda=0.1$**,** $\alpha=0.1$ **and** $\alpha_0=0.1$ **: the left curve is obtained for** $f\left(\lambda x-\lambda_0 t\right)=\left(0.1x-0.t\right)^2$ **and the right for** $f\left(\lambda x-\lambda_0 t\right)=\arctan\left(0.1x-0.1t\right)$ **such that we have** $x\in[-10,10]$**,** $t\in[0,40]$**.**

## ANALYSIS OF SOLUTIONS PROFILES AND EXTERNAL EXCITATIONS: CASE OF THE SECOND SERIES OF SOLUTIONS

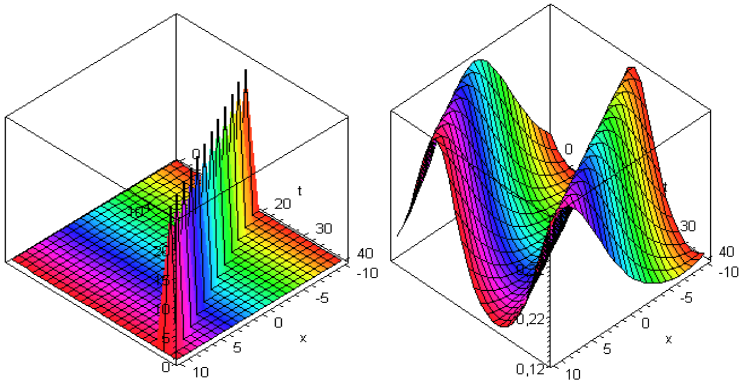


**Figure 6 : Curves representing the solution** $\eta(x,t)=\left(-12\beta\lambda^2/\alpha\right)T_{2,0}\left(f\left(\lambda x-\lambda_0 t\right)\right)$ **For** $\beta=-0.1$**,** $\lambda=0.1$**,** $\alpha=0.1$ **and** $\alpha_0=0.1$ **: the left curve is obtained for** $f\left(\lambda x-\lambda_0 t\right)=\cos\left(0.1x-0.t\right)$ **and the right curve for** $f\left(\lambda x-\lambda_0 t\right)=\cosh\left(0.1x-0.1t\right)$ **such that we have** $x\in[-10,10]$**,** $t\in[0,40]$**.**

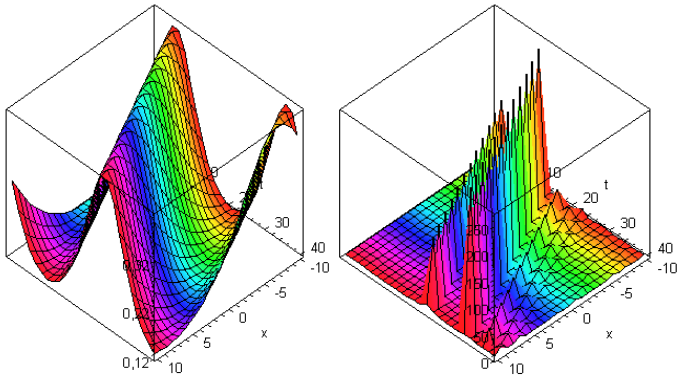


**Figure 7 : Curve representing the solution** $\eta(x,t)=\left(-12\beta\lambda^2/\alpha\right)T_{2,0}\left(f\left(\lambda x-\lambda_0 t\right)\right)$ **for** $\beta=-0.1$**,** $\lambda=0.1$**,** $\alpha=0.1$ **and** $\alpha_0=0.1$ **: the left curve is obtained for** $f\left(\lambda x-\lambda_0 t\right)=\sin\left(0.1x-0.t\right)$ **and the right curve for** $f\left(\lambda x-\lambda_0 t\right)=\sinh\left(0.1x-0.1t\right)$ **such that we have** $x\in[-10,10]$**,** $t\in[0,40]$**.**

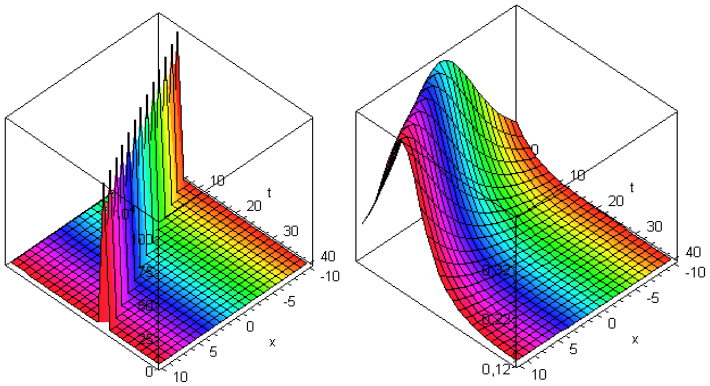


**Figure 8 : Currves representing the solution** $\eta(x,t)=\left(-12\beta\lambda^2/\alpha\right)T_{2,0}\left(f\left(\lambda x-\lambda_0 t\right)\right)$ **for** $\beta=-0.1$**,** $\lambda=0.1$**,** $\alpha=0.1$ **and** $\alpha_0=0.1$ **: the left curve is obteined for** $f\left(\lambda x-\lambda_0 t\right)=\sec\left(0.1x-0.t\right)$ **and the right curve for** $f\left(\lambda x-\lambda_0 t\right)=\operatorname{sech}\left(0.1x-0.1t\right)$ **such that we have** $x\in[-10,10]$**,** $t\in[0,40]$**.**

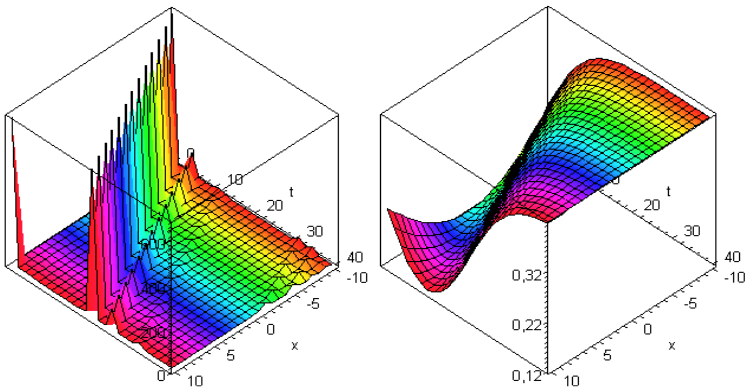


**Figure 9 : Curves representing the solution** $\eta(x,t)=\left(-12\beta\lambda^2/\alpha\right)T_{2,0}\left(f\left(\lambda x-\lambda_0 t\right)\right)$ **pour** $\beta=-0.1$**,** $\lambda=0.1$**,** $\alpha=0.1$ **et** $\alpha_0=0.1$ **: la courbe de gauche est obtenue pour** $f\left(\lambda x-\lambda_0 t\right)=\tan\left(0.1x-0.t\right)$ **et la courbe de droite pour** $f\left(\lambda x-\lambda_0 t\right)=\tanh\left(0.1x-0.1t\right)$ **such that we have** $x\in[-10,10]$**,** $t\in[0,40]$**.**

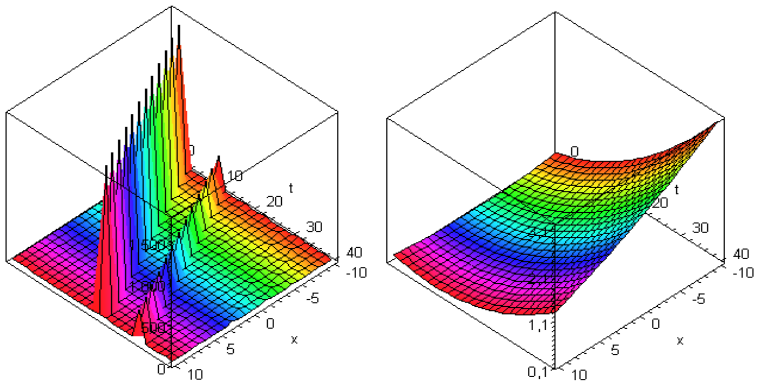


**Figure 10 : Curves representing the solution** $\eta(x,t)=\left(-12\beta\lambda^2/\alpha\right)T_{2,0}\left(f\left(\lambda x-\lambda_0 t\right)\right)$ **for** $\beta=-0.1$**,** $\lambda=0.1$**,** $\alpha=0.1$ **and** $\alpha_0=0.1$ **: the left curve is obtained for** $f\left(\lambda x-\lambda_0 t\right)=\left(0.1x-0.t\right)^2$ **and the right curve for** $f\left(\lambda x-\lambda_0 t\right)=\arctan\left(0.1x-0.1t\right)$ **tel que** $x\in[-10,10]$**,** $t\in[0,40]$**.**

Beyond the curves obtained above, we see that it is possible to obtain as many curves as long as the function f(x) is continuously differentiable in its domain of definition. For example, for f(x) =, we have following curves. But except that not all the curves obtained can properly describe the giant waves as obtained on the sea surface during tsunamis.

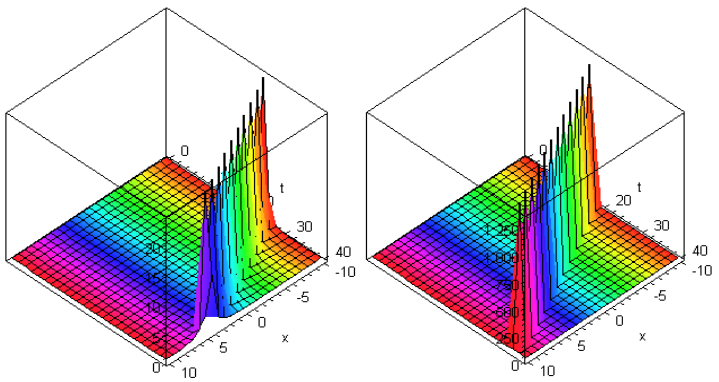


**Figure 11 : Curves representing respectively the solution** $\eta(x,t)=\left(12\beta\lambda^2/\alpha\right)J_{2,0}\left(f\left(\lambda x-\lambda_0 t\right)\right)$ **and** $\eta(x,t)=-12\beta\lambda^2/\alpha T_{2,0}\left(\lambda x-\lambda_0 t\right)$**for ,** $\lambda=0.1$**,** $\alpha=0.1$ **and** $\alpha_0=0.1$ **: the left curve is obtained**

**for** $f\left(\lambda x-\lambda_0 t\right)=\pm\sqrt{10-\left(0.1x-0.t\right)^2}$ , $\beta=0.1$ **and the right curve for** $f\left(\lambda x-\lambda_0 t\right)=\pm\sqrt{10-\left(0.1x-0.t\right)^2}$ , $\beta=-0.1$ **, such that we have** $x\in[-10,10]$ **,** $t\in[0,40]$ **.**

## CONCLUSION

To write this article, we started from the observation that the forced KdV equation which attempts to explain the sliding movements of the seabed, the triggering and the deployment of tsunamis had until now only approximate solutions. This is undoubtedly due to the fact that the second member of the equation which is considered as an external excitation or an external force is chosen randomly. Motivated by this fact, we wanted to demonstrate in this article how to choose the external force of the KdV equation in order to obtain exact solutions. The objective is to obtain solutions whose profiles best approximate the giant waves often observed during tsunamis. To achieve our objective, we first solved the KdV equation which characterizes the free movement of solitary waves, i.e. the basic KdV equation without a second member. Once its solutions were obtained, we constructed the general solutions of the KdV equation, while ensuring that the ansatz-solution to be constructed is close to that of the family of solitary waves. The solution of the nonlinear differential equation without a second member of KdV admitting for solutions $\eta(\xi)=\left(-12\beta\lambda^2/\alpha\right)J_{2,0}(\xi)$, and $\eta(\xi)=\left(-12\beta\lambda^2/\alpha\right)T_{2,0}(\xi)$ where $\xi=\lambda x-\lambda_0 t$ , we take inspiration from this to construct solution to (1) under the form $\eta(\xi)=\left(-12\beta\lambda^2/\alpha\right)J_{2,0}\left(f(\xi)\right)$, and secondly in the form $\eta(\xi)=\left(-12\beta\lambda^2/\alpha\right)T_{2,0}\left(f(\xi)\right)$, where $f(\xi)$ is an arbitrary function continuously differentiable in its domain of definition. We have established in our approach the general expression of the external force so that we have exact solutions capable of characterizing the giant wave resulting from the tsunami surge. This approach allows to build an infinity of solutions; but in this article, we have proposed just a few sample solutions, each time making an adequate choice of the function $f(\xi)$. We have considered two sets of solutions in this manuscript, but it should be noted that in practice it is advisable to consider a single case to search for solutions and subsequently move on to other forms of solutions through transformations.

$$J_{n,m}(i\xi)=(i)^m T_{n,m}(\xi), i^2=-1 \text{ or } T_{n,m}(i\xi)=(i)^m J_{n,m}(\xi), i^2=-1.$$

Figures 1 to 11 show some profiles of giant wave solutions resulting from the results obtained. We humbly believe that this approach to solving and analyzing the forced KdV equation can be a significant contribution to the understanding of tsunami dynamics in case numerical and experimental propagation studies confirm the so-called exact analytical solutions.

## REFERENCES

[1] Zabusky and Kruskal, 1965. Interaction of "solitons" in a collisionless plasma and the recurrence of the initial states, Phys. Rev. Lett. 15, 140-143.

[2] Hasegawa, A, and Tappert, 1973. Transmission of stationary nonlinear optical pulses in dielectric fibers in anomalous dispersion App. Phys. Lett. 23, 142-144.

[3] Hirota R, 1971. Exact solutions of the KdV equation for multiple collisions of solitons Phys. Rev. Lett. 27, 1192-1194.

[4] Wang, M.L, 1996. Exact solutions for a compound KdV-Burgers equation Phys. Lett. A 123, 279-287.

[5] Hirota, R, 1973. Exact N. Soliton solutions of the wave equation of long waves in shallow-water and in

nonlinear lattices J. Math. Phys. 14, 810-814.

[6] Wazwaz, A.M. 2012, A modified KdV-type equation that admits a variety of travelling wave solutions: kinks, solitons, peakons and cuspons, Phys. Scr. Vol 86, 045501-045506.

[7] Mollenauer, L.F, R.F. Stolen and J. P. Gordon, 1980. Experimental observation of picoseconds pulse narrowing and solitons in optical fibers, Phys. Rev. Lett. 27, 1192-1194

[8] Sasa, N and J. Satsuma, 1991. New-type of soliton solutions for a high-order nonlinear Schrödinger equation, J. of Physical society of Japan 60, 409-417.

[9] Wadati, M, 1975. Wave propagation in nonlinear lattice I. J. Phys. Soc. Jpn. 38, 673-680.

[10] Wadati, M, 1975. Wave propagation in nonlinear lattice II. J. Phys. Soc. Jpn. 38, 681-686.

[11] Burger S, K. Bongs, S. Dettmer, W. Ertmer and K. Sengstock, 1999. Dark solitons in Bose-Einstein condensates; Phys. Rev. Lett. 83, 5198-5201.

[12] He, J.H, 1997, Variational interaction method for delay differential equations, Commune Nonlinear Sci. Numer. Simult 2(4) 235-236.

[13] Shikuo, liu, Fu Zontao and Liu Shida et al. 2001. Jacobi elliptic function expansion method and periodic wave solutions of nonlinear wave equations, Physics Letters A, 289 (1) 69-74.

[14] Anupma, B and K.R. Gupta, 2012 Modify (G′/G))-expansion method for finding exact solutions of the coupled Klein-Gordon-Schrödinger equation. Mathematical methods in applied sciences 35(10) 1175-1187.

[15] Wazwaz A.A. 2005. The tanh method, Exact solutions of the sine-Gordon and the sinh-Gordon equation, App. Math. Comput. 167, 1196-1210.

[16] Fan E. and Y. C. Hon, 2003 Applications of extended tanh method to "special" types of nonlinear equations Appl. Math. Comput. 14, 351-358.

[17] J. R. Bogning, C.T. Djeumen Tchaho and T. C. Kofané ,(2012) ,Construction of the soliton solutions of the Ginzburg-Landau equations by the new Bogning-Djeumen Tchaho-Kofané method, Physica Scripta, 85, 025013-025018.

[18] J. R. Bogning, C.T. Djeumen Tchaho and T. C. Kofané, (2012), Generalization of the Bogning- Djeumen Tchaho-Kofane Method for the construction of the solitary waves and the survey of the instabilities, Far East Journal of Dynamical Systems,20(2), 101-119.

[19] E. Pelinovsky, Submarine Landslides and Tsunamis, Kluwer Academic Publisher, Netherlands, 2003.

[20] A.H. Salas, Computing exact solutions to a generalized Lax seventh-order forced KdV equation (KdV7), Applied Mathematics and Computation 216, 8 (2010) 2333-2338.

[21] Alvaro H. Salas, Computing solutions to a forced kdV equations. Nonlinear Analysis; Real world Applications. Vol. 12, Issue 2, April 2011, 1314-1320.

[22] Jx. Zhao, BL. Guo, Analytical solutions to forced KdV equation, Communications in Theoretical Physics 52 (2009) 279-283.

[23] Alvaro H. salas, computing solitons to a forced equation. Nonlinear analysis. Real World Applications. Vol. 12 (2) 2011, 1314-1320.

[24] AH. Salas, Exact solutions for the general fith kdV equation by the exp function method, Applied Mathematics and Computation 205(1) (2008).

[25] Clovis Taki Djeumen Tchaho, Hugues Martial Omanda, Gaston N'tchayi Mbourou, Jean Roger Bogning and Timoléon Crépin Kofané, 2019, Multi-form solitary wave solutions of the KdV-Burgers-Kuramoto, Journal of Physics Communications, 3, 105013

[26] Clovis Taki Djeumen Tchaho, Hugues Martial Omanda, Gaston N'tchayi Mbourou,Jean Roger Bogning and Timoléon Crépin Kofané, 2021, Higher Order Solitary Wave Solutions of the Standard KdV Equations, Open Journal of Applied Sciences, 11, 103-125

[27] J. R. Bogning , R. Njikue , J. P. Ngantcha , H. M. Omanda and C.T. Djeumen Tchaho, Probable solutions of a modified KdV type nonlinear partial differential equation, Asian research journal of mathematics, 18(1): (2022) 1-13.

[28] Wazwaz A. M. 2007, The variational iteration method for rational solutions for KdV, K(2,2) Burgers and cubic Boussinesq equations. Journal of Computational and Applied Mathematics 207 (1) 18-23.

[29] Wazwaz A. M. 2004. The tanh and the sine-cosine methods for the complex modified kdV and the generalized kdV equations. Appl. Math. Comput. 154, 713-723.

[30] Bogning, JR. (2019). Mathematics for nonlinear physics: Solitary wave in the center of the resolution of dispersive nonlinear partial differential equations, Dorrance Publishing Co, USA.

[31] Bogning, JR. (2019). Mathématics for physics: The implicit Bogning functions & applications, Lambert Academic, Publishing, Germany.

[32] Bogning, JR. (2020). Elements of Analytical Mechanics and Quantum Physics , Lambert Academic, Publishing, Germany